Epigenetic Dysregulation in the Basocortical Cholinergic Projection System During the Progression of Alzheimer's Disease

by

Laura J. Mahady

A Dissertation Presented in Partial Fulfillment
of the Requirements for the Degree
Doctor of Philosophy

Approved October 2018 by the
Graduate Supervisory Committee:

Elliott Mufson, Co-Chair
Heather Bimonte-Nelson, Co-Chair
Robert Bowser
Paul Coleman

ARIZONA STATE UNIVERSITY

December 2018

ABSTRACT

Alzheimer's disease (AD) is characterized by the degeneration of cholinergic basal forebrain (CBF) neurons in the nucleus basalis of Meynert (nbM), which provides the majority of cholinergic input to the cortical mantle and together form the basocortical cholinergic system. Histone deacetylase (HDAC) dysregulation in the temporal lobe has been associated with neuronal degeneration during AD progression. However, whether HDAC alterations play a role in cortical and cortically-projecting cholinergic nbM neuronal degeneration during AD onset is unknown. In an effort to characterize alterations in the basocortical epigenome semi-quantitative western blotting and immunohistochemistry were utilized to evaluate HDAC and sirtuin (SIRT) levels in individuals that died with a premortem clinical diagnosis of no cognitive impairment (NCI), mild cognitive impairment (MCI), mild/moderate AD (mAD), or severe AD (sAD). In the frontal cortex, immunoblots revealed significant increases in HDAC1 and HDAC3 in MCI and mAD, followed by a decrease in sAD. Cortical HDAC2 levels remained stable across clinical groups. HDAC4 was significantly increased in prodromal and mild AD compared to aged cognitively normal controls. HDAC6 significantly increased during disease progression, while SIRT1 decreased in MCI, mAD, and sAD compared to controls. Basal forebrain levels of HDAC1, 3, 4, 6 and SIRT1 were stable across disease progression, while HDAC2 levels were significantly decreased in sAD. Quantitative immunohistochemistry was used to identify HDAC2 protein levels in individual cholinergic nbM nuclei immunoreactive for the early phosphorylated tau marker AT8, the late-stage apoptotic tau marker TauC3, and Thioflavin-S, a marker of

mature neurofibrillary tangles (NFTs). HDAC2 nuclear immunoreactivity was reduced in individual cholinergic nbM neurons across disease stages, and was exacerbated in tangle-bearing cholinergic nbM neurons. HDAC2 nuclear reactivity correlated with multiple cognitive domains and with NFT formation. These findings identify global HDAC and SIRT alterations in the cortex while HDAC2 dysregulation contributes to cholinergic nbM neuronal dysfunction and NFT pathology during the progression of AD.

ACKNOWLEDGMENTS

I would like to thank Dr. Sylvia Perez, Dr. Muhammad Nadeem, and Dr. Bin He for their continuous support and technical advice. I would like to thank my dissertation committee co-chair Dr. Heather Bimonte-Nelson for her invaluable mentorship, Dr. Robert Bowser and Dr. Paul Coleman for their input and high level of scientific knowledge which greatly contributed to this work. I would also like to thank my advisor Dr. Elliott Mufson for his mentorship and patience throughout my graduate career, I am extremely grateful to have his support.

TABLE OF CONTENTS

Page

CHAPTER Page

CHAPTER Page

LIST OF TABLES

LIST OF FIGURES

CHAPTER 1

INTRODUCTION

1.1 INTRODUCTION TO ALZHEIMER'S DISEASE

In the early 1900s Dr. Alois Alzheimer, a Bavarian psychiatrist and neuropathologist, first described a form of presenile dementia in a female patient named Auguste Deter (Mufson, Mahady et al. 2015). Auguste developed memory loss and neuropsychiatric symptoms and died at the age of 55. Postmortem evaluation of Auguste's brain revealed extensive cortical atrophy and tissue sections stained using silver impregnation procedures identified senile plaques (SPs) and neurofibrillary tangles (NFTs) (Alzheimer 1906), which are now considered pathological hallmarks of Alzheimer's disease (AD). SPs are present in the extracellular matrix and contain insoluble fibrils of amyloid-beta (Aβ) peptide, which is cleaved from the transmembrane amyloid precursor protein (APP) by β cleavage through the beta-site APP cleaving enzyme 1 (BACE1) and γ secretase (Shoji, Golde et al. 1992; Haass and Selkoe 1993; Thinakaran and Koo 2008). NFTs are agyrophilic aggregates of hyperphosphorylated tau protein (Trojanowski 1993; Yoshiyama, Lee et al. 2013). NFTs also display beta-pleated sheet structures which interfere with cytoskeletal integrity and downstream synaptic function. Synaptic loss is major neuropathological hallmark of the AD brain and correlates with cognitive decline (Scheff and Price 1998; Scheff and Price 2003; Counts, Nadeem et al. 2004; Scheff, Price et al. 2006).

Clinical manifestations of AD include cognitive and neuropsychiatric symptoms. Memory impairment is a primary symptom of AD with declarative episodic memory,

memory of events occurring at a particular time and place, one of the first and most severely affected cognitive domains in AD (Carlesimo and Oscar-Berman 1992; Gold and Budson 2008). This type of memory depends on medial temporal lobe structures (Tulving and Markowitsch 1998). Within episodic memory, memory for recent events is impaired in early AD and is served by the hippocampus, entorhinal cortex, and related structures (Golomb, de Leon et al. 1993; Grady, Furey et al. 2001; Jahn 2013). Subcortical systems supporting procedural memory and motor learning are relatively spared until later stages of the disease, as is semantic memory, memory for factual information (Hirono, Mori et al. 1997). Semantic memory involves neocortical temporal regions including those in the anterior temporal lobe (Bonner and Price 2013).

Deficits in executive function, related to basocortical cholinergic structures (Baudic, Barba et al. 2006), and visuospatial impairment (Quental, Brucki et al. 2009) are affected relatively early in the disease course (Imamura, Takatsuki et al. 1998; Muller-Spahn 2003; Ferris and Farlow 2013). In contrast, language deficits are not present in early stages (McKhann, Knopman et al. 2011). In addition to cognitive deficits, neuropsychiatric symptoms appear in patients with AD including apathy, social disengagement and irritability, depression, agitation, aggression, wandering, and psychosis (Lyketsos, Carrillo et al. 2011). These symptoms usually present at later stages of AD, and are thought to be predictive of more severe dementia (Peters, Rosenberg et al. 2013), neurodegeneration (Namekawa, Baba et al. 2013), loss of independence (Zahodne, Manly et al. 2013), and early death (Vilalta-Franch, Lopez-Pousa et al. 2013).

Clinical indicators of AD occur later in adulthood, usually after the age of 65 in 99% of patients (late onset AD). Whereas less than 1% of patients have an autosomal dominant pattern of inheritance termed "familial AD' due to mutations in genes that code for amyloid metabolism including APP, presenilin 1 (PS1), or presenilin 2 (PS2). The greatest risk factor for late onset AD is age (Hebert, Scherr et al. 1995), but cardiovascular and lifestyle are additional variables (Bruijn and Ikram 2014). The ε4 allele of apolipoprotein E (APOE ε4) is the most important genetic risk factor for AD (Corder, Saunders et al. 1993; Liu, Kanekiyo et al. 2013; Shi, Yamada et al. 2017). Late onset AD is estimated to affect 5.7 million people and is predicted to afflict 13.8 million people in the USA by 2050 (Thies and Bleiler 2013; 2018). The impact of this disease on global healthcare systems is likely to be devastating, with annual expenditures in the US exceeding $232 billion (Wimo, Guerchet et al. 2017; 2018). Understanding the underlying processes in prodromal AD, and defining which cases are true presymptomatic AD cases will be key in determining novel therapeutic strategies aimed at preventing or slowing the emergence of AD. To investigate these types of questions it is imperative to have tissue from a cohort of individuals that received extensive antemortem clinical and postmortem neuropathological characterization. The studies presented in this dissertation were performed using tissue from the Rush Religious Orders Studies, a longitudinal clinical and pathological study of aging and dementia in the elderly.

1.1.1 The Rush Religious Orders Study (RROS)

The Rush Religious Orders Study (RROS) began in 1994 and enrolls nuns, priests, and brothers from more than 40 groups across the US (Bennett, Schneider et al. 2012; Bennett, Buchman et al. 2018). The RROS allows clinicians and scientists to obtain brain tissue from persons on whom risk factor information was obtained prior to the onset of mild cognitive impairment (MCI) and AD for studies linking risk factors to clinical and neuropathologic phenotypes. RROS members undergo yearly clinical evaluations beginning at 65 years of age for medical history, a complete neurological examination, and cognitive performance by a team of investigators led by a neurologist (Bennett, Wilson et al. 2002; Bennett, Schneider et al. 2012). A battery of 21 cognitive performance tests is administered each year. The battery of cognitive tests assess a range of cognitive abilities and are used to construct a global composite measure of cognition and separate measures of five cognitive domains, including episodic memory, semantic memory, working memory, perceptual speed, and visuospatial ability (Bennett, Schneider et al. 2012). All participants agree to organ donation as a condition of entry. Post-mortem data includes neuropathologic evaluation of AD pathology, cerebral infarcts, Lewy body disease, and other pathologies common in aging and dementia (Bennett, Schneider et al. 2012). Pathologic diagnoses of AD include NIA-Reagan measure of likelihood of AD based on CERAD plaque and Braak NFT staging, CERAD criteria for neuritic plaque density and age-adjusted plaque load, and Braak score based on the staging of NFT pathology (Braak and Braak 1991; Mirra 1997). A strength of the RROS is the ability to

study MCI/prodromal AD individuals with cognitive impairment abnormal for their age group who are at greater risk for developing AD (Petersen 2004).

1.2 PRODROMAL AD: MILD COGNITIVE IMPAIRMENT

The preclinical stage of AD has been suggested to begin 15 to 20 years before the emergence of clinical symptoms (Sperling, Mormino et al. 2014). The term MCI is synonymous with the term prodromal AD and is used to describe an intermediate stage between normal brain ageing and dementia. In addition, NFT and Aβ pathology is increased in the brains of individuals with MCI compared to those with no cognitive impairment (NCI) (Guillozet, Weintraub et al. 2003; Markesbery, Schmitt et al. 2006; Markesbery 2010; Mufson, Malek-Ahmadi et al. 2016). The concept of MCI was formed from memory clinics which treated milder cases of dementia, and longitudinal studies of elderly populations that were evaluated annually for cognitive status. Many cases with earlier, milder cognitive loss did not exhibit impairment in two cognitive domains, a criterion that was required for an NINDS/ADRDA diagnosis of AD established by McKhann and coworkers (McKhann, Drachman et al. 1984). In the 1990's these individuals were characterized by an amnestic memory disorder and the term 'MCI' was popularized by Petersen et al. (Petersen, Smith et al. 1999).

Amnestic MCI (aMCI) was the most common form of MCI reported by memory clinics; however, MCI along with other affected single cognitive domains comprise a small component of this clinical presentation. MCI individuals with only memory deficits are classified as single domain aMCI, while those who have a deficit in memory as well as other cognitive domains including language, executive function, and visuospatial skills

are categorized as multi-domain MCI (mdMCI) (Petersen 2004; Johnson, Phillips et al. 2010). The clinical criteria for aMCI include memory impairment corroborated by an informant, objective memory impairment for age, preserved general cognition, mostly intact functional activities, and are not demented (Petersen 2004). If memory is not impaired the individual has nonamnestic MCI (naMCI) and the determination of either a single nonmemory domain or multiple nonmemory domains is made by a clinician (Petersen 2004).

Individuals with aMCI are at a higher risk of developing AD, with an estimated 10-15% conversion rate (Petersen 2004; Johnson, Phillips et al. 2010). However, some individuals clinically diagnosed with NCI or MCI can exhibit SP and NFT pathology equal to or greater than that seen in mild to moderate AD, challenging the pathologically-based idea that these lesions alone cause dementia (Mufson, Chen et al. 1999; Price, McKeel et al. 2009; Markesbery 2010; Mufson, Malek-Ahmadi et al. 2016). Interestingly, individuals with MCI have an upregulation in choline acetyltransferase (ChAT) activity in the frontal cortex and hippocampus that correlate with cognitive impairment (DeKosky, Ikonomovic et al. 2002), thus early cognitive impairment in prodromal AD may be linked to basocortical cholinergic function than the classic pathological hallmarks of AD.

1.3 THE BASOCORTICAL CHOLINERGIC SYSTEM IN AD

1.3.1 Discovery of Cholinergic Transmission in the CNS

In the early 1900s Otto Loewi discovered the cardioactive substance released by the vagus nerve later identified as acetylcholine (ACh) (Loewi 1921). Many years later it

was established that ACh is a neurotransmitter in the central nervous system (CNS), and with the advent of axonally transported tract tracers in the early 1970s monosynaptic projections were demonstrated from the basal forebrain to the cerebral cortex (Divac 1975; Kievit and Kuypers 1975). Innervation of the cortex by cholinergic neurons was visualized using the hydrolytic enzyme acetylcholinesterase (AChE) combined with retrogradely transported horseradish peroxidase (HRP). This methodology was first implemented to determine cholinergic cortical innervation in the monkey brain and demonstrated that cortically injected HRP led to the retrograde labeling of AChE positive basal forebrain neurons (Mesulam and Hoesen 1976). This technique was improved upon by replacing AChE with the immunolabeling of the synthetic enzyme for ACh, choline acetyltransferase (ChAT), since all presynaptic cholinergic basal forebrain (CBF) neurons contain ChAT (Mesulam, Mufson et al. 1986). These improvements helped to identify the anatomical organization of cortically projecting cholinergic neurons in the primate brain and to pinpoint their neuronal origin within cell groups termed the Ch1-4 complex (Figure 1.1) (Mesulam, Mufson et al. 1983; Mesulam, Mufson et al. 1986). In the monkey forebrain, retrograde tracer experiments of cholinergic perikarya identified that CBF neurons located in the medial septal (Ch1) and vertical limb of the diagonal band nucleus (Ch2) provide most of the cholinergic innervation to the hippocampal formation and the hypothalamus, the horizontal limb of the diagonal band nucleus (Ch3) to the olfactory bulb, and Ch4/nbM neurons innervate the entire cerebral cortex and to a lesser extent the amygdala (Figure 1.1) (Mesulam, Mufson et al. 1983; Mesulam, Mufson et al. 1986; Mesulam 2013).

Select cortical areas receive semi-topographic cholinergic innervation from different sectors of the Ch4 complex. Ch4 anteromedial (am) neurons provide cholinergic innervation to medial cortical areas; Ch4 anterolateral (al) to frontoparietal cortex, opercular regions, and the amygdaloid nuclei; Ch4 intermediodorsal and intermedioventral to laterodorsal frontoparietal, peristriate, and midtemporal regions; and Ch4 posterior (p) sectors provide cholinergic input to the superiortemporal and temporopolar regions (Mesulam, Mufson et al. 1983; Mesulam 2013). Cortical projections to Ch4 originate in regions with limbic-paralimbic connections. Cerebral injections of tritiated amino acids in the monkey brain revealed anterograde transport to Ch4 from piriform, orbitofrontal, and frontopolar cortices, as well as anterior insula, temporal pole, entorhinal cortex and anterior cingulate. While injections in parietal cortex, peristriate, lateral temporal, and dorsolateral prefrontal cortex were not anterogradely transported to Ch4 (Mesulam and Mufson 1984). Ch4 also receives input from the hypothalamus and amygdala (Price and Amaral 1981; Mesulam and Mufson 1984). Thus, Ch4 can influence cholinergic transmission in all parts of the cortex in a fashion that is particularly responsive to neural activity within areas of the limbic system highlighting a key role in systems-based neuroanatomy in AD.

Approximately 90% of nbM neurons are cholinergic and are magnocellular and hyperchromic (Mesulam 2013). NbM perikaryal shapes are diverse; from multipolar to fusiform and pyramidal. These neurons are found in compact groups within the nbM and dispersed interstitial neurons embedded within the anterior commissure, internal and external medullary laminae of the globus pallidus, ansa peduncularis, ansa lenticularis,

and the internal capsule (Mesulam, Mufson et al. 1983). In the human brain cholinergic nbM neurons express AChE, the vesicular acetylcholine transporter, calbindin-d28k, high affinity nerve growth factor receptor trkA, and low-affinity p75 nerve growth factor receptor ($p75^{NTR}$) (Mufson, Bothwell et al. 1989; Geula, Schatz et al. 1993; Kordower, Chen et al. 1994; Gilmor, Erickson et al. 1999; Mesulam 2013).

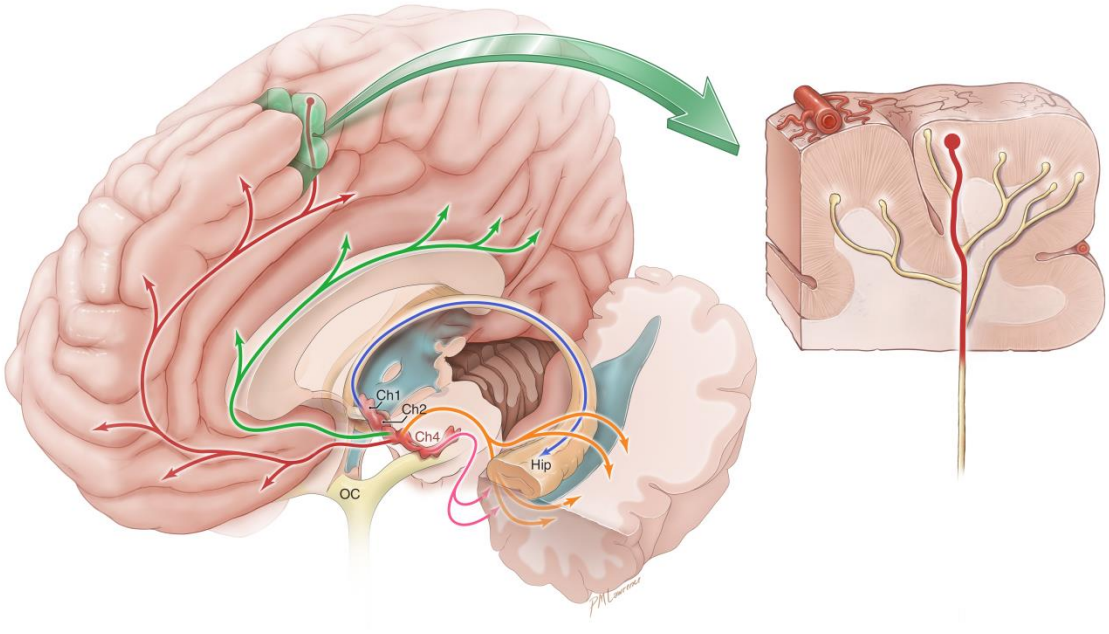

Figure 1.1 The Basocortical Cholinergic Projection System

CBF neurons located in the medial septal (Ch1) and vertical limb of the diagonal band nucleus (Ch2) provide the majority of cholinergic innervation for the hippocampal formation and the hypothalamus, and Ch4/nbM neurons innervate the entire cerebral cortex and the amygdala. OC; optic chiasm; Hip; hippocampal formation.

1.3.2 CBF Neuron Survival and Maintenance

CBF neuronal survival is dependent upon nerve growth factor (NGF), which is derived from the precursor protein proNGF (Fahnestock, Michalski et al. 2001; Fahnestock, Yu et al. 2004). The NGF family of proteins includes brain derived nerve growth factor (BDNF), neurotrophin 3 (NT-3), and neurotrophin 4 (NT-4). The NGF neurotrophin family binds with nanomolar affinity to the low affinity pan-neurotrophin receptor, $p75^{NTR}$, and with picomolar affinity to specific high affinity tyrosine kinase receptors (Trks) (Huang and Reichardt 2001). ProNGF binds with a higher affinity to the $p75^{NTR}$ receptor compared to trkA (Lee, Kermani et al. 2001), with its coreceptor sortilin (Nykjaer, Lee et al. 2004) and NH2. NGF binds TrkA, BDNF and NT-4 binds TrkB, and NT-3 binds with TrkC (Huang and Reichardt 2001). TrkA receptors are produced in CBF neurons, are anterogradely transported to cortical sites where they bind with cortically produced NGF, and promote/maintain synaptic contact with the neurons of the hippocampus and cortex (Conner, Franks et al. 2009). In the 1980s, normal brain levels of NGF mRNA were shown to correlate with the degree of CBF innervation, with the highest NGF protein and mRNA levels present in the cortex and hippocampus (Korsching, Auburger et al. 1985). In addition, radiolabelled NGF injection into the hippocampus or cortex was demonstrated to bind trkA and be retrogradely transported to CBF neurons (Seiler and Schwab 1984). NGF interacts with $p75^{NTR}$ and the high affinity NGF-specific receptor TrkA on the surface of cholinergic neurons (Chao, Bothwell et al. 1986; Kaplan and Miller 2000; Nykjaer, Lee et al. 2004). Using radiolabeling, immunohistochemistry, and in situ hybridization $p75^{NTR}$ was shown to be located on CBF

neurons in the rat, monkey, and human brain (Riopelle, Verge et al. 1987; Dawbarn, Allen et al. 1988) while other studies have shown $p75^{NTR}$ immunolabeling of trigeminal and cerebellar neurons (Mufson, Higgins et al. 1991; Mufson, Brashers-Krug et al. 1992). Since over 80% of CBF neurons are $p75^{NTR}$ positive, this NGF receptor is a fiduciary marker for cholinergic nbM neurons (Mufson, Bothwell et al. 1989). TrkA mRNA and protein is present in CBF neurons, with over 90% colocalization with $p75^{NTR}$ (Sobreviela, Clary et al. 1994). CBF neurons also express TrkB or TrkC or a combination of these (Mufson, Ginsberg et al. 2003).

Cholinergic neurons located within the nbM produce the NGF receptors trkA and $p75^{NTR}$, which are anterogradely transported to the cortex (Conner, Franks et al. 2009). Mature NGF is produced following cleavage from its precursor protein, proNGF. Alterations in cortical NGF extracellular metabolism elevate levels of proNGF and exacerbate NGF degradation leading to atrophy of the cortical cholinergic system and cognitive deficits in adult rats (Allard, Leon et al. 2012). ProNGF is the predominant form in the human brain, and levels of proNGF increase during the disease process beginning in MCI and are associated with poor performance on cognitive tests (Fahnestock, Michalski et al. 2001; Peng, Wuu et al. 2004). Thus, NGF maturation and degradation may also explain cholinergic nbM neuronal atrophy in AD. Signaling through the $p75^{NTR}$ receptor is complex due to its many interactions with co-receptors and its ability to elicit ligand-dependent and independent trophic or apoptotic events (Barker 2004). $P75^{NTR}$-mediated apoptosis occurs following proNGF binding with the co-receptor sortilin, however proNGF can also have trophic effects by binding TrkA,

although at a lower affinity than $p75^{NTR}$ (Fahnestock, Yu et al. 2004; Clewes, Fahey et al. 2008; Masoudi, Ioannou et al. 2009). Cholinotrophic enhancement strategies have been proven to be effective in improving lesion-induced cognitive deficits in murine models, including cholinesterase inhibitors, neurotrophic factors, and transplantation of NGF-enriched fetal implants in the CBF (Dunnett 1990; Tuszynski, Roberts et al. 1996; Jonhagen, Nordberg et al. 1998; Winkler, Power et al. 1998). Cholinesterase inhibitors prevent the breakdown of ACh and sustain its activity at cholinergic synapses (Colovic, Krstic et al. 2013). Three cholinesterase inhibitors are approved by the FDA for symptomatic treatment of AD including donepezil, rivastigmine, and galantamine (Colovic, Krstic et al. 2013). A meta-analysis showed a modest benefit of these drugs for stabilizing cognition and behavior (Hansen, Gartlehner et al. 2008; Massoud and Gauthier 2010; Hampel, Mesulam et al. 2018).

Cholinesterase inhibitors not only provide symptomatic benefit, but may reduce the enormous financial and emotional burdens of AD on the healthcare system and caregivers. A Medicare beneficiary study determined that each additional month of cholinesterase inhibitors treatment is associated with a reduction in all-cause healthcare costs (Mucha, Shaohung et al. 2008). Additionally, for each year of treatment the use of cholinesterase inhibitors in AD reduces the risk for nursing home placement by ~30% (Feldman, Pirttila et al. 2009). Finally, these drugs reduce caregiver burden by reducing time devoted to the patient, caregiver stress, and some of the behavioral symptoms (Feldman, Gauthier et al. 2003; Hashimoto, Yatabe et al. 2009; Schoenmakers, Buntinx et al. 2009; Adler, Yarchoan et al. 2014). Encouraging results have also been obtained

using ex vivo gene transfer to deliver nerve growth factor or acetylcholine to compromised regions of the basocortical cholinergic system (Dekker, Winkler et al. 1994; Chen and Gage 1995; Winkler, Power et al. 1998; Tuszynski, Thal et al. 2005). These data highlight the importance of understanding the mechanisms driving cholinergic projection system dysfunction during the progression of AD.

1.3.3 Cholinotrophic Alterations in MCI and AD

Three landmark studies revealed the dysfunction of the basocortical cholinergic system in AD: the finding that cholinergic presynaptic markers are reduced in the cerebral cortex (Bowen, Smith et al. 1976; Davies and Maloney 1976); the loss and degeneration of cholinergic Ch4/nbM neurons in AD (Mesulam and Hoesen 1976; Whitehouse, Price et al. 1981); and the discovery that the cholinergic antagonist scopolamine impairs memory in cognitively normal aged individuals (Drachman and Leavitt 1974). Together these observations lead to the formation of the "cholinergic hypothesis" of AD (Bartus, Dean et al. 1982), which propelled the development of cholinesterase inhibitors for the treatment of AD (Hampel, Mesulam et al. 2018). Numerous *in vivo* and *in vitro* studies have investigated alterations underlying cholinergic and cholinotrophic deficits in AD. Associated with the selective degeneration of CBF neurons in severe AD is a reduction in cortical ChAT activity (DeKosky, Harbaugh et al. 1992) that correlates with disease duration and degree of cognitive impairment in AD (Wilcock, Esiri et al. 1982; Bierer, Haroutunian et al. 1995). The number of ChAT and vesicular acetylcholine transporter (VAChT) positive neurons were shown to be unchanged within the nbM early in the disease process, indicating viable but perhaps

dysregulated cholinergic function (Gilmor, Erickson et al. 1999). Interestingly, immunohistochemistry using antibodies against the NGF receptors, trkA and $p75^{NTR}$, combined with unbiased counting revealed a significant reduction in nbM neurons positive for these receptors compared to ChAT stained perikarya (Mufson, Ma et al. 2002).

Single-cell gene profiling studies indicate a downregulation in trkA, trkB, and trkC expression, while $p75^{NTR}$ and ChAT transcript levels are unchanged in individual cholinergic nbM neurons (Ginsberg, Che et al. 2006). Although a reduction of trkA transcripts supports the loss of neurons positive for the trkA protein, the stability of $p75^{NTR}$ expression conflicts with the loss of protein in neurons early in AD. The latter observation suggests that $p75^{NTR}$ nbM neuronal expression is maintained at a normal level or upregulated in the face of the disease process. Interestingly, age of disease onset may play crucial role cholinergic neuronal vulnerability, since it has been reported that early-onset AD was associated with a greater reduction in cholinergic nbM neurons compared to late-onset cases (Tagliavini and Pilleri 1983; Allen, Dawbarn et al. 1988). Similarly, ChAT activity in the frontal cortex is not as severely decreased in late-onset AD compared to early onset (Bird, Stranahan et al. 1983; Rossor and Mountjoy 1986; Perry, Johnson et al. 1992; Sparks, Hunsaker et al. 1992). During the past several years clinical pathological investigations have indicated that changes in cortical ChAT activity is regionally and disease-stage specific. For example, ChAT activity is reduced in severe AD, while it was unchanged in inferior parietal, superior temporal, and anterior cingulate cortices in MCI and mild AD compared to NCI cases (DeKosky, Ikonomovic et al.

2002). Furthermore, ChAT activity in the superior frontal cortex and hippocampus is significantly elevated in MCI, but unchanged in mild AD compared to NCI or MCI. In addition to cholinotrophic alterations present in AD, the nbM is one of the first subcortical structures to be affected by NFT pathology identifying it as an early site of pathogenesis.

1.3.4 Neurofibrillary Tangle Pathology Within the nbM in AD

Braak and Braak described the spread of NFT pathology in the AD brain and indicated that the area containing the nbM was affected prior to the medial temporal lobe suggesting that a toxic moiety is propagated along axonal projections to interrelated brain regions (Braak and Braak 1991; Mesulam 1999; de Calignon, Polydoro et al. 2012; Liu, Drouet et al. 2012). In prodromal AD the nbM contains NFT densities that are as high as those in any other region in the brain (Mesulam, Shaw et al. 2004). A linear model for NFT evolution has been proposed that can be observed by antibodies directed against oligomeric, phosphorylated, and truncated tau epitopes marking early, intermediate, and late stages of NFT development during the progression of AD (Binder, Guillozet-Bongaarts et al. 2005). For example, tau phosphorylation at Serine 422 (pS422) was identified as an early event using the pS422 antibody, phosphorylation at Ser202 and Thr205 is another early tau posttranslational modification identified with the AT8 antibody, whereas tau truncation at aspartate 421 by caspase 3 (Asp421) detected with the TauC3 antibody occurs later during NFT formation (Ghoshal, Garcia-Sierra et al. 2001; Ghoshal, Garcia-Sierra et al. 2002; Garcia-Sierra, Ghoshal et al. 2003; Binder, Guillozet-

Bongaarts et al. 2005; Guillozet-Bongaarts, Garcia-Sierra et al. 2005; Guillozet-Bongaarts, Cahill et al. 2006).

Oligomeric and pretangle tau isoforms have been found in the nbM in early AD and MCI. A recent study identified tau oligomeric complex (TOC1) immunostaining in the nbM, and stereological estimates identified that numbers of TOC1 positive neurons increase with a concomitant decrease in $p75^{NTR}$ positive neurons during the transition from MCI to AD (Tiernan, Mufson et al. 2018). In addition, TOC1 positive nbM neurons colocalize with the pretangle marker pS422 and persist in late stage NFTs immunoreactive for MN423, truncation at glutamic $acid^{391}$ (Tiernan, Mufson et al. 2018). Another report demonstrated that the presence of pS422 positive pretangles, and TauC3 positive mature tangles increase during disease progression and occur parallel to a loss of $p75^{NTR}$ positive neurons (Vana, Kanaan et al. 2011). Numbers of pS422 immunoreactive neurons significantly correlate with cognitive measures such as global cognitive score and mini-mental state examination, while numbers of TauC3 positive cholinergic nbM neurons correlated with Braak score (Vana, Kanaan et al. 2011). Numerous pS422 and TauC3 positive neuropil threads were present in MCI and AD, indicating impaired axonal/dendritic processes in cholinergic neurons early during disease progression (Vana, Kanaan et al. 2011), and suggesting that the degenerative process begins in the axon and is retrogradely transported to the cell body.

A report investigating AT8 and Alz-50 immunostaining in cholinergic nbM neurons of MCI and early AD identified that the presence of pretangle-bearing neurons is correlated with cognitive impairment (Mesulam, Shaw et al. 2004). Interestingly, the

authors identified five early Braak stages (I/II) with extensive nbM NFT pathology that was not seen in any other structures outside of medial temporal areas, further confirming the selective vulnerability of the nbM to age-related and NFT pathology (Mesulam, Shaw et al. 2004). The mechanism linking early pathological tau formation and loss of cholinergic phenotype is unknown. However, epigenetic studies have shown that histone acetylation and deacetylation are involved in the regulation of ChAT expression (Aizawa and Yamamuro 2010; Aizawa, Teramoto et al. 2012) and in the hyperphosphorylation and acetylation of pathologic tau (Julien, Tremblay et al. 2009; Min, Chen et al. 2015; Min, Sohn et al. 2018), suggesting a role for epigenetics in the selective vulnerability of cholinergic nbM neurons in AD.

1.4 INTRODUCTION TO EPIGENETIC REGULATION

Epigenetics is the study of changes in gene expression, chromatin structure, and cell function in the absence of alterations to the underlying DNA sequence. Epigenetic modifications are capable of altering transcriptional activity in numerous biological pathways. Epigenetic status is modified by environmental factors such as diet, exposure to hazardous conditions, and life events such as pregnancy (Mastroeni, Grover et al. 2011).These modifications not only influence gene expression but also may determine phenotypic age, which can differentiate mortality risk between individuals of the same chronological age (Levine, Lu et al. 2015; Levine, Lu et al. 2018). Thus, epigenetic mechanisms may provide a point of intersection for diverse risk factors and pathophysiologic processes in AD. Unlike mutations and other genetic abnormalities, which are stable in the genome through time, epigenetic modifications are dynamic and

potentially reversible with the use of drugs and therapeutic approaches (Rodenhiser and Mann 2006). Characterizing the complex spectrum of epigenetic modifications including DNA methylation, RNA-related mechanisms, and posttranslational modifications to histone proteins which build upon each other and affect gene transcription and posttranscriptional expression will have a paramount effect in the area of personalized AD therapeutics.

1.4.1 DNA Methylation

DNA methylation (Figure 1.2) is highly interactive with histone acetylation and other posttranslational histone modifications, contributing to the complexity of the epigenome. In the 1970's discoveries by Bird established that adjacent cytosine-guanine (CpGs) dinucleotides in DNA are methylated by DNA methyltransferases (DNMTs) including DNMT1, DNMT2, DNMT3a/b, and DNMT4 (Bird 1978; Mastroeni, Grover et al. 2011; Cacabelos and Torrellas 2015). DNMT1 maintains methylation of hemimethylated DNA after DNA replication, while de novo DNA methylation is carried out by DNMT3a and DNMT3b (Mastroeni, Grover et al. 2011). DNMT2 has 5-cytosine DNA methyltransferase activity, but is also a RNA methyltransferase (Tang, Reddy et al. 2003). DNMTs transfer methyl groups derived from methyltetrahydrofolate to cytosine to form 5-methylcytosine. As a result, around 70% of CpG dinucleotides within the human genome are methylated (Mastroeni, Grover et al. 2011). DNA methylation can occur in coding or non-coding regions at any CpG dinucleotide, but previous studies have indicated that CpG-rich sections (CpG islands) within the promoter region are some of the most highly methylated. Gene expression can be modified by methylated CpG

sequences through induction of histone modifications, interfering with the binding of transcription factors to promoter sites, recruiting transcriptional repressors, and altering chromatin structure (Bird and Wolffe 1999; Zhang, McKinsey et al. 2002; Cacabelos and Torrellas 2015).

DNA hydroxymethylation has been identified as another modification to CpGs that may make them more inaccessible to transcription. This process involves the hydroxylation of 5-methylcytosine to form 5-hydroxymethylcytosine (Valinluck and Sowers 2007; Kriaucionis and Heintz 2009; Tahiliani, Koh et al. 2009). It has been suggested that hydroxymethylated DNA is a result of oxidative enzymes and oxidative damage in neurons (Kriaucionis and Heintz 2009; Tahiliani, Koh et al. 2009). Normally, glycosylases remove 5-hydroxymethylcytosines from DNA by utilizing the base excision repair (BER) system (Mastroeni, Grover et al. 2011), which allows 5-hydroxymethylcytosines to be replaced with unmodified cytosines which are then methylated de novo by the DNMTs. However, when 5-hydroxymethylcytosines are not removed they reduce the interaction of DNA with DNA-binding proteins (Valinluck, Tsai et al. 2004; Valinluck and Sowers 2007) and when present in the gene promoter are associated with transcriptional repression (Robertson, Robertson et al. 2011).

DNA methylation also modifies gene expression through methyl-CpG-binding proteins (MeCPs). MeCP2 binds to methylated DNA and recruits HDACs which results in a more condensed chromatin state and reduced or silenced gene transcription (Jones, Veenstra et al. 1998; Wade, Jones et al. 1998). Earlier reports suggested that MeCP2 required a methylated chromatin substrate for direct binding (Lewis, Meehan et al. 1992),

but more recent work identified that MeCP2 can condense chromatin directly even if DNA methylation, histone deacetylase activity, or the cooperation of other transcriptional co-repressors are absent (Wade 2001). In contrast, another methyl-CpG-binding protein, MeCP1, mediates DNA methylation and histone acetylation. MeCP1 can identify and bind to CpG dinucleotides, recruit HDACs, and induce transcriptional repression (Feng and Zhang 2001). Unlike MeCP2, MeCP1 does not bind directly to methylated DNA, but to a methyl-CpG-binding domain protein, MBD2 (Mastroeni, Grover et al. 2011). These proteins maintain DNA methylation of CpGs by recruiting DNMT1, which recognizes and repairs CpGs that have lost methyl groups on one DNA strand.

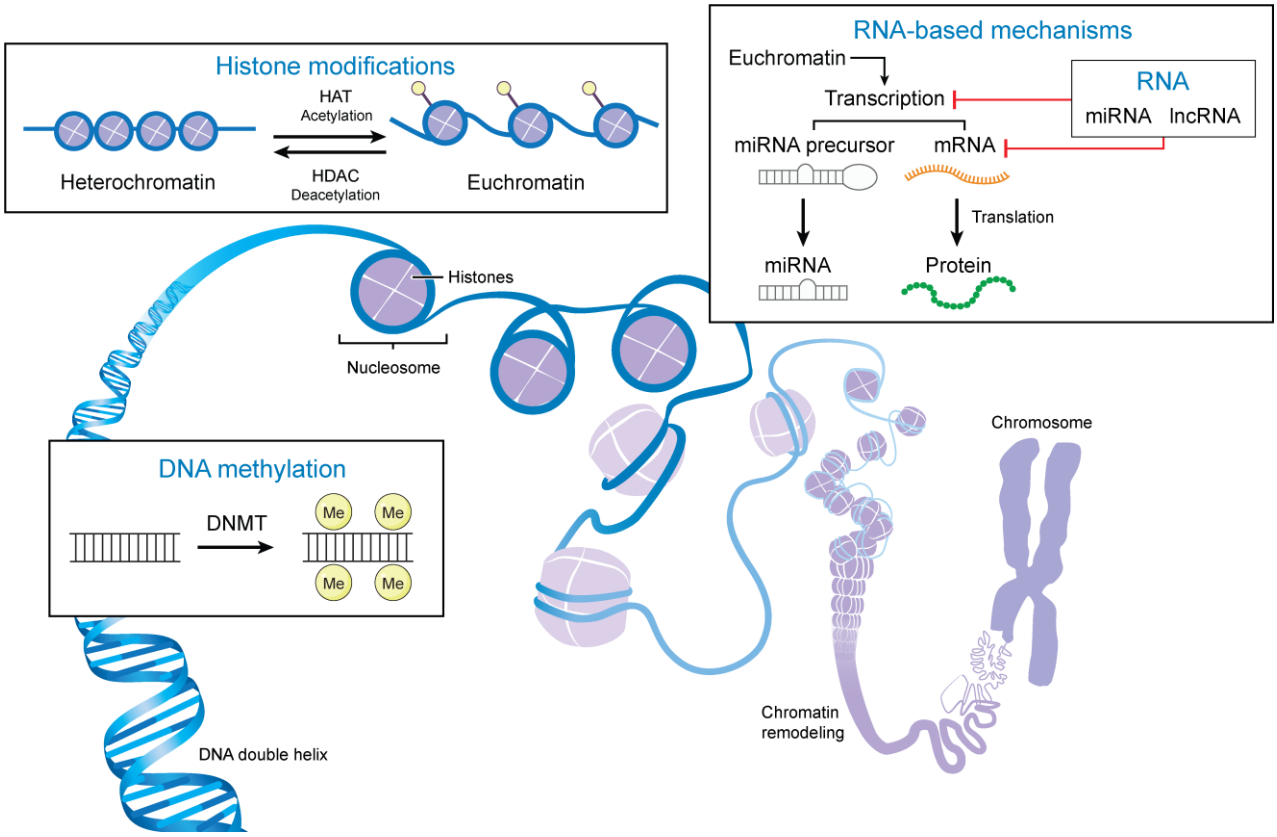

Figure 1.2 Mechanisms of Epigenetic Regulation

Epigenetic regulation depends on interaction between DNA methylation, histone modifications and RNA-based mechanisms. DNA methylation occurs largely at CpG islands. HATs acetylate lysine residues on histone tails contributing to chromatin relaxation or euchromatin, while HDACs remove acetyl groups leading to heterochromatin or highly compact chromatin. Two classes of non-coding RNA, miRNA and lncRNA, can modulate gene expression by interrupting translation of mRNAs by inhibition of post-transcriptional events, transcript degradation, or direct translational suppression. DNMT, DNA methyltransferase; Me, methyl group; HAT, histone acetyltransferase; HDAC, histone deacetylase; miRNA, micro RNA; mRNA, messenger RNA; lncRNA, long non-coding RNA.

1.4.2 RNA-related Epigenetic Mechanisms

Epigenetic regulation also extends to mechanisms involving non-protein-coding RNAs such as long non-coding RNAs (lncRNAs), micro-RNAs (miRNAs), and small interfering RNAs (siRNA). NcRNAs have numerous functions in epigenetic regulation including silencing of transposable elements, controlling gene expression, X-chromosome inactivation, DNA methylation, and histone modifications (Cacabelos and Torrellas 2015). LncRNAs are adaptors between specific chromatin loci, chromatin-remodeling and transcription factors (Cacabelos and Torrellas 2015). LncRNAs can also guide epigenetic-modifier complexes to distinct genomic sites, or act as scaffolds, which recruit multiple proteins simultaneously (Roberts, Morris et al. 2014). Small non-coding RNAs associate with a family of proteins called the Argonaute (AGO) proteins, and play a central role in RNA interference/activation (RNAi/a) pathways. Posttranscriptional regulation is facilitated by miRNAs and siRNAs which block translation and promote transcript degradation (Jiao, Zheng et al. 2014; Zusso, Barbierato et al. 2018). MiRNAs (Figure 1.2) inhibit translation through the RISC (RNA-induced silencing complex) and promote mRNA degradation by binding to the 3' untranslated region (3'UTR) (Pratt and MacRae 2009). However, miRNAs can also bind to the promoter region of a target gene and promote mRNA translation. MiRNAs also inhibit the expression of mRNAs by reducing their stability and translation rate (Cacabelos and Torrellas 2015). Similar to protein coding genes, miRNAs are susceptible to epigenetic modulation and are affected by DNA methylation. Recently, enhancer of zeste homolog 2 (EZH2) and HDACs were identified as critical histone modifiers of deregulated miRNAs in cancer that can be

recruited to a miRNA promoter by transcription factors (Liu, Chen et al. 2013). Whether these symbiotic relationships between HDACs and miRNAs are dysregulated during the onset of AD remains to be determined.

1.4.3 Posttranslational Histone Modifications

Histone proteins have a central globular domain and an N-terminal tail with multiple sites for modifications. These include posttranslational modifications such as methylation, phosphorylation, ubiquitination, sumoylation, biotinylation, citrullination, ADP ribosylation, glycosylation and histone acetylation (Konsoula and Barile 2012), and not only affect gene transcription (Allfrey 1966), but also DNA repair and replication (Wang, Yu et al. 2013). Histone lysine acetyltransferases (HATs/KATs) catalyze the transfer of acetyl groups from acetyl-coenzyme A to lysine residues on the N-termini of histones (Figure 1.2). Five families of HATs catalyze histone acetylation: KAT2A/GCN5, KAT2B/PCAF, KAT6-8, CREBBP/CBP, and EP300 (Huynh and Casaccia 2013). Acetylation neutralizes the positive charge of the histone proteins and decreases interactions with negatively-charged phosphate groups on DNA (Mastroeni, Grover et al. 2011; Cacabelos and Torrellas 2015), resulting in conformational relaxation of the chromatin and active transcription.

Histone deacetylases (HDACs) promote condensed chromatin state and decreased or silenced gene transcription by transferring acetyl groups from histone tails to coenzyme A (Mastroeni, Grover et al. 2011; Cacabelos and Torrellas 2015). Mammalian HDACs can be classified into four families based to their homology to yeast (class I, IIa, IIb and IV). Each class differs in structure, enzymatic function, subcellular localization

and expression patterns (Cacabelos and Torrellas 2015). Classes I and II are zinc-dependent and bind acetylated lysines via a water molecule (Fiorino, Giudici et al. 2014). Class I HDACs include HDAC1, 2, 3 and 8. These HDACs are ubiquitous, have high enzymatic activity for histone substrates, and are localized primarily in the nucleus (Haberland, Montgomery et al. 2009). HDAC1 and HDAC2 are very similar in sequence and function together as co-repressors in the Sin3, NuRD, CoREST and PRC2 complexes (Cacabelos and Torrellas 2015). HDAC2's role in biology and disease is ascribed to its ability to regulate transcription. On the other hand, HDAC2 possesses deacetylase-independent SUMO E3 ligase-like activity and activates protein synthesis of a subset of genes related to proliferation and apoptosis (Xu, Vatsyayan et al. 2010). Since HDAC2 is unique in its ability to regulate gene expression at both transcriptional and translational levels, it not only is a transcription co-repressor but also a translational activator.

Class IIa HDACs include HDAC4, 5, 7 and 9. The N-termini of Class IIa HDACs have binding sites for the transcription factor myocyte enhancer factor 2 (MEF2) and the chaperone protein 14-3-3, allowing these deacetylases to be signal responsive (Haberland, Montgomery et al. 2009). These HDACs shuttle from the nucleus to the cytoplasm when phosphorylated by calcium/calmodulin-dependent protein kinase (CaMK) and protein kinase D (PKD) and bind the 14-3-3 chaperone (Haberland, Montgomery et al. 2009). In contrast to other HDACs, class IIa HDACs show comparatively restricted expression patterns. HDAC5 and HDAC9 are present the heart, brain and in muscles (Haberland, Montgomery et al. 2009). HDAC4 is enriched in the brain and in skeletal growth plates, while HDAC7 is present in endothelial cells and

thymocytes (Haberland, Montgomery et al. 2009). The mechanism(s) by which class IIa HDACs repress transcription has not been elucidated. However, they have been shown to recruit class I HDACs through their C-terminal domain, which may account for some of their repressive activity (Fischle, Dequiedt et al. 2002). These HDACs have also been shown interact with other transcriptional repressors, like heterochromatin protein 1 (HP1) and C-terminal-binding protein (CTBP) (Dressel, Bailey et al. 2001; Zhang and Reinberg 2001; Zhang, McKinsey et al. 2002). Thus, these HDACs are adaptors for other transcriptional regulators and confer signal-responsiveness to downstream target genes (Haberland, Montgomery et al. 2009).

HDAC6 and HDAC10 comprise the class IIb HDACs. HDAC6 is a primarily cytoplasmic deacetylase, while little is known about the actions of HDAC10 (Fischer, Cai et al. 2002; Guardiola and Yao 2002). HDAC6 primarily deacetylates cytoskeletal proteins including α-tubulin and cortactin, transmembrane proteins such as interferon receptor IFNαR, and chaperone proteins (Hubbert, Guardiola et al. 2002; Kovacs, Murphy et al. 2005; Tang, Gao et al. 2007; Zhang, Yuan et al. 2007). HDAC6 is unique because it contains two deacetylase domains and a C-terminal zinc finger. HDAC11 is a class IV deacetylase expressed in the brain, heart, muscle, kidney and testis. Similar to HDAC10 little is known about its function, however, it possesses a deacetylase domain with small N- and C-terminal extensions comparable to the class I and II HDACs (Gao, Cueto et al. 2002; Liu, Hu et al. 2008).

Sirtuins (SIRTs) are class III nicotinamide adenine dinucleotide (NAD^+)-dependent deacetylases which transfer an acetyl group from the lysine side chain of a

substrate to cofactor. These enzymes are related to the yeast orthologous silent information regulator 2 (Sir2), which is involved in increasing yeast longevity. Calorie restriction in yeast activates Sir2 leading to lifespan extension, thus a growing number of studies have investigated the role of SIRTs in calorie restriction, metabolic homeostasis, and aging-related diseases like AD (Fiorino, Giudici et al. 2014). There are seven SIRT proteins with diverse subcellular locations including nuclear (SIRT1, 2, 6, 7), mitochondrial (SIRT3, 4, 5), and cytoplasmic (SIRT1, 2) family members. SIRT1 is the most studied due to its close homology to Sir2. SIRT1 deacetylates lysine residues on histones H1, H3 and H4 in addition to reducing methylation of histone H3 (Imai, Armstrong et al. 2000; Vaquero, Scher et al. 2004). SIRT1 also deacetylates and represses the activities of p53 (Vaziri, Dessain et al. 2001), and forkhead transcription factors (FOXO)3a, FOXO1, and FOXO4 (Motta, Divecha et al. 2004; Yang, Hou et al. 2005). SIRT1 increases the ability of FOXO3 to induce the cell cycle or to withstand oxidative stress, it also reduces the apoptotic ability of FOXO3 (Brunet, Sweeney et al. 2004). Thus, HDACs and SIRTs are in a unique position to regulate expression and function of numerous nuclear and cytoplasmic proteins across many different pathways, and merit investigation in AD.

1.5 EPIGENETIC ALTERATIONS IN THE AD BRAIN

1.5.1 DNA Methylation in AD

Numerous AD-related genes contain methylated CpG sites in their promoter regions and a genome-wide decrease in methylation is reported in AD (Mastroeni, Grover et al. 2011; Jager, Srivastava et al. 2014; Cacabelos and Torrellas 2015). Mastroeni and

colleagues analyzed DNA methylation in a pair of monozygotic twins discordant for AD (Mastroeni, McKee et al. 2009). Immunohistochemical detection of 5mC revealed that global DNA methylation within the anterior temporal neocortex and the superior frontal gyrus was significantly decreased in the twin with AD compared to the non-demented twin (Mastroeni, McKee et al. 2009). However, other studies using similar antibody-based methods have found that individuals with AD tend to have a higher level of DNA methylation than individuals without the disease. For example, DNA methylation was higher in the middle frontal gyrus of individuals with AD than in the same region of age-matched controls (Coppieters, Dieriks et al. 2014). Similarly, Rao et al. also found increased global DNA methylation in the frontal cortex of AD patients compared with cognitively normal controls (Rao, Keleshian et al. 2012). A study of DNA methylation in the entorhinal cortex also revealed a significant decrease in global DNA methylation in individuals with AD (Mastroeni, Grover et al. 2010). Immunoreactivity for 5mC was not significantly different in AD-spared regions such as the cerebellum, suggesting that this effect is region specific (Mastroeni, Grover et al. 2010). Though the results of this study in combination with those from the twin study suggest that individuals with AD have lower levels of DNA methylation in the temporal cortex than those without the disease, other groups have reported opposite findings. For example, one group demonstrated an increase in global DNA methylation in the middle temporal gyrus of subjects with AD compared with age-matched, cognitively normal controls (Coppieters and Dragunow 2011). Another group found no significant difference in global DNA methylation in the entorhinal cortex of individuals with and without AD (Lashley, Gami et al. 2015).

A recent immunohistochemical study found a reduction in extranuclear 5mC and 5hmC in astrocytes and neurofilament-labeled pyramidal neurons (Phipps, Vickers et al. 2016), the latter which display NFT pathology (Hof and Morrison 1990; Vickers, Riederer et al. 1994; Thangavel, Sahu et al. 2009), in the inferior temporal gyrus in AD compared to age-matched controls. Interestingly, AD-spared calretinin interneurons and microglia did not have significant alterations in 5mC or 5hmC, thus DNA methylation alterations in AD may be cell type dependent. Similar to DNA methylation findings within the temporal cortex and frontal cortex, the results in the hippocampus are inconclusive. A study by Chouliaras et al. found a significant decrease in hippocampal DNA methylation in AD cases compared to age-matched controls. In addition, the authors found that glial cell DNA methylation was significantly different in the CA1 and CA3 subregions, whereas neuronal DNA methylation was significantly different only in the CA1 subregion (Chouliaras, Mastroeni et al. 2013), suggesting that cell type specific alterations in DNA methylation vary depending on hippocampal subregion. By contrast, higher levels of DNA methylation were found in the hippocampus compared to individuals without AD (Bradley-Whitman and Lovell 2013).

Gene-specific DNA methylation studies have identified inconsistent results in regards to hypermethylated and hypomethylated genes in AD. Analysis of DNA methylation of APP, PSEN1 and MAPT found no significant differences in the frontal cortex and hippocampus of non-demented controls and individuals in various stages of AD (Barrachina and Ferrer 2009). Iwata et al. used pyrosequencing to analyze DNA methylation of various CpG sites of AD-related genes in the inferior temporal lobe, the

superior parietal lobe, and the cerebellum in AD subjects and non-demented control subjects. This investigation found significant differences in DNA methylation profiles of APP, MAPT and GSK3B, but not of PSEN1, BACE1 or APOE and these changes in methylation resulted in changes in gene expression (Iwata, Nagata et al. 2014). Thus DNA methylation can directly impact gene transcription in AD.

Using MALDI-TOF mass spectrometry in postmortem brain tissue samples derived from the prefrontal cortex of individuals with AD and age-matched controls, it was discovered that the promoter region of APOE was hypermethylated in AD (Wang, Oelze et al. 2008). In addition to the genes classically associated with AD, numerous genome-wide association studies have identified genetic variants associated with increased AD susceptibility. This includes the sortilin-related receptor, low-density lipoprotein receptor class A repeat-containing protein (SORL1), ATP-binding cassette, sub-family A, member 7 (ABCA7), and bridging integrator 1 (BIN1) (Lambert, Ibrahim-Verbaas et al. 2013; Humphries, Kohli et al. 2015; Yu, Li et al. 2015). Yu and colleagues analyzed DNA methylation in the dorsolateral prefrontal cortex of subjects with and without AD at 28 gene loci associated with AD pathology (Yu, Li et al. 2015). DNA methylation of five genes (SORL1, ABCA7, HLA-DRB5, SLC2A4 and BIN1) was significantly associated with AD. Several components of the cell cycle (P16, P21, P27, P53, RB1, cyclin B2) and apoptotic proteins (caspases 1, 3, 7-9) are regulated by DNA methylation and are upregulated in AD neurons (Cacabelos and Torrellas 2015). S100A2, a calcium-binding protein, has an age-dependent decrease in DNA methylation and is hypermethylated in AD (Wang, Oelze et al. 2008).

A significant decrease in 5hmC was reported in the entorhinal cortex and cerebellum of individuals with AD compared with age-matched controls (Condliffe, Wong et al. 2014). On the other hand, another group demonstrated a significant increase in 5hmC in the hippocampus, but not in the cerebellum (Bradley-Whitman and Lovell 2013). In contrast, immunoreactivity for 5hmC was reduced by 20.2% in the hippocampus of AD compared with non-demented, age-matched controls (Chouliaras, Mastroeni et al. 2013). Similar results were obtained when analyzing monozygotic twins discordant for AD. 5hmC immunoreactivity was lower in the CA1 region of the hippocampus of the AD twin compared with the non-demented twin. Others found a significant increase in 5hmC in the mid-frontal gyrus and mid-temporal gyrus in AD but low levels in astrocytes and microglia (Coppieters, Dieriks et al. 2014).

1.5.2 RNA-related changes in AD

Numerous miRNAs have been linked to AD via direct regulation of genes such as APP and BACE1 or indirectly via their effects on genes involved in neurogenesis and immune responses (Hebert, Horre et al. 2008; Lindsay 2008; Hebert, Horre et al. 2009; Soreq and Wolf 2011). Let-7b belongs to the let-7 miRNA gene family and is increased in the CSF of AD patients (Lehmann, Kruger et al. 2012). Among its downstream targets are members of chromatin remodeling proteins such as enhancer of zeste homolog 2 (EZH2) and the transcript of the miRNA processing enzyme dicer (DICER1), indicating a reciprocal interaction between let-7b expression, miRNA maturation, and epigenetic regulation (Forman, Legesse-Miller et al. 2008; Kong, Li et al. 2012). MiRNAs, miR-9, miR-125b, and miR-148 are abundantly expressed in the fetal hippocampus but miR-9

and miR-148 are significantly downregulated while miR-125b is significantly upregulated in postmortem AD tissue (Krichevsky, King et al. 2003; Lukiw 2007; Cogswell, Ward et al. 2008; Schonrock, Ke et al. 2010). MiR-9 targets include fibroblast growth factor (FGFR1), CDK6, caudal-type homeobox 2 (CDX2), NFKB1, and sirtuin 1 (SIRT1), the latter which provides feedback via its HDAC activity (O'Hagan, Mohammad et al. 2008; Rodriguez-Otero, Roman-Gomez et al. 2011; Rotkrua, Akiyama et al. 2011; Schonrock, Humphreys et al. 2012).

MiR-34c levels have been shown to be elevated in the hippocampus in both AD and aged mutant APP/PS1-21 mice, where reducing miR-34c levels rescues learning abilities in this mouse model (Zovoilis, Agbemenyah et al. 2011). MiR-107 is a miRNA with decreased expression in the temporal cortex in AD, specifically in Braak stage III and has been suggested to accelerate AD progression (Wang, Rajeev et al. 2008; Nelson and Wang 2010). The same study found significant negative correlations between miR-107 expression, neuritic plaque and NFT counts, and BACE1 mRNA levels (Wang, Rajeev et al. 2008; Nelson and Wang 2010). The family of miR-200 has been studied in drosophila where a mutation in the miR-200a/b ortholog leads to behavioral deficits and increased apoptosis and HDAC activity within the brain (Karres, Hilgers et al. 2007). MiR-200c levels are increased in the hippocampus and medial frontal gyrus in AD (Cogswell, Ward et al. 2008), whereas miR-200a levels are increased in peripheral blood mononuclear cells of patients with AD (Schipper, Maes et al. 2007). Thus, dysregulated miRNA expression combined with compromised regulatory crosstalk between miRNAs

and histone-modifying proteins like SIRT1 may contribute to abnormal expression of pathogenic genes in AD.

1.5.3 Histone Modifications in AD

Learning and memory were first linked to histone acetylation when it was demonstrated that acetylation of histones is altered when rats undergo memory consolidation (Schmitt and Matthies 1979). Later studies demonstrated that specific forms of learning correlate with increased HAT activity (Swank and Sweatt 2001), and histone acetylation (Levenson, O'Riordan et al. 2004). Since then, the therapeutic potential of HDAC inhibitors in AD was tested in a mouse model that allowed inducible overexpression of the p25 protein (CK-p25 mice) (Fischer, Sananbenesi et al. 2005), a pathological subunit of cdk5 that is dysregulated in human AD patients (Patrick, Zukerberg et al. 1999). Overexpression of p25 causes amyloid and tau pathology, severe neurodegeneration and memory impairment (Cruz, Tseng et al. 2003; Fischer, Sananbenesi et al. 2005; Cruz, Kim et al. 2006; Graff, Rei et al. 2012). Intraperitoneal administration of the HDAC inhibitor sodium butyrate for 4 weeks was able to reinstate learning behavior and restore retrieval of consolidated memories in CK-p25 mice. This correlated with synaptogenesis and rewiring of the neuronal network suggest neuroprotective actions of HDAC inhibition (Fischer, Sananbenesi et al. 2007).

Epigenetic alterations have been suggested to be a major force of aging (Chouliaras, Hove et al. 2012; Heyn, Li et al. 2012; Chouliaras, Mastroeni et al. 2013) which is the most predominant risk factor for AD (2015). Histone modifications have been widely implicated in the phenotypic alterations that occur during cellular senescence

and the aging of various organisms (Wilson and Jones 1983; Bandyopadhyay and Medrano 2003; Liu, Wylie et al. 2003; Fraga and Esteller 2007), and may provide a link between aging and AD. Histone acetylation mechanisms, particularly those involving the Sir2 family of histone deacetylases, have been linked to aging and senescence in yeast and invertebrates (Bandyopadhyay and Medrano 2003). However, it is not understood how the molecular processes of aging predispose to AD, or become dysregulated in AD. A recent study compared genome-wide enrichment of H4k16ac in the lateral temporal lobe of AD individuals compared to younger and elderly cognitively normal controls and found that while normal aging leads to increased H4k16ac, in AD loss of H4k16ac is found in proximity to genes linked to aging and AD (Nativio, Donahue et al. 2018). An association was discovered between the genomic locations of significant H4k16ac changes with genetic variants identified in genome-wide association studies. These data are congruent with analyses of histone acetylation in mouse models of AD, in which loss of acetylation occurs at neuronal genes (Graff, Rei et al. 2012)

Manipulation of histone tail acetylation has been investigated in several animal models of AD using HDAC inhibitors. For example, it has been reported that after fear conditioning training in APP/PS1 mice, levels of hippocampal acetylated histone 4 (H4) were about 50% lower than in wild-type littermates (Francis, Fa et al. 2009). Treatment with the HDAC inhibitor Trichostatin A increased the levels of acetylated H4 and contextual freezing performance to wild-type levels (Francis, Fa et al. 2009). Treatment with HDAC inhibitors has also been shown to induce sprouting of dendrites, increase the number of synapses, and reinstate learning behavior and access to long-term memories in

CK-p25 transgenics (Fischer, Sananbenesi et al. 2007). In a cortical neuron culture model, overexpression of APP resulted in a decrease in histone 3 and histone 4 acetylation, as well as a decrease in CREB-binding protein levels (Lonze and Ginty 2002; Rouaux, Jokic et al. 2003).

Additionally, a targeted proteomics approach in human brains showed reduction of H3k18ac and H3k23ac in AD (Zhang, Schrag et al. 2012). H4k16ac changes between aging and AD revealed that changes during aging and changes during disease are negatively correlated. In addition to histone acetylation, histone 3 trimethylation on lysine 4 (H3k4me3) not only plays a role in chromatin structure regulation and gene expression but is ectopically located in the neuronal cytoplasm in AD (Mastroeni, Delvaux et al. 2015). These authors observed increasing cytoplasmic localization of H3k4me3 with increasing Braak stage, and ectopic localization preceded the early tau phosphorylation markers MC1 and PG5 (Mastroeni, Delvaux et al. 2015). These data suggest that AD is a state of dysregulated aging that may induce specific transcriptional and chromatin structural changes.

In addition to histone acetylation, histone deacetylation has been indirectly studied in a handful of studies by examination of HDAC levels in the AD cortex. Class I and II HDACs are the best characterized in the AD brain, however, results measuring HDAC protein levels examined in the medial temporal lobe memory circuit, which displays tau pathology early in the onset of AD (Braak and Braak 1991), have been inconsistent across studies. For example, immunohistochemical analysis of entorhinal cortex neurons containing HDAC1 and HDAC2 (Dawson and Kouzarides 2012; Graff

and Tsai 2013; Volmar and Wahlestedt 2015), revealed that levels of both these proteins are decreased in the entorhinal cortex (Mastroeni, Grover et al. 2010), while HDAC2 but not HDAC1 or HDAC3 was increased in CA1 hippocampal and entorhinal cortex nuclei in AD compared to non-cognitively impaired aged controls (Graff, Rei et al. 2012). The same study found enrichment of HDAC2 at the promoter and coding regions of genes important for learning and memory including synaptophysin (*Svp*), synaptotagmin (*Stg*), brain-derived nerve growth factor (*Bdnf*), immediate early gene *Arc*, and cyclin dependent kinase 5 (*Cdk5*) (Graff, Rei et al. 2012). Knockdown of HDAC2 levels using short hairpin RNA in a mouse model of neurodegeneration increased H4k12 acetylation and rescued expression of these genes (Graff, Rei et al. 2012). Similar to results reported by Mastroeni and colleagues (Mastroeni, Grover et al. 2010), a recent mass spectrometry study demonstrated a reduction of HDAC1 expression in the AD frontal cortex and the retina compared to age-matched controls (Anderson, Chen et al. 2015).

HDACs 4 and 6, are predominantly cytosolic deacetylases, and have histone and non-histone targets in the AD brain (Ding, Dolan et al. 2008; Gao, Hubbert et al. 2010; Shen, Chen et al. 2016). HDAC4 is upregulated by endoplasmic reticulum stress and accumulates in the nuclei of neurons in the frontal cortex and hippocampus when dephosphorylated in AD (Shen, Chen et al. 2016). The same study observed a parallel increase in H3k27me3 and the appearance of cell cycle proteins including cyclin A2 in the same regions (Shen, Chen et al. 2016). HDAC5 expression levels in the AD frontal cortex are increased, but little is known about HDAC5's function in AD (Anderson, Chen et al. 2015). HDAC6 is involved in autophagic regulation (Pandey, Taylor et al. 2007),

mitochondrial transport (Chen, Owens et al. 2010), and facilitation of tau hyperphosphorylation (Ding, Dolan et al. 2008; Perez, Santa-Maria et al. 2009). Acetylated alpha-tubulin, which serves as a marker of stable microtubules, is reduced in neurons in the AD brain (Ding, Dolan et al. 2008). Ding and collaborators observed that HDAC6 levels increased by 52% in the cortex and by 91% in the hippocampus of AD patients relative to controls, and that the acetylation of alpha-tubulin showed a corresponding decrease in AD patients (Ding, Dolan et al. 2008). These findings suggest that HDAC6 decreases the level of acetylated alpha-tubulin and subsequently reduces the stability of microtubules, which are a crucial component of the cytoskeleton and transport system and are dysregulated in AD. HDAC6 overexpression in AD disturbs mitochondrial transport, probably in a glycogen synthase kinase 3ß(GSK3ß)-dependent manner (Chen, Owens et al. 2010). One study showed that HDAC6 regulated mitochondrial transport in hippocampal neurons, depending on the status of GSK3ß. GSK3ß is one of the major kinases that phosphorylates tau. GSK3ß also interacts with HDAC6, increasing the phosphorylation of HDAC6 at Ser22 and impairing the microtubule-based transport of mitochondria (Chen, Owens et al. 2010).

Hyperphosphorylated tau collapses the transport system in neurons via microtubule disintegration (Mietelska-Porowska, Wasik et al. 2014). Both HDAC6 and tau proteins are associated with microtubules, and it was reported that they can also interact with each other (Ding, Dolan et al. 2008; Perez, Santa-Maria et al. 2009). Reports indicate that HDAC6 interacts with tau protein *in vitro*, *in situ*, and in the human brain (Ding, Dolan et al. 2008) and that tau acts as an HDAC6 deacetylase inhibitor (Perez,

Santa-Maria et al. 2009). Tubacin can attenuate tau phosphorylation by inhibiting HDAC6; however, the underlying mechanism of this site-specific effect is not understood. In addition, evidence suggests that the HDAC6-PP1 (Protein phosphatase 1) complex reduces the dephosphorylation activity of PP1 on tau. In a recent study, it was reported that tau is acetylated by HAT p300 in an AD mouse model, and that acetylated tau protein was significantly reduced by SIRT1 overexpression; in contrast, HDAC6 overexpression did not significantly reduce levels of acetylated tau (Min, Cho et al. 2010).

SIRT1 protein and mRNA levels are decreased in the parietal cortex but not in the cerebellum (Julien, Tremblay et al. 2009). In the hippocampus, SIRT1 transcripts are downregulated in the CA1 and CA3 subfields, but not in the dentate gyrus. Hippocampal CA1 and CA3 subregions are the target site of entorhinal cortex projecting neurons, which are among the first to develop neurofibrillary tangles in AD (Braak and Braak 1991). Clinical molecular pathological investigations have shown that cortical SIRT1 levels correlate with global cognitive score, episodic memory and perceptual speed test scores, disease duration, and tau accumulation (Julien, Tremblay et al. 2009) suggesting a key role in the pathogenesis of cognitive dysfunction in AD. This study also revealed that individuals with MCI did not show a decrease in SIRT1 but there was a significant loss of SIRT1 in patients with the highest indices of AD neuropathology. Transgenic mice that overexpress SIRT1 display improved glucose homeostasis and increased metabolic rates (Bordone, Cohen et al. 2007), two processes suggested to be dysregulated in AD (Pasinetti and Eberstein 2008). More specifically, a reduction of SIRT1

deacetylation could limit the capacity of AcetylCoA synthetase to generate AcetylCoA, a key molecule in cellular metabolism and production of acetylcholine (Hallows, Lee et al. 2006). Additional evidence from experiments in cultured neurons suggests that decreased SIRT1 activity accelerates neurodegeneration by upregulating nicotinamide mononucleotide adenylyl-transferase1 activity (Araki, Sasaki et al. 2004) or by repressing p25-mediated cell death (Kim, Nguyen et al. 2007). Another target of SIRT1 deacetylation is the mitochondrial deacetylase SIRT3 (Kwon, Seok et al. 2017). Frontal cortex SIRT3 mRNA and protein are significantly reduced and are associated with altered mitochondrial respiratory activity and neuronal damage in AD (Lee, Kim et al. 2018). Levels of mitochondrial SIRT3 are inversely correlated with mitochondrial p53 levels in the AD cortex, suggesting that mitochondrial SIRT3 and p53 alterations contribute to AD pathogenesis (Lee, Kim et al. 2018). Thus, numerous alterations to HDAC and SIRT levels are present in the AD cortex, are highly interactive, and affect many biological pathways dysregulated during the disease process.

While there is strong evidence that HDAC and SIRT proteins are dysregulated in cortical and hippocampal regions in AD, whether these proteins are altered in basocortical cholinergic neurons and are associated with cognitive function and neuropathological criteria remain unknown. Given the importance of this cholinergic projection system in working memory, executive function, and attention (Baxter and Chiba 1999; Ballinger, Ananth et al. 2016; Maurer and Williams 2017; Blake and Boccia 2018), the numerous studies demonstrating its early selective vulnerability in AD (Vana, Kanaan et al. 2011; Mesulam 2013; Schmitz and Spreng 2016; Tiernan, Mufson et al.

2018), and evidence that enhancement of cholinergic transmission is one of the only drug therapies approved by the FDA shown to be clinically useful in the treatment of AD, (Cavedo, Dubois et al. 2016; Cavedo, Grothe et al. 2017; Hampel, Mesulam et al. 2018), identification of HDAC and SIRT dysregulation in basocortical cholinergic neurons and their role in the onset and pathogenesis of dementia is of paramount interest in the AD drug therapy space. The following series of clinical pathological investigations examine the role that epigenetics plays in the degeneration of CBF neurons and their relation to cognitive and neuropathological endpoints during the prodromal stages of AD.

CHAPTER 2

FRONTAL CORTEX EPIGENETIC DYSREGULATION DURING THE PROGRESSION OF ALZHEIMER'S DISEASE

2.1 ABSTRACT

Although the frontal cortex plays an important role in cognitive function and undergoes neuronal degeneration in Alzheimer's disease (AD), the factors driving these cellular changes remain unknown. Recent studies suggest that alterations in epigenetic regulation play a pivotal role in this process in AD. We evaluated frontal cortex histone deacetylase (HDAC) and sirtuin (SIRT) levels in tissue obtained from subjects with a premortem diagnosis of no cognitive impairment (NCI), mild cognitive impairment (MCI), mild to moderate AD (mAD) and severe AD (sAD) using quantitative Western blotting. Immunoblots revealed significant increases in HDAC1 and HDAC3 in MCI and mAD, followed by a decrease in sAD compared to NCI. HDAC2 levels remained stable across clinical groups. HDAC4 was significantly increased in MCI and mAD, but not in sAD compared to NCI. HDAC6 significantly increased during disease progression, while SIRT1 decreased in MCI, mAD, and sAD compared to NCI. HDAC1 levels negatively correlated with perceptual speed, while SIRT1 positively correlated with perceptual speed, episodic memory, global cognitive score and mini-mental state examination. HDAC1 positively, while SIRT1 negatively correlated with cortical neurofibrillary tangle (NFT) counts. These findings suggest that dysregulation of epigenetic proteins contribute to neuronal dysfunction and cognitive decline in the early stages of AD.

2.2 INTRODUCTION

Alzheimer's disease (AD) is an irreversible progressive neurodegenerative disorder resulting in cognitive decline, with an enormous societal cost (Wimo, Guerchet et al. 2017). With the rapidly expanding elderly population in the USA and other countries, understanding the cellular and molecular mechanism(s) driving the onset of AD are of paramount importance. AD-related cognitive decline is manifest by deficits in working memory and executive function, memory modalities associated with the prefrontal cortex (Salat, Kaye et al. 2001; Levine, Lu et al. 2015). The frontal cortex is a major hub of the dorsal memory network (DMN) that displays extensive amyloid pathology associated with the onset of cognitive decline early in AD (Buckner, Snyder et al. 2005; Buckner, Sepulcre et al. 2009; Simic, Babic et al. 2014). However, the underlying cellular and molecular mechanism(s) driving frontal cortex neuronal dysfunction remain unknown. Recent studies have linked epigenetic modifications including DNA methylation and posttranslational modifications of histone proteins (Bredy, Wu et al. 2007; Kouzarides 2007; Graff and Tsai 2013; Volmar and Wahlestedt 2015), to cognitive impairment and synaptic plasticity in the medial temporal memory circuit (i.e., entorhinal cortex and hippocampus) (Bredy, Wu et al. 2007; Graff, Rei et al. 2012; Kosik, Rapp et al. 2012). By contrast, there are virtually no epigenetic studies of frontal cortex protein levels and their relation to clinical measures of cognitive performance and neuropathological criteria during AD progression.

Recently, research exploring the potential contribution of epigenetic proteins, regulators of gene expression not associated with modifications to DNA sequence (Dawson and Kouzarides 2012; Graff and Tsai 2013), has been of great interest in the

field of AD. Histone acetylation, a posttranslational epigenetic process, is regulated by the opposite actions of histone acetyltransferases (HATs), and histone deacetylases (HDACs), which provide or block access to cellular transcriptional machinery, resulting in the tight control of gene expression (Mastroeni, Grover et al. 2011; Dawson and Kouzarides 2012; Graff and Tsai 2013; Volmar and Wahlestedt 2015). HDACs, including sirtuins (SIRTs), are a family of enzymes with deacetylase activity that have been linked to learning and memory (Guan, Haggarty et al. 2009; McQuown, Barrett et al. 2011; Bahari-Javan, Maddalena et al. 2012; Graff, Rei et al. 2012; Gupta-Agarwal, Franklin et al. 2012; Kim, Akhtar et al. 2012; Graff and Tsai 2013) and AD pathogenesis (Ding, Dolan et al. 2008; Julien, Tremblay et al. 2009; Kumar, Chaterjee et al. 2013; Shen, Chen et al. 2016; D'Addario, Candia et al. 2017). Interestingly, monozygotic twins with identical genetic information display discordant outcomes for AD, with decrements in DNA methylation found in neurons of the temporal cortex of the AD twin (Poulsen, Esteller et al. 2007; Mastroeni, McKee et al. 2009), suggesting that alterations of the epigenome may mediate molecular pathways that contribute to AD pathogenesis.

Although HDAC protein levels have been examined in the medial temporal lobe memory circuit, which displays tau pathology early in the onset of AD (Braak and Braak 1991), the results have been inconsistent across studies. For example, immunohistochemical analysis of entorhinal cortex neurons containing HDAC1 and HDAC2, nuclear enzymes associated with transcriptional complexes and modulation of chromatin plasticity (Dawson and Kouzarides 2012; Graff and Tsai 2013; Volmar and Wahlestedt 2015), revealed that levels of both these proteins are decreased in the

entorhinal cortex (Mastroeni, Grover et al. 2010), while HDAC2 but not HDAC1 or HDAC3 was increased in CA1 hippocampal and entorhinal cortex nuclei in AD compared to non-cognitively impaired aged controls (Graff, Rei et al. 2012). A recent study demonstrated a reduction of HDAC1 expression in the AD frontal cortex compared to age-matched controls using mass spectrometry (Anderson, Chen et al. 2015). Others have examined HDACs 4 and 6, which are predominantly cytosolic deacetylases, with histone and non-histone targets in the AD brain (Ding, Dolan et al. 2008; Gao, Wang et al. 2010; Shen, Chen et al. 2016). HDAC4 is upregulated by endoplasmic reticulum stress and accumulates in the nuclei of neurons in the frontal cortex when dephosphorylated in AD (Shen, Chen et al. 2016). HDAC6 is involved in autophagic regulation (Pandey, Nie et al. 2007; Pandey, Taylor et al. 2007), mitochondrial transport (Chen, Owens et al. 2010), facilitation of tau hyperphosphorylation (Ding, Dolan et al. 2008; Perez, Santa-Maria et al. 2009), and is increased the cortex in animal models of AD and the human condition (Ding, Dolan et al. 2008). SIRT1 protein and mRNA levels were decreased in the parietal cortex but protein levels were not altered in the hippocampus or cerebellum. Parietal cortex SIRT1 levels correlated with global cognition test scores and tau accumulation (Julien, Tremblay et al. 2009). Together these findings suggest that members of the HDAC family are dysregulated in cortical regions related to cognitive impairment and neurofibrillary tangle (NFT) pathology in AD. However, to our knowledge no report has examined HDAC and SIRT protein levels in the frontal cortex obtained from cognitively and neuropathologically well-characterized cases during the

progression of AD, and more importantly, subjects classified with mild cognitive impairment (MCI) a prodromal AD stage (Petersen 2004).

Thus, the aim of the current study was to identify alterations in HDAC and SIRT1 protein levels and their association with cognitive test scores, neuropathological criteria and demographic variables in the frontal cortex during the progression of AD. HDAC protein levels were examined in frontal cortex samples obtained from individuals who died with an antemortem clinical diagnosis of no cognitive impairment (NCI), mild cognitive impairment (MCI), mild/moderate AD (mAD), and severe AD (sAD). Information from this study will inform the use of HDAC inhibitors as disease modifying therapeutics in pre-symptomatic AD.

2.3 METHODS

2.3.1 Subjects

Frozen frontal cortex tissue was obtained from individuals who died with an ante-mortem clinical diagnosis of NCI (n=14), MCI (n=13), and mild/moderate AD (n=13) from the Rush Religious Orders study (RROS), a longitudinal clinicopathological study of aging and AD in Catholic nuns, priests, and brothers (Mufson, Chen et al. 1999; Bennett, Schneider et al. 2005; Bennett, Schneider et al. 2006). Additional cases with a diagnosis of severe AD (n=8) were obtained from the Rush Alzheimer's Disease Center (RADC). The Human Research Committees of Rush University Medical Center approved this study and written informed consent for research and autopsy was obtained from the participants or their family/guardians.

2.3.2 Clinical and Neuropathologic Evaluations

Details of the clinical evaluation of the RROS cohort have been previously reported (Mufson, Chen et al. 1999; Bennett, Schneider et al. 2005; Mufson, He et al. 2012; Perez, Getova et al. 2012). Briefly, a team of investigators led by a neurologist performed annual neurological examinations and a cognitive battery in addition to reviewing each subject's medical history. The average time from the last clinical evaluation to death was ~8 months. Neuropsychological testing included the mini-mental state examination (MMSE), global cognitive score (GCS), a composite z-score compiled from a battery of 19 cognitive tests (Mufson, Chen et al. 1999), including episodic memory z-score, semantic memory z-score, working memory z-score, perceptual speed z-score, and visuospatial ability z-score (Wilson, Beckett et al. 2002). Subjects with MCI had cognitive impairment insufficient to meet criteria for dementia (Bennett, Wilson et al. 2002). Among the MCI cases, 3 were amnestic and 10 were non-amnestic. A final clinical diagnosis was assigned after a team of neurologists and neuropsychologists reviewed the clinical data. Neuropathological diagnosis was based on Braak staging of NFTs (Braak and Braak 1991), National Institute on Aging (NIA) Reagan criteria (Newell, Hyman et al. 1999), and recommendations of the Consortium to Establish a Registry for Alzheimer's disease (CERAD) (Mirra 1997). Neuritic plaque (NP), diffuse plaque (DP), and neurofibrillary tangle (NFT) counts in the mid-frontal cortex were obtained from modified Bielschowsky silver stained sections (6 μm) (Schneider, Aggarwal et al. 2009). Counts for amyloid density in the mid-frontal cortex, anterior cingulate, and superior frontal gyrus were obtained from sections (20μm) stained with the

anti-β-amyloid (Aβ) antibody 4G8 (1:9000, Covance, WI, USA) (Bennett, Schneider et al. 2004). Cases with mixed pathologies (e.g. stroke, Parkinson's disease, Lewy body dementia, vascular dementia and hippocampal sclerosis) were excluded.

2.3.3 Antibodies

Table 2.1 summarizes the antibodies used, respective dilution, and specificity. Rabbit polyclonal antibodies raised against HDAC1 (1:500, Abcam, Cambridge, MA) (Poleshko, Palagin et al. 2008; Rashid, Pilecka et al. 2009; Mastroeni, Grover et al. 2010; Bicknell, Walker et al. 2011; Slack, LE et al. 2011; Lutz, Fitzner et al. 2016), HDAC2 (1:500, Abcam) (Saito, Nagai et al. 2006; Burd, Kinyamu et al. 2008; Poleshko, Palagin et al. 2008; Fritah, Col et al. 2009; Lee, Murthy et al. 2011), HDAC3 (1:500, Abcam) (Chuang, Wu et al. 2013; Huang, Langdon et al. 2016), HDAC4 (1:500, Abcam) (Gupta, Samant et al. 2008; Ronn, Volkov et al. 2013), HDAC6 (1:500, Cell Signaling, Danvers, MA) (Pernet, Faure et al. 2014; Ratti, Ramond et al. 2015; Pujol Lopez, Kenis et al. 2016), SIRT1 (1:500, Cell Signaling) (Ringholm, Bienso et al. 2011; van Gent, Di Sanza et al. 2014; Bao, Zheng et al. 2016), and a mouse monoclonal antibody for β-tubulin (1:2000, Sigma, St. Louis, MO) were used for western blotting experiments.

Antigen	Description of Immunogen	Source, Host Species, Cat. #	Dilution	Published antibody specificity	Reference in text
HDAC1	Synthetic peptide conjugated to KLH derived from within residues 450 to the C-terminus of Human HDAC1.	Abcam, rabbit polyclonal, ab19845	1:500	Human tissue, WB; IHC-P	Lutz et al., 2016; Slack et al., 2011; Bicknell et al., 2011; Mastroeni et al., 2010; Rashid et al., 2009; Poleshko et al., 2008;
HDAC2	Synthetic peptide conjugated to KLH derived from within residues 450 to the C-terminus of Human HDAC2.	Abcam, rabbit polyclonal, ab16032	1:500	Human tissue; WB	Lee et al., 2011; Fritah et al., 2009; Poleshko et al., 2008; Burd et al., 2008; Saito et al., 2006
HDAC3	Synthetic peptide corresponding to Human HDAC3 amino acids 411-428 conjugated to Keyhole Limpet Haemocyanin (KLH).	Abcam, rabbit polyclonal, ab32369	1:500	Human tissue; WB, IHC-P	Huang et al., 2016; Chuang et al., 2013
HDAC4	Synthetic peptide to amino acids 1-19 of Human HDAC4 conjugated to KLH with C-terminal added lysine.	Abcam, rabbit polyclonal, ab12172	1:500	Human and mouse tissue; WB	Ronn et al., 2013; Gupta et al., 2008
HDAC6	Synthetic peptide corresponding to residues surrounding Pro681 of human HDAC6 protein.	Cell Signaling, rabbit monoclonal, D21B10	1:500	Mouse tissue; WB	Pujol Lopez et al., 2016; Ratti et al., 2015; Pernet et al., 2014
SIRT1	Synthetic peptide corresponding to the carboxy terminus of human SIRT1	Cell Signaling, rabbit polyclonal, D739	1:1000	Human and mouse tissue; WB	Bao et al., 2016; van Gent et al., 2014; Ringholm et al., 2011

Table 2.1 Summary of Antibodies

Antibodies used for western blotting, their respective dilution, and published specificity. WB, Western blot; IHC-P, Immunohistochemistry-paraffin.

2.3.4 Quantitative Immunoblotting

Frozen tissue samples from the frontal cortex were denatured in sodium dodecyl sulfate (SDS) loading buffer to a final concentration of 5 mg/ml. Proteins (50 μg/sample) were separated by 4-20% SDS-PAGE (Lonza, Rockland, ME) and transferred to polyvinylidene fluoride membranes (Immobilon P, Millipore, Billerica, MA) electrophoretically (Counts, Nadeem et al. 2004; Mufson, He et al. 2012). Membranes were first blocked in Tris-buffered saline (TBS)/0.05%Tween-20/5% milk for 60 minutes at room temperature and primary antibodies against HDAC1, HDAC2, HDAC3, HDAC4, HDAC6, and SIRT1 were added to the blocking buffers. Membranes were incubated at room temperature for 30 minutes; and then incubated overnight at 4°C. After washes (TBS/0.05% Tween-20), membranes were incubated for 1 hour at room temperature with horseradish peroxidase-conjugated goat anti-rabbit and anti-mouse IgG secondary antibodies (1:5,000 and 1:3,000, respectively). Immunoreactivity was visualized by enhanced chemiluminescence (Pierce, Rockford, IL) on a Kodak Image Station 440CF (Perkin-Elmer, Wellesley, MA) and bands quantified with Kodak 1D. Frontal cortex protein immunoreactive signals were normalized to β-tubulin signals. Samples were analyzed in three independent experiments, and only one band was visualized at the appropriate kilodalton (kDa) weight for each antibody. Controls included elimination of primary antibodies and a non-specific IgG.

2.3.5 Statistical Analysis

The Kruskal-Wallis test was used to detect differences between clinical groups in the protein levels, age at death, education, post-mortem interval (PMI), brain weight at

autopsy, and time between last clinical assessment and autopsy. The Conover-Iman test was used to discern group pair-wise comparisons that were statistically significant. Chi-square analysis was used to determine significance of frequency differences for gender, APOE ε4 allele status, Braak stage, CERAD diagnosis, and NIA-Reagan diagnosis present between clinical groups. Spearman correlations were used to assess associations between protein levels and age at death, education, PMI, brain weight at autopsy, time between last clinical assessment and autopsy, along with cognitive variables, count data for diffuse plaques (DP), neuritic plaques (NP), NFTs, and amyloid load in the frontal cortex, anterior cingulate, and superior frontal gyrus. Within-group differences among the deacetylases were tested using the Wilcoxon signed-rank test. Within each of the clinical groups, HDAC and SIRT1 differences between low and high Braak stages were assessed using the Mann-Whitney test. For correlation analyses, false discovery rate (FDR) was used to correct for multiple comparisons (Benjamini and Hochberg 1995; Glickman, Rao et al. 2014). All p-values were corrected for multiple comparisons to avoid the risk of Type I error. Statistical significance was set at $p < 0.05$ (two-tailed) and measurements were graphically represented using Sigma Plot 12.5 software (Systat Software, San Jose, CA). A power analysis showed that a correlation of $r = 0.40$ could be detected with 80% power (two-sided alpha = 0.05) using a sample size of 46. Given the sample size of $n = 48$ for this study, there was adequate statistical power for our studies. Statistical analyses were carried out using SYSTat 13.0 (SYSTAT, Inc., San Jose, CA). G*Power 3.1 was used for the estimate of statistical power.

2.4 RESULTS

2.4.1 Case Demographics

Clinical, demographic, and neuropathological data for RROS individuals are presented in Tables 2.2 and 2.3. No statistically significant group differences were found for age at death ($p = 0.15$), education ($p = 0.67$), PMI ($p = 0.06$), brain weight at autopsy ($p = 0.15$), and time between last clinical assessment ($p = 0.48$) (Table 2.2). No significant differences were found in the frequencies of gender ($p = 0.98$), APOE ε4 carrier status ($p = 0.28$), Braak stage ($p = 0.87$), CERAD diagnosis ($p = 0.50$), and NIA-Reagan diagnosis ($p = 0.34$) (Table 2.2). Among the cognitive variables (Table 2.3), the MMSE showed significant group differences as the NCI and MCI groups had significantly higher scores than the mAD group ($p < 0.001$). However, the NCI and MCI groups were not significantly different. A similar pattern was noted for the perceptual speed domain (Table 2.3) (NCI>mAD and MCI>mAD $p < 0.001$, NCI vs MCI $p = 0.07$). For GCS and episodic memory, significant group differences were noted for all group pair-wise comparisons ($p < 0.001$) (Table 2.3). Neuropathology revealed that 69% of mAD, 85% MCI, and 79% of NCI subjects were Braak stages III-VI. Using the NIA-Reagan criteria, 50% of NCI, 46% of MCI, and 69% of mAD cases were classified as intermediate to high likelihood of AD (Table 2.2). The CERAD diagnosis revealed that 43% of NCI, 23% of MCI, and 54% of mAD cases were probable or definite AD.

	NCI	MCI[a]	mAD	p-value
Number	14	13	13	-
Gender (M/F)	6/8	6/7	6/7	0.98[c]
ApoE ε4 (Carrier/Non-Carrier)	1/13	4/9	2/10[d]	0.28[c]
Age at Death (years)	85.07±4.34	86.63±5.18	88.35±4.75	0.15[b]
Education (years)	17.21±4.00	17.31±3.12	18.46±4.27	0.67[b]
PMI (hours)	5.77±2.13	5.97±2.27	4.42±2.27	0.06[b]
Brain Weight at Autopsy	1,223.00±88.80	1194.77±144.71	1132.46±108.44	0.15[b]
Duration between last clinic visit and autopsy (years)	0.70±0.83	0.92±0.98	0.77±0.54	0.48[b]
Braak Stage				
0	0	0	0	
I	2	1	2	
II	1	1	2	0.87[c]
III	6	5	2	
IV	4	4	4	
V	1	2	3	
VI	0	0	0	
CERAD Diagnosis				
No AD	4	5	2	
Possible AD	4	5	4	0.50[c]
Probable AD	3	1	1	
Definite AD	3	2	6	
NIA Reagan Diagnosis				
Not AD	0	0	0	
Low Likelihood	7	7	4	0.34[c]
Intermediate Likelihood	7	4	6	
High Likelihood	0	2	3	

Table 2.2 Clinical, Demographic, and Neuropathological Characteristics by Clinical Diagnosis

AD, Alzheimer's disease; ApoE, apolipoprotein E; CERAD, Consortium to Establish a Registry for Alzheimer's Disease; PMI, Postmortem Interval; MCI, mild cognitive impairment; MMSE, Mini-Mental State Examination; NCI, no cognitive impairment; NIA, National Institute on Aging. [a]n=3 MCI cases were amnestic. [b]Kruskal-Wallis test, with Conover-Inman test for multiple comparisons. [c]Chi-square test. [d]One mAD case did not have ApoE genotype information.

Neuropsychological tests	NCI	MCI	mAD	*p* Value[a]	Groupwise Comparisons
MMSE	28.14±1.35	27.23±2.68	20.08±5.57	<0.001	NCI, MCI>mAD
GCS (z-score)	0.03±0.26	-0.44±0.38	-1.19±0.60	<0.001	NCI>MCI>mAD
Episodic Memory (z-score)	0.47±0.28	-0.25±0.46	-1.49±0.89	<0.001	NCI>MCI>mAD
Semantic Memory (z-score)	-0.18±0.77	-0.40±0.60	-0.83±0.87	0.09	-
Working Memory (z-score)	-0.13±0.48	-0.34±0.68	-0.59±0.63	0.22	-
Perceptual Speed (z-score)	-0.43±0.75	-0.98±0.61	-2.21±0.80	<0.001	NCI, MCI>mAD
Visuospatial (z-score)	-0.35±0.60	-0.85±0.69	-0.99±0.71	0.07	-

Table 2.3 Summary of Neuropsychological Tests by Clinical Diagnosis Category

Values represent mean ± SD. [a]Kruskal-Wallis test, with Conover-Inman test for multiple comparisons. AD, Alzheimer's disease; GCS, Global Cognitive Score; MMSE, Mini-Mental State Examination; MCI, mild cognitive impairment; NCI, no cognitive impairment.

The RADC sAD group had an average age at death of 78.75 ± 5.23 years (range 71-86), 63% were female, average PMI was 5.08 ± 1.45 hours (range 2-6.4) and average brain weight at autopsy was 1,105.71 ± 98.30 grams (range 980-1220). The average MMSE score was 2.50 ± 3.50 (range 0-9). This group was evaluated for Braak stage and MMSE scores only. Data from all eight sAD cases were included in the boxplots and summary diagram but not in the demographic tables.

2.4.2 Frontal Cortex Epigenetic Protein Levels

Prompted by evidence linking dysregulated HDAC levels to AD pathogenesis, we utilized quantitative western blotting to investigate whether HDACs are altered in the frontal cortex, a key component of the dorsal memory network (Buckner, Sepulcre et al. 2009; Simic, Babic et al. 2014), during AD progression. We chose to evaluate HDACs from all three major classes, which display both nuclear and cytoplasmic subcellular locations. HDACs 1 and 2 are nuclear proteins involved in gene transcription, and have been implicated in dysregulation of genes involved in learning and memory (Guan, Haggarty et al. 2009; McQuown, Barrett et al. 2011; Bahari-Javan, Maddalena et al. 2012; Graff, Rei et al. 2012; Gupta-Agarwal, Franklin et al. 2012; Kim, Akhtar et al. 2012; Graff and Tsai 2013). HDAC1 levels (Table 2.4**,** Figure 2.1A) in the NCI, MCI, and mAD groups were significantly higher than the sAD group ($p < 0.05$, $p < 0.001$, $p < 0.001$, respectively), while HDAC2 levels were not significantly different between groups ($p = 0.63$; Table 2.4, Figure 2.1B). HDAC3 is primarily cytoplasmic but can shuttle between the nucleus and cytoplasm. HDAC3 levels (Table 2.4, Figure 2.2A) were significantly lower in the NCI than the MCI group ($p = 0.02$), while levels in the NCI,

MCI, and mAD groups were significantly higher than the sAD group ($p = 0.04$, $p < 0.001$, $p < 0.001$, respectively). HDAC4 is a cytoplasmic class II deacetylase, which can be translocated to the nucleus in neurodegenerative disease conditions such as AD (Shen, Chen et al. 2016). Cortical HDAC4 levels (Table 2.4, Figure 2.2B) in the MCI cases were significantly higher than the NCI ($p < 0.001$) and the mAD ($p = 0.04$) groups, whereas no significant changes were found between sAD and the other clinical groups. We also evaluated levels of a Class IIb deacetylase, HDAC6, which interacts with numerous cytoplasmic proteins. HDAC6 levels (Table 2.4, Figure 2.3A) in the sAD group were significantly higher than the NCI ($p < 0.001$) and the mAD ($p < 0.001$) groups, while MCI levels were significantly higher than the NCI group ($p = 0.01$). SIRT1 was the only class III deacetylase evaluated, due to its link to tau accumulation in AD (Julien, Tremblay et al. 2009). For SIRT1, the only groupwise comparison that was not statistically significant was the comparison between the mAD and sAD groups ($p = 0.18$; Figure 2.3B). All other comparisons were statistically significant (NCI > MCI, $p = 0.03$; NCI > mAD, $p < 0.001$; NCI > sAD, $p < 0.001$; MCI > mAD, $p = 0.02$) (Table 2.4, Figure 2.3B). Thus deacetylases from each class are dysregulated during the progression of AD, contributing to the complexity of frontal cortex epigenetic changes in AD.

	NCI (n=14)	MCI (n=13)	mAD (n=13)	sAD (n=8)	*p*-value[a]	Groupwise Comparisons
HDAC1	0.22±0.15 (0.08-0.58)	0.44±0.43 (0.04-1.61)	0.41±0.36 (0.08-1.09)	0.09±0.05 (0.03-0.19)	0.01	MCI>sAD; mAD>sAD
HDAC2	0.53±0.18 (0.32-1.01)	0.59±0.24 (0.28-1.05)	0.56±0.18 (0.33-0.90)	0.65±0.20 (0.33-0.94)	0.63	-
HDAC3	0.38±0.39 (0.05-1.18)	0.90±0.80 (0.06-2.68)	0.55±0.48 (0.04-1.51)	0.08±0.04 (0.02-0.14)	<0.001	NCI, MCI, mAD>sAD; NCI<MCI
HDAC4	0.12±0.03 (0.08-0.17)	0.21±0.13 (0.10-0.58)	0.13±0.06 (0.06-0.27)	0.14±0.05 (0.07-0.21)	0.03	NCI<MCI; MCI>mAD
HDAC6	0.08±0.03 (0.04-0.15)	0.12±0.05 (0.05-0.25)	0.10±0.04 (0.05-0.17)	0.14±0.02 (0.12-0.18)	<0.001	NCI<MCI; NCI, mAD<sAD
SIRT1	0.73±0.33 (0.05-1.18)	0.49±0.30 (0.02-0.77)	0.20±0.14 (0.03-0.43)	0.09±0.05 (0.01-0.18)	<0.001	NCI>MCI, mAD, sAD; MCI>mAD, sAD

Table 2.4 Clinical Group Differences for HDAC and SIRT1 Proteins

Values represent mean±standard deviation (range). NCI, no cognitive impairment; MCI, mild cognitive impairment; mAD, mild/moderate Alzheimer's disease; sAD, severe Alzheimer's disease. [a]Kruskal-Wallis test, with Conover-Inman test for multiple comparisons.

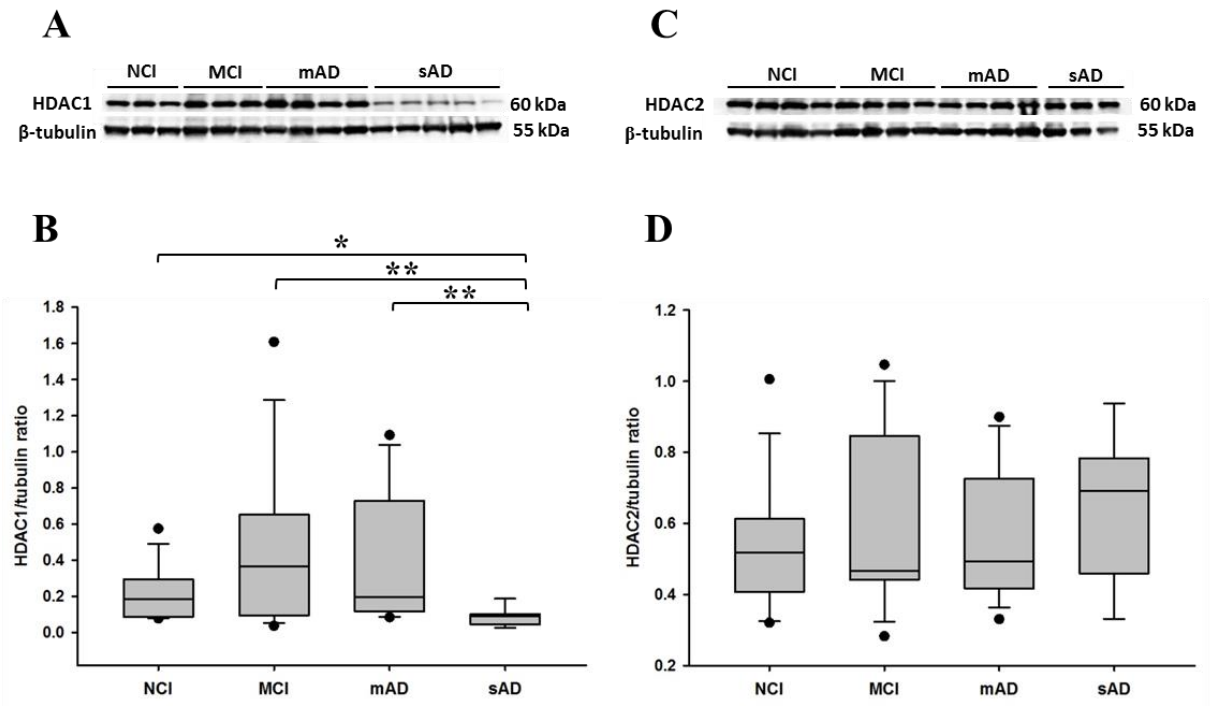

Figure 2.1 HDAC1 and HDAC2 Immunoblots and Boxplots

Representative immunoblots and boxplots of HDAC1 and HDAC2 frontal cortex levels in cases clinically diagnosed as non-cognitively impaired (NCI), mildly cognitively impaired (MCI), mild/moderate AD (mAD), and severe AD (sAD). Immunoreactive signals obtained by densitometry were normalized to levels of beta-tubulin. (A) HDAC1 levels were significantly decreased in sAD compared with NCI ($p < 0.05$), MCI ($p < 0.001$), and mAD ($p < 0.001$). (B) HDAC2 levels were stable across clinical groups. Black dots in box-plots indicate outliers. Single asterisk indicates a $p < 0.05$, double asterisks indicate a $p < 0.001$.

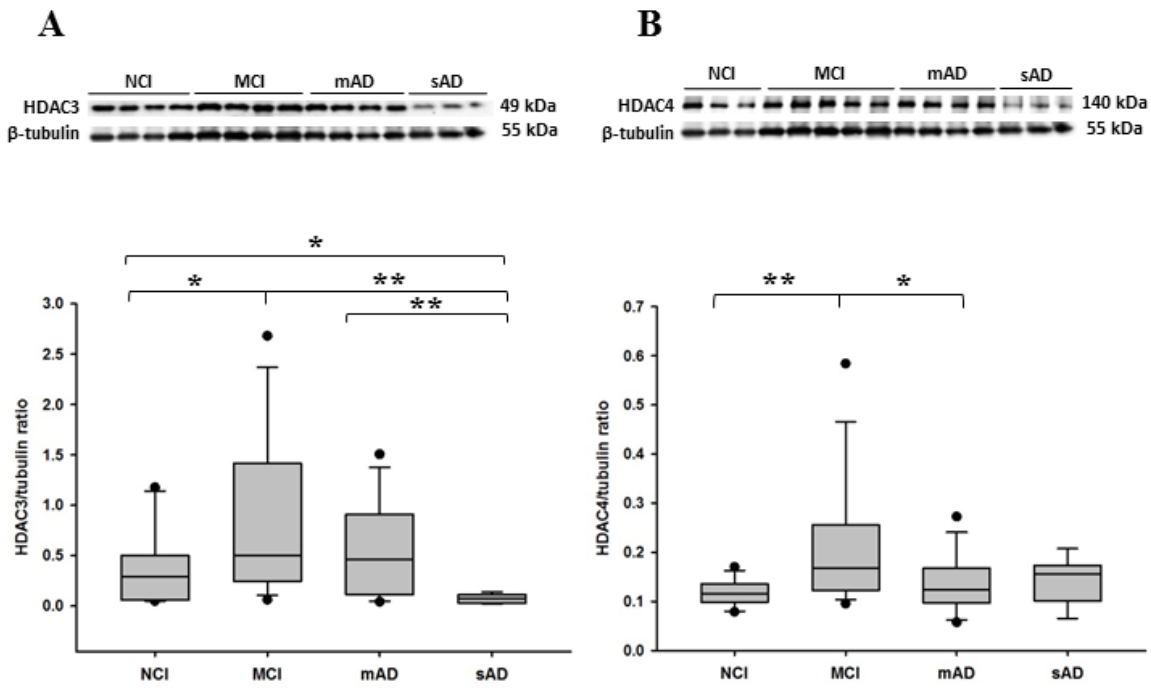

Figure 2.2 HDAC3 and HDAC4 Immunoblots and Boxplots

Representative immunoblots and boxplots of HDAC3 and HDAC4 frontal cortex levels in cases clinically diagnosed as non-cognitively impaired (NCI), mildly cognitively impaired (MCI), mild/moderate AD (mAD), and severe AD (sAD). Immunoreactive signals obtained by densitometry were normalized to levels of beta-tubulin. (A) HDAC3 levels were significantly increased in MCI compared to NCI ($p < 0.05$), and significantly decreased in sAD compared to NCI ($p < 0.05$) and MCI ($p < 0.001$). (B) HDAC4 levels were significantly increased in MCI compared to NCI ($p < 0.001$) and mAD ($p < 0.05$). Black dots in boxplots indicate outliers. Single asterisk indicates a $p < 0.05$, double asterisks indicate a $p < 0.001$.

We examined within-group differences between HDAC proteins across the four clinical groups to determine whether select HDACs are significantly upregulated across disease progression. Significant differences in HDACs were found in all four clinical groups ($p < 0.05$), with SIRT1 being the highest protein level in NCI, HDAC3 and HDAC2 the highest in MCI, mAD, and HDAC2 the highest in sAD (Table 2.5).

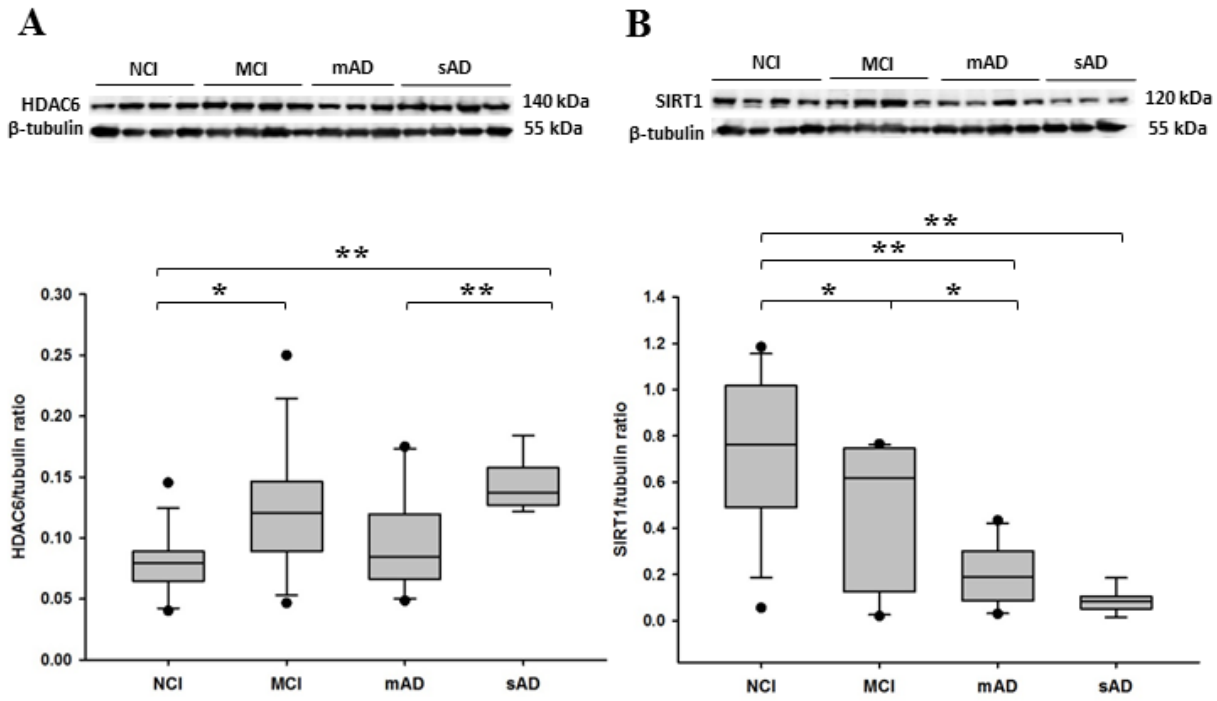

Figure 2.3 HDAC6 and SIRT1 Immunoblots and Boxplots

Representative immunoblots and boxplots of HDAC6 and SIRT1 frontal cortex levels in cases clinically diagnosed as non-cognitively impaired (NCI), mildly cognitively impaired (MCI), mild/moderate AD (mAD), and severe AD (sAD). Immunoreactive signals obtained by densitometry were normalized to levels of beta-tubulin. (A) HDAC6 levels were significantly increased in MCI compared to NCI, and mAD ($p < 0.05$), and were significantly increased in sAD compared to NCI, and mAD ($p < 0.001$). (B) SIRT1 levels were significantly higher in NCI compared to MCI ($p < 0.05$), mAD ($p < 0.001$), and sAD ($p < 0.001$), and in MCI compared to mAD ($p < 0.05$). Black dots in boxplots indicate outliers. Single asterisk indicates a $p < 0.05$, double asterisks indicate a $p < 0.001$.

Clinical Group	Protein Within-Group Comparisons
NCI	SIRT1>HDAC6, HDAC4, HDAC3, HDAC1; HDAC2>HDAC3, HDAC4, HDAC6; HDAC1>HDAC6; HDAC2>HDAC1; HDAC3>HDAC6
MCI	HDAC2>HDAC6, HDAC4, HDAC1; HDAC3>HDAC6, HDAC4, HDAC1; HDAC1>HDAC6; HDAC4>HDAC6; SIRT1>HDAC6
mAD	HDAC2> HDAC1, HDAC4, HDAC6, SIRT1; HDAC3> HDAC4, HDAC6, SIRT1; HDAC1>HDAC6, HDAC4>HDAC6; SIRT1>HDAC6
sAD	HDAC2>HDAC1, HDAC3, HDAC4, HDAC6, SIRT1; HDAC4>HDAC1, HDAC3, SIRT1; HDAC6> HDAC1, HDAC3, SIRT1

Table 2.5 Within-Group Significant Comparisons of HDAC Protein Differences

All within-group comparisons $p<0.05$. NCI, no cognitive impairment; MCI, mild cognitive impairment; mAD, mild/moderate Alzheimer's disease; sAD, severe Alzheimer's disease.

2.4.3 Association Between Biochemical, Clinical and Neuropathological Measures

Having established that frontal cortex HDAC levels are altered during disease progression, we next sought to identify their association to each other and to demographic, cognitive, and neuropathologic variables. Interprotein correlations and their association with cognitive measurements are shown in Tables 2.6 and 2.7, respectively. SIRT1 showed no correlation with any of the HDAC proteins (Table 2.6). Whereas HDAC1 and HDAC3 were moderately correlated (Figure 2.4A) ($r = 0.53$, $p < 0.001$), as well as HDAC2 and HDAC4 (Figure 2.4B) ($r = 0.40$, $p = 0.005$); and HDAC4 and HDAC6 (Figure 2.4C) ($r = 0.50$, $p < 0.001$) across clinical groups (Table 2.6). Given evidence that HDACs are involved in the aberrant expression of genes involved in learning, memory, and synaptic plasticity, we probed the association between cortical HDAC levels and cognitive measures in the RROS cases. After adjusting for multiple comparisons, HDAC1 and SIRT1 were the only proteins that significantly correlated with cognitive measures (Table 2.7). Levels of HDAC1 were negatively correlated with perceptual speed z-scores (Figure 2.5A; $r = -0.45$, $p = 0.004$), whereas SIRT1 was positively correlated with perceptual speed z-scores (Figure 2.5B; $r = 0.61$, $p < 0.001$). SIRT1 levels were moderately correlated with GCS (Figure 2.5C; $r = 0.40$, $p = 0.01$), episodic memory scores (Figure 2.5D; $r=0.36$, $p < 0.05$) and MMSE status (Figure 2.5E; $r = 0.37$, $p = 0.02$). Since SIRT1 and HDAC6 have been linked to tau accumulation and deacetylation (Hempen and Brion 1996; Julien, Tremblay et al. 2009; Perez, Santa-Maria et al. 2009; Cook, Gendron et al. 2012), respectively, we examined the association

between altered levels of HDACs and NFT counts in the frontal cortex between the NCI, MCI, and mAD groups.

	HDAC1	HDAC2	HDAC3	HDAC4	HDAC6	SIRT1
HDAC1		0.22	0.53[b]	0.09	-0.14	-0.07
HDAC2	0.22		-0.106	0.40[a]	0.25	-0.01
HDAC3	0.53[b]	-0.11		-0.14	-0.20	0.02
HDAC4	0.09	0.40[a]	-0.14		0.50[b]	0.14
HDAC6	-0.14	0.25	-0.20	0.50[b]		0.01
SIRT1	-0.07	-0.01	0.02	0.14	0.01	

Table 2.6 Summary of Interprotein Correlations

[a] $p = 0.005$, [b] $p < 0.001$

	MMSE	GCS	Episodic Memory	Semantic Memory	Working Memory	Visuospatial Ability	Perceptual Speed
HDAC1	0.04	-0.27	-0.26	-0.003	0.02	-0.03	-0.45[a]
HDAC2	0.26	-0.07	-0.13	0.11	-0.13	0.06	-0.12
HDAC3	-0.08	-0.21	-0.22	-0.04	-0.13	0.13	-0.25
HDAC4	0.09	-0.11	-0.19	0.07	-0.21	-0.11	-0.04
HDAC6	0.003	-0.09	-0.12	-0.07	0.04	0.01	-0.03
SIRT1	0.37[a]	0.40[a]	0.36[a]	0.24	-0.004	0.19	0.61[b]

Table 2.7 Correlations Between Neuropsychological tests and Protein Levels

[a] $p<0.05$, [b] $p<0.001$; GCS, Global Cognitive Score; MMSE, Mini-Mental State Examination.

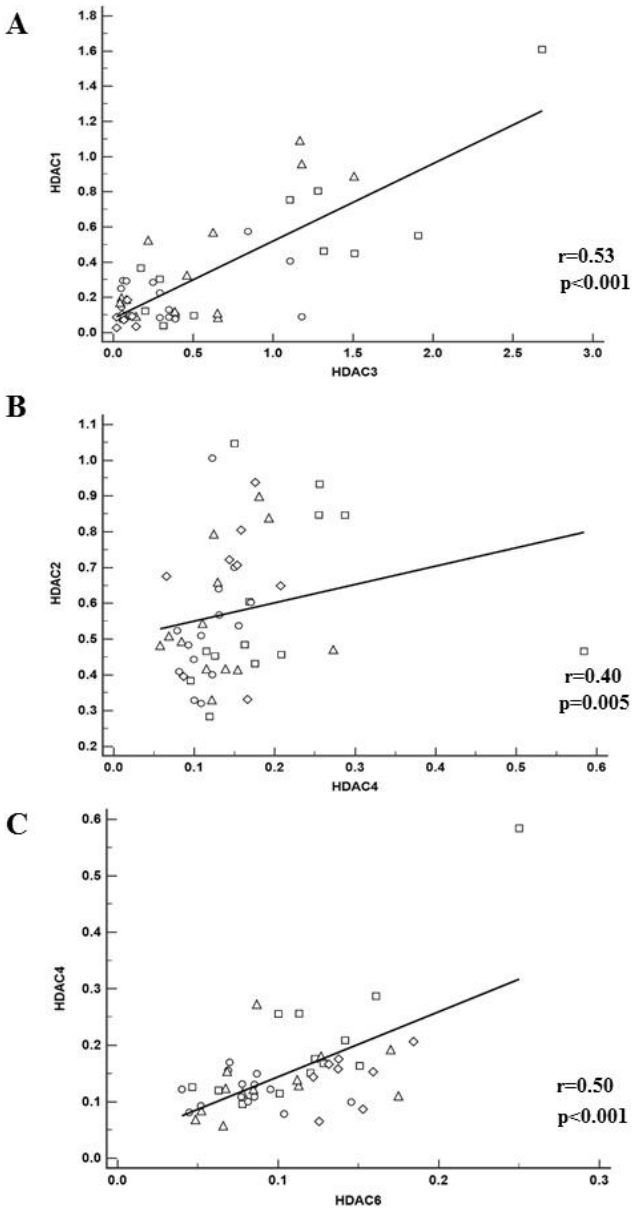

Figure 2.4 Interprotein Correlation Plots

(A) Frontal cortex HDAC3 levels correlated positively with HDAC1 levels (r=0.53, p < 0.001). (B) Significant positive correlations were found between HDAC4 and HDAC2 (r=0.40, p = 0.005), and (C) between HDAC6 and HDAC4 (r=0.50, p < 0.001). NCI, open circles; MCI, open squares; mAD, open triangles; sAD, open diamonds.

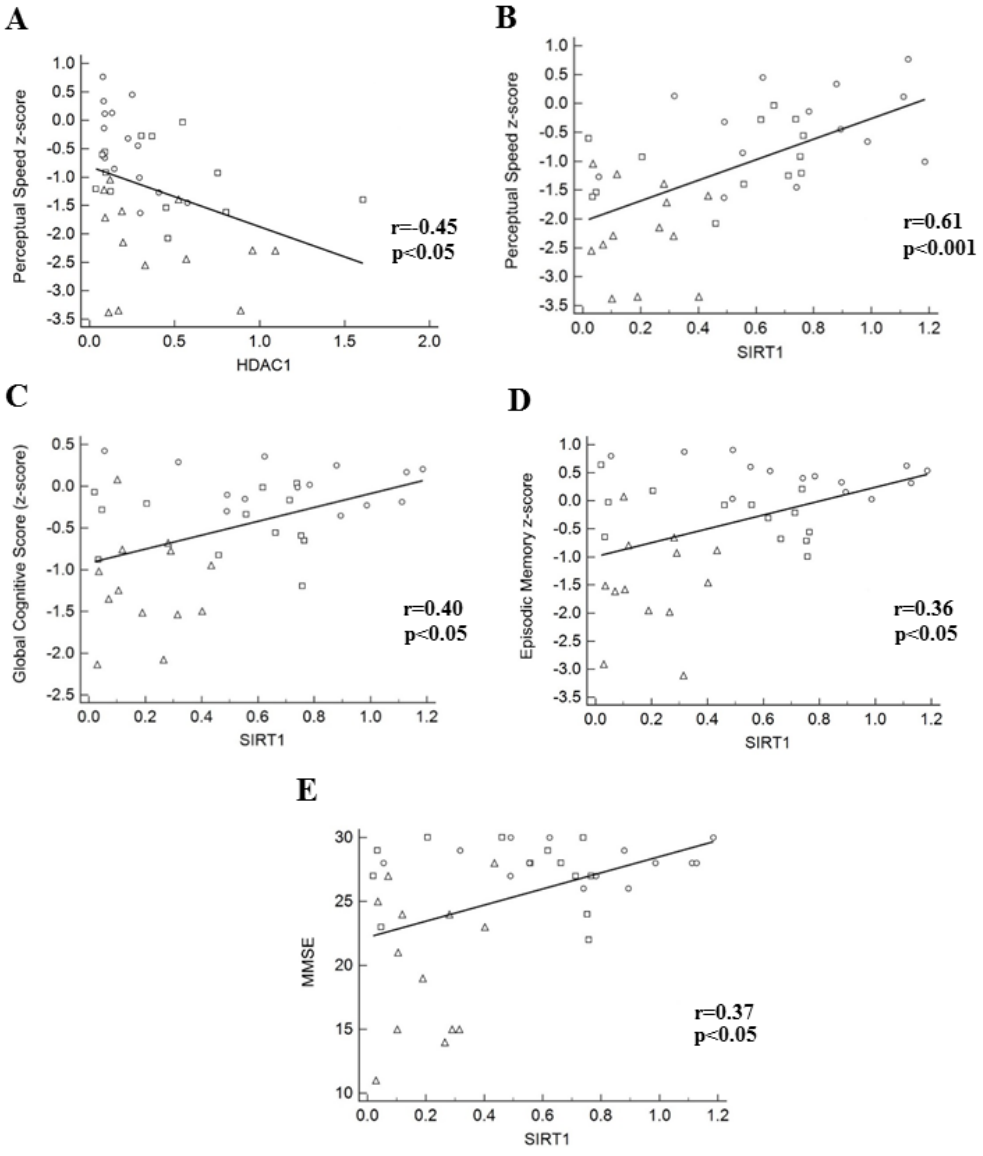

Figure 2.5 HDAC and Cognitive Test Correlation Plots

(A) Frontal cortex levels of HDAC1 correlated negatively with perceptual speed z-score (r=-0.45, $p < 0.05$), while SIRT1 levels correlated positively with perceptual speed z-score (B) (r=0.61, $p < 0.001$), Global Cognitive score (C) (r=0.40, $p < 0.05$), episodic memory z-score (D) (r=0.36, $p < 0.05$), and MMSE (E) (r=0.37, $p < 0.05$). NCI, open circles; MCI, open squares; mAD, open triangles. MMSE, Mini-Mental State examination.

HDAC1 (Figure 2.6A) and SIRT1 (Figure 2.6B) showed weak correlations with frontal NFT counts (Table 2.8, $r = 0.37$, $p = 0.02$; $r = -0.31$, $p = 0.05$; respectively), none of the other HDACs correlated with NFT counts (Figure 2.7). Comparisons between low (0-III) and high (IV-VI) Braak stages revealed no significant differences between groups ($p = 0.64$) (Table 2.9). No significant differences in protein levels were noted for HDAC or SIRT1 proteins in cases with low or high Braak stages (Table 2.10). No significant differences were found in NCI protein levels between high and low Braak groups, indicating that in controls Braak stage did not have a significant effect on HDAC levels (Table 2.11). In addition, levels of HDAC proteins were not correlated with NPs, DPs, or NPs+DPs (Figures 2.8, 2.9, 2.10A-F). The demographic variables (age at death, education, PMI, brain weight at autopsy, time between last clinical assessment and autopsy) did not correlate with any of the proteins examined.

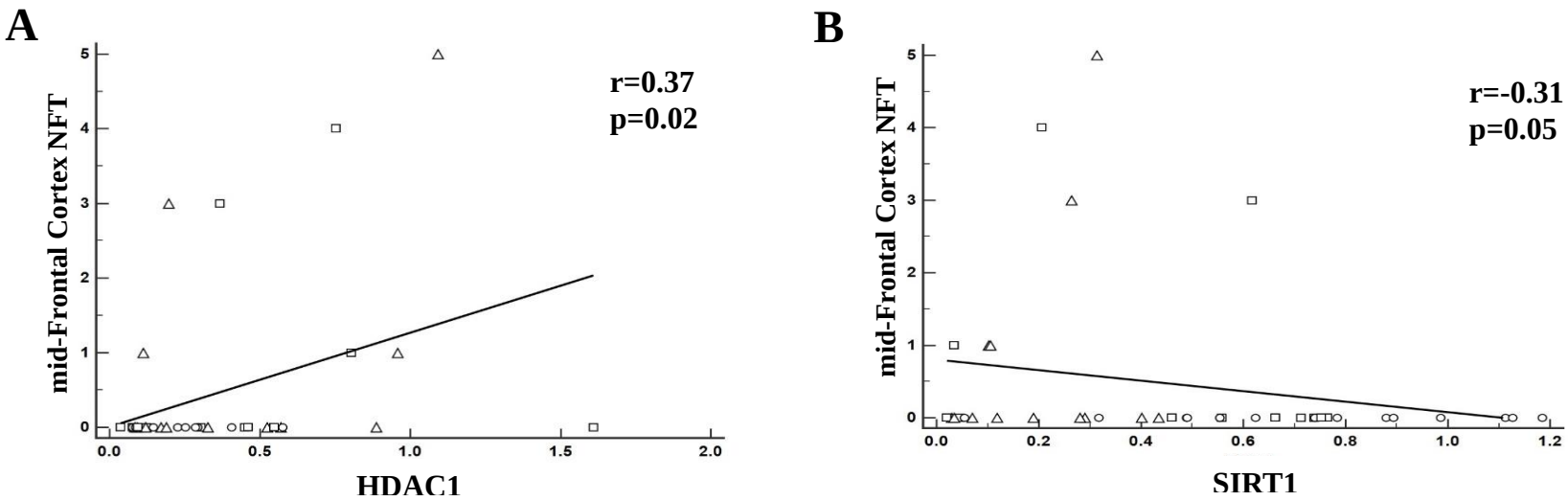

Figure 2.6 Correlational Plots Between HDAC Levels and mid-Frontal Cortex NFT Counts

Frontal cortex levels of HDAC1 (A) correlated positively with mid-Frontal cortex NFT counts (r=0.37, p = 0.02), whereas SIRT1 levels (B) negatively correlated with mid-Frontal NFT counts (r=-0.31, p < 0.05). NCI, open circles; MCI, open squares; mAD, open triangles; NFT, neurofibrillary tangle.

	HDAC1	HDAC2	HDAC3	HDAC4	HDAC6	SIRT1
Diffuse plaques	0.12	-0.11	-0.03	-0.05	0.02	-0.06
Neuritic plaques	0.01	-0.29	-0.01	-0.04	-0.06	-0.15
Diffuse + Neuritic plaques	0.16	-0.20	-0.02	-0.07	-0.04	-0.15
Mid-frontal NFT counts	0.37 [a]	-0.01	0.16	0.07	0.14	-0.31 [a]

Table 2.8 Correlations Between Protein Levels and Neuropathological Variables

[a] $p < 0.05$, all other correlations not statistically significant. NFT, neurofibrillary tangle.

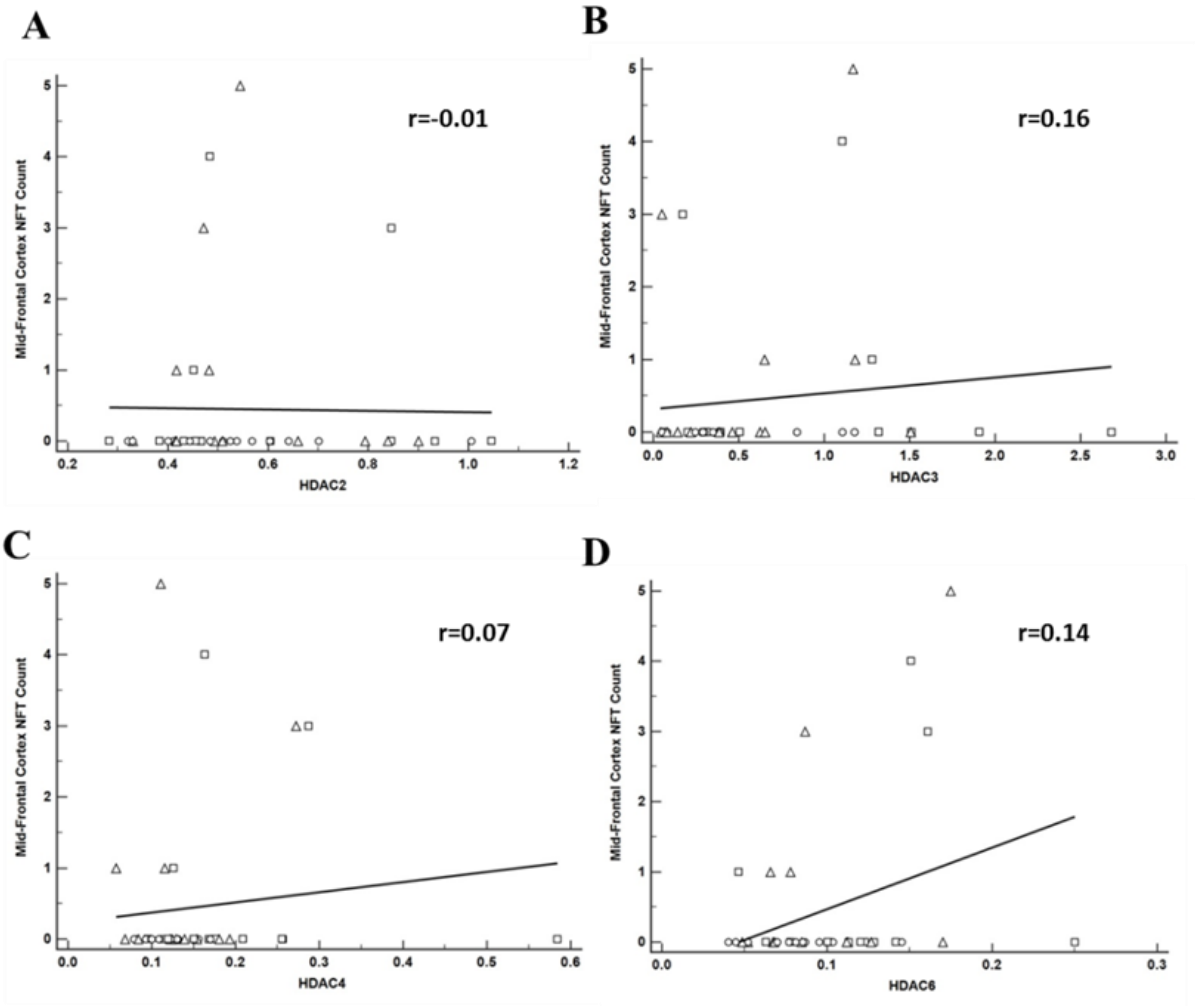

Figure 2.7 Correlation Plots Between HDAC Proteins and NFT Counts

Frontal cortex levels of HDAC2 (A), HDAC3 (B), HDAC4 (C), and HDAC6 (D) were not significantly correlated with mid-frontal cortex neurofibrillary tangles (NFTs) counts. NCI, open circles; MCI, open squares; mAD, open triangles.

Braak Stage	NCI (n = 14)	MCI (n = 13)	mAD (n = 13)	Total (n = 40)
Low Braak Stage (0-III)	5	6	7	18
High Braak Stage (IV-V)	9	7	6	22

Table 2.9 Low and High Braak Stage Classification by Clinical Group

No Braak stage VI cases were present in the sample; Braak stage information was not available for the sAD group; Chi-square p-value = 0.64.

	NCI	MCI	mAD
HDAC1	p = 0.64	p = 0.15	p = 0.57
HDAC2	p = 0.16	p = 0.78	p = 0.06
HDAC3	p = 0.32	p = 0.99	p = 0.32
HDAC4	p = 0.55	p = 0.89	p = 0.57
HDAC6	p = 0.64	p =0.89	p = 0.67
SIRT1	p = 0.13	p = 0.67	p = 0.48

Table 2.10 Low and High Braak Stage Differences for HDAC and SIRT1 Proteins

No statistically significant differences were found in HDAC or SIRT levels between low and high Braak stage NCI, MCI and mAD cases. NCI, no cognitive impairment; MCI, mild cognitive impairment; mAD, mild/moderate AD.

	High Braak Stage	Low Braak Stage	p-value
HDAC1	0.25±0.20	0.20±0.12	p = 0.64
HDAC2	0.45±0.10	0.58±0.19	p = 0.16
HDAC3	0.27±0.34	0.44±0.41	p = 0.32
HDAC4	0.12±0.03	0.12±0.03	p = 0.55
HDAC6	0.07±0.02	0.08±0.03	p = 0.64
SIRT1	0.60±0.22	0.81±0.37	p = 0.13

Table 2.11 NCI HDAC and SIRT1 Levels for Low and High Braak Stage Groups

No significant differences were found in NCI protein levels between high and low Braak groups.

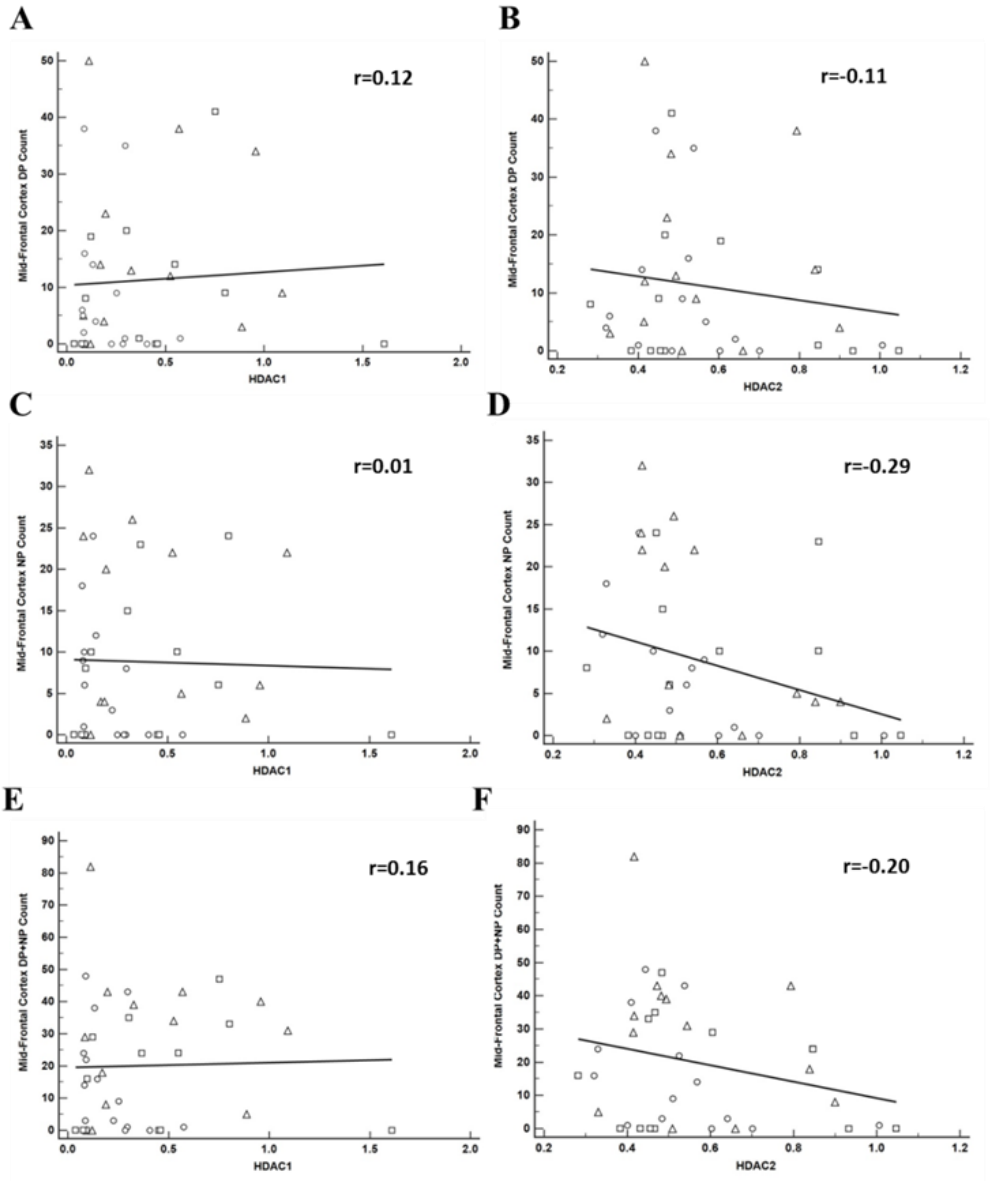

Figure 2.8 Correlation Plots Between HDAC1 and HDAC2 Proteins and Plaque Counts

Frontal cortex levels of HDAC1 and HDAC2 were not significantly correlated with mid-frontal cortex diffuse plaque (DP) (A, B), neuritic plaque (NP) (C, D), or DP+NP (E, F) counts. NCI, open circles; MCI, open squares; mAD, open triangles.

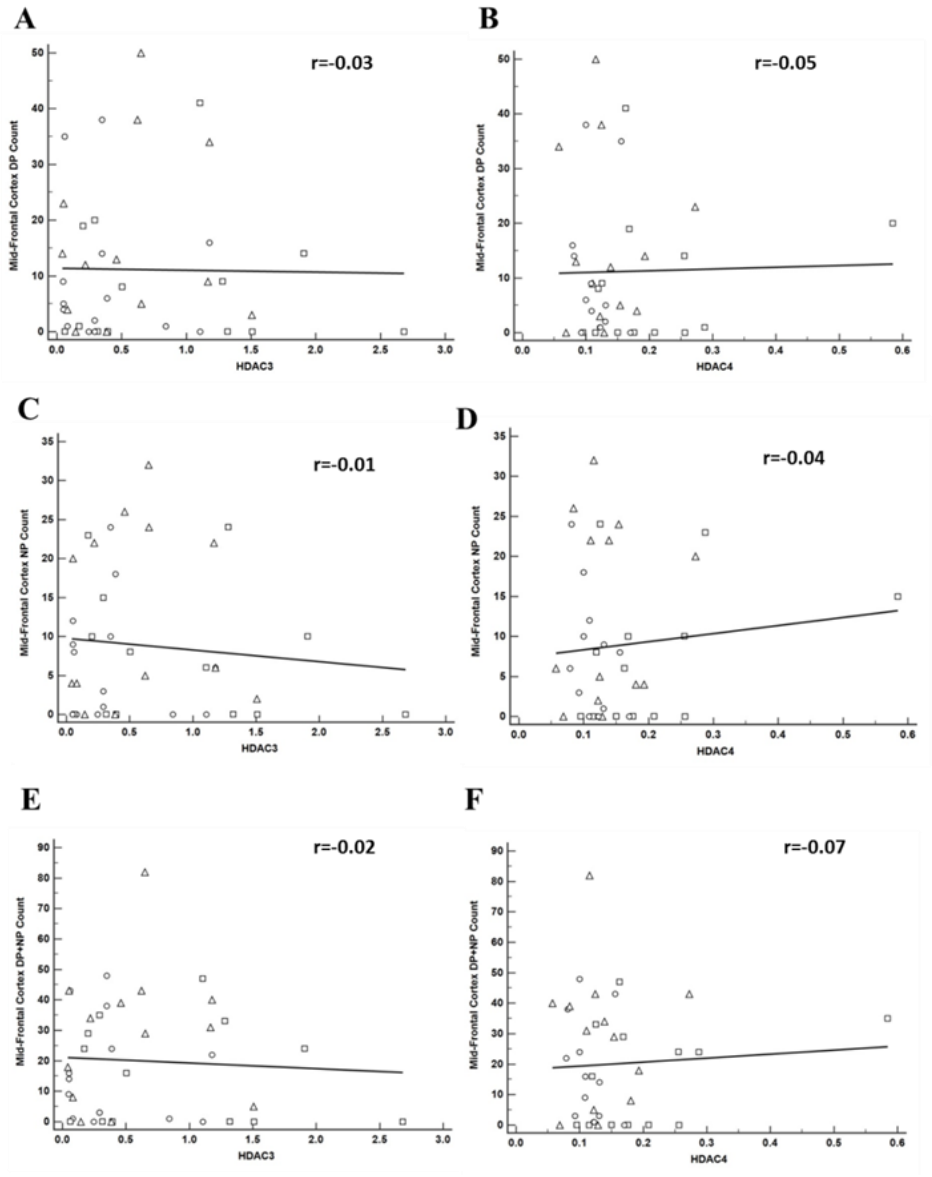

Figure 2.9 Correlation Plots Between HDAC3 and HDAC4 Proteins and Plaque Counts

Frontal cortex levels of HDAC3 and HDAC4 were not significantly correlated with mid-frontal cortex diffuse plaque (DP) counts (A, B), neuritic plaque (NP) (C, D), or DP+NP (E, F) counts. NCI, open circles; MCI, open squares; mAD, open triangles.

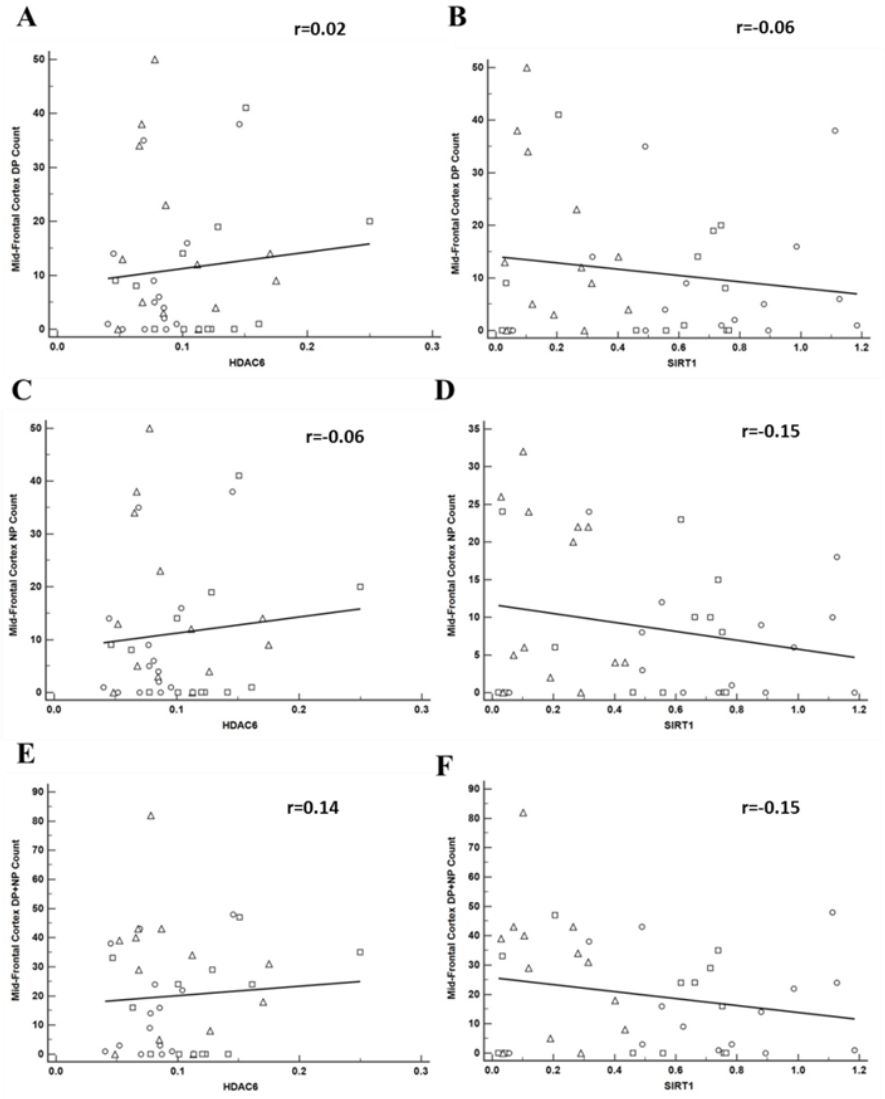

Figure 2.10 Correlation Plots Between HDAC6 and SIRT1 Proteins and Plaque Counts

Frontal cortex levels of HDAC6 and SIRT1 were not significantly correlated with mid-Frontal cortex diffuse plaque (DP) (A, B), neuritic plaque (NP) (C, D), or DP+NP (E, F) counts. NCI, open circles; MCI, open squares; mAD, open triangles.

2.5 DISCUSSION

HDACs are modulators of chromatin plasticity that interact with other epigenetic regulators to influence genomic and cellular stability. These proteins are associated with the promoter regions of memory-associated genes, including immediate early genes (Guzowski, Lyford et al. 2000; French, O'Connor et al. 2001), brain-derived neurotrophic factor (Linnarsson, Bjorklund et al. 1997; Hall, Thomas et al. 2000), and synaptic genes (Kouzarides 2007; Graff, Rei et al. 2012) in corticolimbic regions. Increasing evidence from animal studies suggests that perturbations to the balance of HDAC proteins and acetylation/deacetylation levels in the frontal cortex play a negative role in memory and learning (Bredy, Wu et al. 2007; Jakovcevski and Akbarian 2012; Morris, Mahgoub et al. 2013). Whether alterations in cortical HDAC protein levels are neuroprotective or neurotoxic during AD progression is controversial. These proteins may have different functions dependent on disease stage, cellular milieu, and environmental factors. Our data demonstrate that frontal cortex HDAC proteins are differentially dysregulated depending upon antemortem clinical classification and selectively correlate with cognitive tests and NFT pathology during the onset of AD.

Here, we found that frontal cortex levels of HDAC1 and HDAC3 were significantly increased in MCI and mAD followed by a significant decrease in sAD compared to NCI subjects. These protein levels were significantly correlated with each other across disease progression. Functionally, HDAC1 exhibits dual roles in the regulation of neuronal activity (Kim, Frank et al. 2008; Jeong, Then et al. 2009; Reynolds, Casaccia et al. 2010; Bardai, Price et al. 2012; Dobbin, Madabhushi et al.

2013), subserving neuroprotection and neurotoxicity based on its interaction with either SIRT1 or HDAC3 (Kim, Frank et al. 2008; Bardai, Price et al. 2012; Dobbin, Madabhushi et al. 2013). HDAC1 promotes cell survival via interaction with DNA damage response and repair pathways (Miller, Tjeertes et al. 2010; Wang, Pan et al. 2013), while SIRT1 deacetylates HDAC1 to promote non-homologous end joining in the face of DNA damage (Dobbin, Madabhushi et al. 2013), which has been reported in the AD brain (Adamec, Vonsattel et al. 1999). Previous reports show that the interaction between HDAC1 and HDAC3 is increased in neurons primed to die when compared with healthy neurons (Bardai, Price et al. 2012). A recent study demonstrated a reduction of HDAC1 expression in the AD frontal cortex compared to age-matched controls using mass spectrometry (Anderson, Chen et al. 2015). Whether increases in cortical levels of HDAC1 and HDAC3 during prodromal AD reflect the activation of neuronal death pathways or a concerted effort to maintain cellular homeostasis is unknown. However, we have previously proposed that an upregulation in choline acetyltransferase activity in the MCI frontal cortex is indicative of an compensatory reorganizational response (DeKosky, Ikonomovic et al. 2002); therefore, it is possible that the increase in HDAC1 and HDAC3 protein levels reported here in MCI may also be an example of neuroplasticity occurring in the prodromal stage of AD. A possible downstream consequence of epigenomic plasticity may be the suppression of gene transcription. Increased cortical levels of HDAC1 were negatively correlated with perceptual speed z-scores across disease progression, indicating an association between HDAC1 and poorer performance on perceptual speed tasks. Functionally, the frontal cortex plays a critical

role in perceptual decision-making (Rahnev, Lau et al. 2011; Fleming, Huijgen et al. 2012; Rahnev, Nee et al. 2016) and binds perceptual and executive control information to guide goal-driven behavior (Opris, Santos et al. 2013). Thus, increased HDAC1 levels in the frontal cortex may affect downstream molecular pathways associated with perceptual speed domains during AD progression. In addition, increased levels of HDAC1 were positively correlated with frontal cortex NFT counts, indicating that both increased HDAC1 and NFT burden may contribute to AD neuropathogenesis, however, to our knowledge there are no neurobiological reports directly associating HDAC1 and NFT formation.

The present study did not observe changes in HDAC2 levels in the frontal cortex. By contrast two immunohistochemical studies have demonstrated both increases and decreases in HDAC2 in the entorhinal cortex and hippocampus (Mastroeni, Grover et al. 2010; Graff, Rei et al. 2012). This may reflect regional-specific changes related to specific cellular populations. Interestingly, a case report of monozygotic twins discordant for AD reported increased HDAC2 gene expression in peripheral blood cells of the AD twin (D'Addario, Candia et al. 2017), suggesting that global levels of HDAC2 expression may increase in AD, but depending on the region evaluated may not be translated or post-translationally modified to yield a functional protein.

Intracellular trafficking of HDAC4 has been implicated in neuronal survival and transcriptional repression. HDAC4 is localized in the cytoplasm under normal conditions; in response to low potassium or excitotoxic glutamate conditions, it rapidly accumulates in neuronal nuclei where it suppresses myocyte enhancer factor-2 (MEF-2) and cAMP

response element-binding protein (CREB)-dependent transcription (Bolger and Yao 2005; Herrup, Li et al. 2013). HDAC4 is dephosphorylated and translocated to the nucleus in neurodegenerative diseases including AD, where it selectively accumulates in frontal cortex layer III nuclei (Shen, Chen et al. 2016). Although we did not find increases in total cortical HDAC4 levels in mAD and sAD, it is possible that using other HDAC4 antibodies directed against its dephosphorylated form would reveal differences across clinical groups. By contrast, we found a significant increase in HDAC4 levels in MCI compared to NCI, which may reflect a epigenetic plasticity response to an initial disease insult.

HDAC6 levels were increased in MCI and sAD compared to NCI and mAD in the frontal cortex, suggesting that similar to HDAC1 and HDAC3, HDAC6 levels may increase in response to disease onset, plateau in mild/moderate AD before an increase during severe AD. HDAC6 is involved in both the ubiquitin-proteasome system and autophagic pathways (Kopito 2000; Boyault, Gilquin et al. 2006; Hildmann, Riester et al. 2007), where it can regulate the formation and transportation of aggresomes, as well as promote proteasome or lysosome-mediated degradation of misfolded proteins. Lysosomal-endosomal and autophagic upregulation occurs in cortical, hippocampal, and basal forebrain neurons in MCI and AD even before plaque and tangle pathology (Nixon and Yang 2011; Orr and Oddo 2013; Perez, He et al. 2015). Perhaps increased HDAC6 levels in the frontal cortex in MCI reflect augmented protein clearance and degradation. HDAC6 has also been implicated in tubulin acetylation and acetylated α-tubulin, a marker for microtubule stability, is reduced in the AD brain (Ding, Dolan et al. 2008). By

contrast, HDAC6 levels have been reported to be increased in the cortex and hippocampus, which is paralleled by a decrease in acetylation of α-tubulin in AD compared to controls (Ding, Dolan et al. 2008). Perhaps the increase in frontal cortex HDAC6 levels destabilizes microtubules impairing intracellular transport (Chen, Zhou et al. 2005; Dompierre, Godin et al. 2007; Gao, Wang et al. 2010). A few reports have demonstrated a reduction in acetylated alpha-tubulin immunoreactivity in NFT-bearing neurons in the human CA1 region of the hippocampus, suggesting that HDAC6 is also involved in tau microtubule destabilization in AD (Hempen and Brion 1996; Perez, Santa-Maria et al. 2009; Cook, Gendron et al. 2012). Although these findings suggest an interaction between HDAC6 and tau, we did not find a correlation between HDAC6, NFT counts, or Braak stage. We did observe a significant positive correlation between HDAC4 and HDAC6 levels, indicating that these cytoplasmic HDACs may interact at the cellular level.

In the present study, frontal cortex SIRT1 levels steadily decreased across the clinical groups. Decreased expression of SIRT1 in Braak stages I-II has been previously shown by Bossers et al. in the AD prefrontal cortex, suggesting that loss of SIRT1 may be associated with early NFT formation (Bossers, Wirz et al. 2010). Decreases in SIRT1 mRNA and protein have been demonstrated in the parietal cortex in AD (Julien, Tremblay et al. 2009) but were not significantly decreased in MCI in comparison to our data which showed a significant decrease in SIRT1 levels in MCI compared to NCI. This earlier study also found a significant positive correlation between parietal cortex SIRT1 levels and global cognitive z-scores in AD (Julien, Tremblay et al. 2009), similar to the

findings reported here for the frontal cortex. We also found significant correlations between SIRT1 levels and perceptual speed, episodic memory z-scores, as well as MMSE, indicating that a reduction of frontal cortex SIRT1 protein levels may affect multiple cognitive domains during AD progression. SIRT1 knockout mice exhibit a significant deficit in both short and long-term hippocampal-dependent memory, while mice expressing high levels of SIRT1 in the hippocampus show normal long term potentiation and memory function, suggesting that SIRT1 may be critical for hippocampal-dependent memory tasks (Gao, Wang et al. 2010; Michan, Li et al. 2010). What role cortical SIRT1 plays in episodic memory is unknown. However, it is possible that a concomitant change in hippocampal and cortical levels of SIRT1 may indicate a double hit to different memory circuits. Given the functional disconnection between the frontal cortex and hippocampus in AD (Grady, Furey et al. 2001), alterations in cortical levels of SIRT1 may exacerbate hippocampal dysfunction.

SIRT1 directly modulates synaptic plasticity and memory formation (Gao, Wang et al. 2010). Although we have shown in tissue from the RROS cohort that drebrin, a postsynaptic dendritic spine marker, is decreased in the AD hippocampus (Counts, He et al. 2012), whether decreases in SIRT1 and drebrin levels are related to alterations in synaptic plasticity has not been established. In cell culture models, SIRT1 is suggested to be protective against cellular stress and inflammation by inhibiting NF-kappaB signaling to mediate protection against microglia-dependent amyloid-beta toxicity (Chen, Zhou et al. 2005). However, we did not find any association between SIRT1 levels and CERAD or amyloid density counts in the frontal cortex. We did observe a moderate negative

correlation between SIRT1 levels and frontal cortex NFT counts, indicating as others have suggested that a reduction in SIRT1 is associated with tau accumulation in the AD cortex (Julien, Tremblay et al. 2009).

Interestingly, when we divided our NCI cases into high and low Braak groups no difference in HDAC and SIRT1 protein levels was found between these NFT defined groups. In this regard, many studies have shown that NCI cases display both high Braak NFT and amyloid plaque pathology (Mufson, Chen et al. 1999; Price and Morris 1999; Erten-Lyons, Woltjer et al. 2009; Mufson, Malek-Ahmadi et al. 2016; Mufson, Malek-Ahmadi et al. 2016; Wegiel, Flory et al. 2017) but do not differ in the level of different molecular and cellular markers (Perez, Nadeem et al. 2017). The concepts of cognitive reserve and "super agers" have been used to explain these findings (Arnold, Louneva et al. 2013; Mufson, Malek-Ahmadi et al. 2016; Mufson, Malek-Ahmadi et al. 2016; Wegiel, Flory et al. 2017). Despite these concepts, a clear biological explanation remains to be defined. Aged people with Braak stage III, IV and V display significant neuronal damage to the medial temporal lobe (MTL) memory circuit consisting of the transentorhinal and entorhinal cortex and hippocampus (Buckner, Snyder et al. 2005; Buckner, Sepulcre et al. 2009; Simic, Babic et al. 2014), which may disconnect multimodal neocortical information from reaching the MTL. However, despite an apparent MTL disconnection and extensive amyloid plaque pathology, aged people remain cognitively intact (Mufson, Malek-Ahmadi et al. 2016; Mufson, Malek-Ahmadi et al. 2016). These observations suggest that NFT and amyloid lesions may not be a necessary precondition for cognitive impairment in the elderly or AD. Therefore, the

biological factors that maintain cognitive stability in the face of extensive AD lesions in cognitively intact elders remain to be defined. Perhaps dysregulation of epigenetic factors play a more pivotal role in cellular alterations during the course of AD.

A caveat of this or any other human tissue study is what role end of life agonal state has upon HDAC protein levels in the brain. The effects of agonal conditions on RNA and DNA are well documented. An average postmortem interval of 3-4 hours is considered suitable for gene expression analysis (Blair, Wang et al. 2016). On the other hand, studies indicate that proteins such as actin and GAPDH, often used as internal loading controls for Western blot studies, remain intact even at longer PMIs (i.e., over 48 hours) (Blair, Wang et al. 2016). Our postmortem intervals were ~5 hours, which is slightly higher than what would be considered appropriate for gene expression studies, but well within time limits for protein assay usage.

Figure 2.11 summarizes our findings of HDAC alterations in the frontal cortex during the clinical progression of AD. Whether HDAC profiles can be monitored as biomarkers for disease progression remains to be determined. The advent of HDAC PET tracers ([^{11}C]Martinostat) (Schroeder, Wang et al. 2014; Wang, Schroeder et al. 2014; Wey, Gilbert et al. 2016) make it possible to image neuroepigenetic proteins in the human brain. Combining this technology with peripheral blood cell (D'Addario, Candia et al. 2017), and serum HDAC analyses (Kumar, Chaterjee et al. 2013) will aid in the development of a more accurate bioassay for determining the transition from NCI to MCI. Mapping epigenetic alterations in different brain regions and uncovering the molecular and cellular mechanisms related to disease pathogenesis may provide the basis

for novel therapeutic platforms for the treatment of dementia and perhaps personalized medicine. In this regard, we are presently examining epigenetic alterations in other components of the DMN in tissue obtained from the RROS. Interestingly, HDAC inhibitors are used for treating cancer (Gallinari, Di Marco et al. 2007; Marks and Xu 2009; Arrighetti, Corno et al. 2015; Behera, Jayprakash et al. 2015; Ceccacci and Minucci 2016) and possibly for AD (Xu, Dai et al. 2011; Delcuve, Khan et al. 2012; Cacabelos and Torrellas 2015).

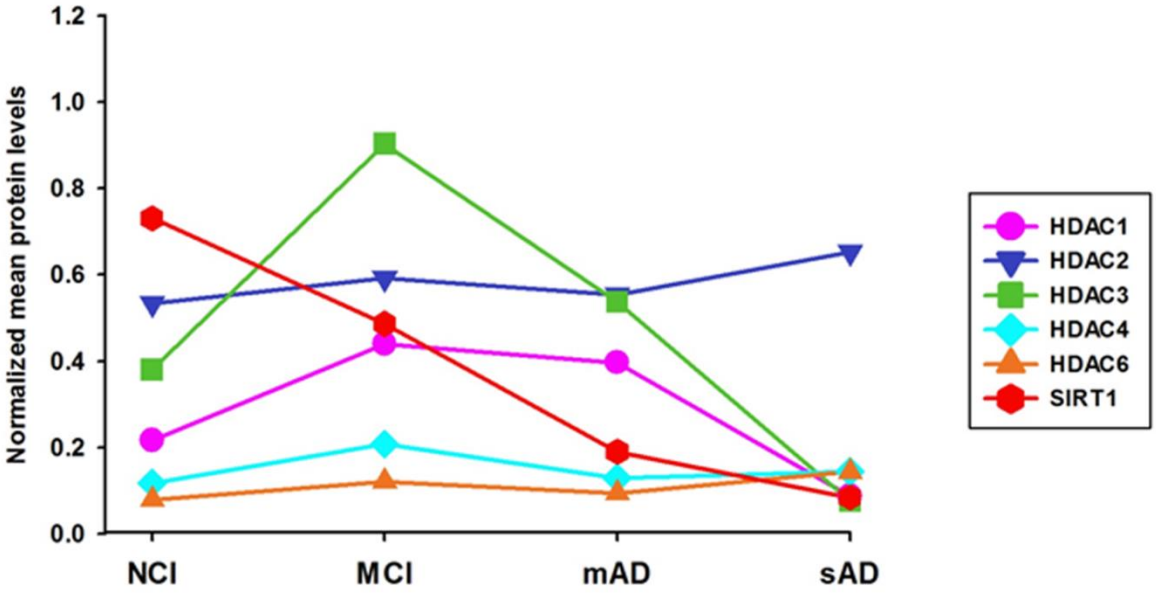

Figure 2.11 Summary of Deacetylase Levels in the Frontal Cortex Across AD Progression

Summary diagram showing changes in histone deacetylase levels in the frontal cortex during the progression of Alzheimer's disease. NCI, no cognitive impairment; MCI, mild cognitive impairment; mAD, mild/moderate Alzheimer's disease; sAD, severe Alzheimer's disease.

CHAPTER 3

HDAC2 DYSREGULATION IN THE NUCLEUS BASALIS OF MEYNERT DURING THE PROGRESSION OF ALZHEIMER'S DISEASE

3.1 ABSTRACT

Aims: Alzheimer's disease (AD) is characterized by degeneration of cholinergic basal forebrain (CBF) neurons in the nucleus basalis of Meynert (nbM), which provides the major cholinergic input to the cortical mantle and is related to cognitive decline in patients with AD. Cortical histone deacetylase (HDAC) dysregulation has been associated with neuronal degeneration during AD progression. However, whether HDAC alterations play a role in CBF degeneration during AD onset is unknown. We investigated global HDAC protein levels and nuclear HDAC2 immunoreactivity in tissue containing the nbM and their association with neurofibrillary tangle (NFT) development during AD progression.

Methods: We used semi-quantitative western blotting and immunohistochemistry to evaluate HDAC and sirtuin (SIRT) levels in individuals that died with a premortem clinical diagnosis of no cognitive impairment (NCI), mild cognitive impairment (MCI), mild/moderate AD (mAD), or severe AD (sAD). Quantitative immunohistochemistry was used to identify HDAC2 protein levels in individual cholinergic nbM nuclei and their localization with the early phosphorylated tau marker AT8, the late-stage apoptotic tau marker TauC3, and Thioflavin-S, a marker of mature NFTs.

Results: In AD patients, HDAC2 protein levels were dysregulated in the basal forebrain region containing cholinergic neurons of the nbM. HDAC2 nuclear

immunoreactivity was reduced in individual cholinergic nbM neurons across disease stages. HDAC2 nuclear reactivity correlated with multiple cognitive domains and with NFT formation.

Conclusions: These findings suggest that HDAC2 dysregulation contributes to cholinergic nbM neuronal dysfunction, NFT pathology, and cognitive decline during the clinical progression of AD.

3.2 INTRODUCTION

Alzheimer's disease (AD) is characterized by degeneration of cholinergic basal forebrain (CBF) neurons (Mesulam, Mufson et al. 1983) in the nucleus basalis of Meynert (nbM) (Whitehouse, Price et al. 1981; Doucette 1986; Etienne, Robitaille et al. 1986; Rinne, Paljarvi et al. 1987; Mufson, Bothwell et al. 1989; Iraizoz, Lacalle et al. 1991; Iraizoz, Guijarro et al. 1999), which are the main source of acetylcholine to the cortical mantle (Rye, Wainer et al. 1984). Cholinergic neuron loss in the nbM contributes to cognitive and attentional deficits (Iraizoz, Guijarro et al. 1999; Mufson, He et al. 2012) and correlates with disease severity in AD (Perry, Tomlinson et al. 1978; Wilcock, Esiri et al. 1982; DeKosky, Harbaugh et al. 1992). Alterations in the balance between the high-affinity trkA (cell survival) and the low-affinity pan neurotrophin receptor ($p75^{NTR}$) (cell death) nerve growth factor (NGF) receptors (Mufson, Ma et al. 2000; Mufson, Ma et al. 2002), dysregulation of NGF metabolism (Peng, Wuu et al. 2004; Cuello, Bruno et al. 2007; Iulita and Cuello 2016) and development of neurofibrillary tangle (NFT) pathology (Rasool, Svendsen et al. 1986; Sassin, Schultz et al. 2000; Mesulam, Shaw et al. 2004;

Vana, Kanaan et al. 2011) have been suggested to play a role in the pathogenesis of CBF neurons in AD. Interestingly, histone acetylation and deacetylation have been shown to be involved in the regulation of choline acetyltransferase (ChAT) expression, the synthetizing enzyme for the neurotransmitter acetylcholine (Aizawa and Yamamuro 2010; Aizawa, Teramoto et al. 2012; Bekdash 2016), suggesting a role for epigenetics in the selective vulnerability of cholinergic nbM neurons in AD.

Histone deacetylases (HDACs), a class of enzymes with deacetylase activity, are found in the nucleus and cytoplasm and are believed to play a role in the pathogenesis of AD (Ding, Dolan et al. 2008; Guan, Haggarty et al. 2009; Xu, Dai et al. 2011; Cook, Gendron et al. 2012; Graff, Rei et al. 2012). Multiple HDAC classes are associated with cellular events that are dysfunctional in AD, including endoplasmic reticulum stress (HDAC4) (Shen, Chen et al. 2016), autophagic regulation (HDAC6) (Pandey, Nie et al. 2007), mitochondrial transport (HDAC6) (Chen, Owens et al. 2010), tau hyperphosphorylation (HDAC6) (Ding, Dolan et al. 2008), and amyloid beta (Aβ) and tau accumulation (SIRT1) (Julien, Tremblay et al. 2009; Lalla and Donmez 2013). Studies also indicate that dysregulation of HDACs is associated with brain regions susceptible to NFT formation, including the hippocampus and entorhinal cortex, in AD (Mastroeni, Grover et al. 2010; Graff, Rei et al. 2012). Although reports indicate that basal forebrain pathology precedes and predicts cortical pathology and memory impairment (Teipel, Flatz et al. 2005; Schmitz and Spreng 2016), whether epigenetic dysregulation occurs and associates with the formation of NFTs in nbM cholinergic neurons is unknown.

Of the various HDACs, HDAC2 has received extensive investigation because of its role in the regulation of genes involved in learning and memory via modulation of chromatin plasticity (Dawson and Kouzarides 2012; Graff and Tsai 2013; Volmar and Wahlestedt 2015). Immunohistochemical analysis of HDAC1 and HDAC2 has revealed decreased reactivity in the entorhinal cortex (Mastroeni, Grover et al. 2010). However, HDAC2 (but not HDAC1 or HDAC3) is increased in the nuclei of hippocampal CA1 and entorhinal cortex neurons in AD compared with non-cognitively impaired aged controls (Graff, Rei et al. 2012). A western blotting study of the frontal cortex revealed significant increases in HDAC1, HDAC3, HDAC4, and HDAC6 in MCI and mAD compared with NCI, whereas HDAC2 levels remained stable across clinical groups (Mahady, Nadeem et al. 2018). Conversely, cortical SIRT1 levels decreased during disease progression (Mahady, Nadeem et al. 2018). However, to our knowledge, no reports have examined HDAC modifications in the basal forebrain region containing the cholinergic cortical projection neurons during the progression of AD and their relation to cognitive performance and neuropathological criteria.

In the present study, we investigated the role of HDACs, especially HDAC2, in cholinergic nbM neuronal degeneration during the progression of AD. Using semi-quantitative western blotting, we analyzed global levels of HDACs and SIRT1 proteins in basal forebrain tissue containing the nbM obtained from individuals who died with an antemortem clinical diagnosis of no cognitive impairment (NCI), mild cognitive impairment (MCI), mild/moderate AD (mAD), and severe AD (sAD) and who received a postmortem neuropathological evaluation. In addition, we examined HDAC2 nuclear

immunoreactivity and its association with early (AT8) and late (TauC3) tau epitopes that mark NFT evolution (Garcia-Sierra, Ghoshal et al. 2003; Binder, Guillozet-Bongaarts et al. 2005; Guillozet-Bongaarts, Garcia-Sierra et al. 2005; Vana, Kanaan et al. 2011; Combs, Hamel et al. 2016; Tiernan, Mufson et al. 2018) in individual nbM cholinergic neurons in tissue from the same clinicopathological groups. Our data provide evidence that reduced HDAC2 levels in the nbM are coincident with early posttranslational tau modifications in prodromal AD (MCI), and are associated with cognitive decline.

3.3 METHODS

3.3.1 Subjects

Frozen and free-floating tissue containing cholinergic nbM neurons was obtained from individuals who died with an antemortem clinical diagnosis of NCI (n=20), MCI (n=13), or mild/moderate AD (n=12) from the Rush Religious Orders Study (RROS) (Mufson, Chen et al. 1999; Bennett, Wilson et al. 2002; Bennett, Schneider et al. 2005; Mufson, He et al. 2012). Additional cases with a diagnosis of severe AD (n=16) were obtained from the Rush Alzheimer's Disease Center (RADC). The Human Research Committees of Rush University Medical Center approved this study and written informed consent for research and autopsy was obtained from the participants or their family/guardians.

3.3.2 Clinical and Neuropathologic Evaluations

Details of the clinical evaluation of the RROS cohort have been reported previously (Mufson, Chen et al. 1999; Bennett, Schneider et al. 2005; Mufson, He et al. 2012; Perez, Getova et al. 2012). Briefly, a team of investigators led by a neurologist

performed annual neurological examinations and a cognitive battery in addition to reviewing each participant's medical history. The average time from the last clinical evaluation to death was about 8 months. Neuropsychological testing included the Mini-Mental State Examination (MMSE), the Global Cognitive Score (GCS), and a composite z-score compiled from a battery of 19 cognitive tests (Mufson, Chen et al. 1999), including episodic memory z-score, semantic memory z-score, working memory z-score, perceptual speed z-score, and visuospatial ability z-score (Wilson, Beckett et al. 2002). The 13 MCI cases had cognitive impairment insufficient to meet the criteria for dementia (Bennett, Wilson et al. 2002). MCI subtypes include: amnestic MCI (aMCI) which is characterized by memory impairment and progression to AD at a higher rate than non-amnestic MCI (naMCI), which involves a cognitive domain(s) other than memory such as executive function, language, and visuospatial processing. Amnestic and non-amnestic MCI can be subcategorized into single (sdMCI) or multiple domain MCI (mdMCI) depending on how many cognitive domains are affected (Petersen 2004). Of the 13 MCI cases, 6 were amnestic and 7 were non-amnestic. A final clinical diagnosis was applied to these cases after a team of neurologists and neuropsychologists reviewed the clinical data. Neuropathological diagnosis was based on Braak staging of NFTs (Braak and Braak 1991), the National Institute on Aging (NIA) Reagan criteria (Newell, Hyman et al. 1999), and recommendations of the Consortium to Establish a Registry for Alzheimer's disease (CERAD) (Mirra 1997). The recent criteria for the diagnosis of AD are currently being applied to all RROS cases (Dubois, Feldman et al. 2007). Participants were excluded if they had mixed pathologies other than AD (e.g., TAR DNA-binding protein

43, large strokes, Parkinson's disease, Lewy body dementia, vascular dementia, hippocampal sclerosis).

3.3.3 Antibodies

Table 3.1 summarizes the antibodies used and their respective dilution and specificity. Antibodies used for quantitative western blotting included rabbit polyclonal antibodies raised against HDAC1 (1:500, Abcam, Cambridge, MA), HDAC2 (1:500, 1:20 immunofluorescence, Abcam), HDAC3 (1:500, Abcam), HDAC4 (1:500, Abcam), HDAC6 (1:500, Cell Signaling Technology, Danvers, MA), SIRT1 (1:500, Cell Signaling Technology), a goat polyclonal antibody against choline acetyltransferase ChAT (1:200, Millipore, Billerica, MA), and a mouse monoclonal antibody for β-tubulin (1:2000, Sigma, St. Louis, MO). Tissue sections were immunostained using either a rabbit polyclonal $p75^{NTR}$ (1:500, Promega Corp., Madison, WI) or a goat polyclonal $p75^{NTR}$ (1:20, immunofluorescence, Abcam) antibody and the mouse monoclonal antibody AT8 (tau phosphorylation at Ser202 and Thr205; 1:800 for 3,3′-diaminobenzidine tetrahydrochloride-dihydrate (DAB) immunohistochemistry, 1:50 for immunofluorescence, Thermo Fisher Scientific, Waltham, MA), and a mouse monoclonal antibody against the tau Asp421 cleavage neoepitope TauC3, a late-stage NFT marker (1:50 immunofluorescence, Thermo Fisher Scientific, Waltham, MA). Fluorescence signals were shown with Cy3-, Cy2-, and Cy5-conjugated anti-mouse, anti-goat, and anti-rabbit IgGs (1:200, Jackson ImmunoResearch Laboratories, West Grove, PA).

Antigen	Description of Immunogen	Source, Host Species	Dilution
HDAC1	Synthetic peptide conjugated to KLH derived from within residues 450 to the C-terminus of Human HDAC1.	Abcam, rabbit polyclonal	1:500 WB
HDAC2	Synthetic peptide conjugated to KLH derived from within residues 450 to the C-terminus of Human HDAC2.	Abcam, rabbit polyclonal	1:500 WB, IHC 1:20 IF
HDAC3	Synthetic peptide corresponding to Human HDAC3 amino acids 411-428 conjugated to Keyhole Limpet Haemocyanin (KLH).	Abcam, rabbit polyclonal	1:500 WB
HDAC4	Synthetic peptide to amino acids 1-19 of Human HDAC4 conjugated to KLH with C-terminal added lysine.	Abcam, rabbit polyclonal	1:500 WB
HDAC6	Synthetic peptide corresponding to residues surrounding Pro681 of human HDAC6 protein.	Cell Signaling, rabbit monoclonal	1:500 WB
SIRT1	Synthetic peptide corresponding to the carboxy terminus of human SIRT1	Cell Signaling, rabbit polyclonal	1:1000 WB
ChAT	Directed against the human placental enzyme choline acetyltransferase	Millipore, goat polyclonal	1:200 WB
$p75^{NTR}$	Purified rabbit IgG recognizes the cytoplasmic domain of the human p75 neurotrophin receptor	Promega, rabbit polyclonal; Abcam, goat polyclonal	1:500 IHC, 1:20 IF
AT8	Partially purified human PHF-tau, recognizes tau phosphorylated at Ser202 and Thr205	ThermoFisher, mouse monoclonal	1:800 IHC, 1:50 IF
TauC3	KLH-CSSTGSIDMVD, corresponding to the C terminus of tau truncated at Asp421	ThermoFisher, mouse monoclonal	1:50 IF

Table 3.1 Summary of Antibodies

WB, Western blot; IHC, Immunohistochemistry. IF, Immunofluorescence.

3.3.4 Semi-quantitative Immunoblotting

Frozen basal forebrain regions were dissected rostrally at the crossing of the anterior commissure, and caudally where the anterior commissure recedes into the temporal pole containing the anterior, anteromedial, anterolateral, and intermediate subregions of the nucleus basalis. Dissections did not include the hypothalamus, ventral globus pallidus, or the ventral putamen. Frozen tissue samples containing the nbM were denatured in sodium dodecyl sulfate (SDS) loading buffer to a final concentration of 5 mg/ml. Proteins (50 μg/sample) were separated by 4-20% SDS–polyacrylamide gel electrophoresis (SDS-PAGE; Lonza, Rockland, ME) and transferred to polyvinylidene fluoride membranes (Immobilon P, Millipore, Billerica, MA) electrophoretically (Counts, Nadeem et al. 2004; Mufson, He et al. 2012). Membranes were first blocked in tris-buffered saline (TBS)/0.05%Tween-20/5% milk for 60 minutes at room temperature and primary antibodies against HDACs 1, 2, 3, 4, HDAC6, and SIRT1 were added to the blocking buffers. Membranes were incubated at room temperature for 30 minutes; and then incubated overnight at 4°C. After membranes were washed in TBS/0.05% Tween-20, they were incubated for 1 hour at room temperature with horseradish peroxidase-conjugated goat anti-rabbit and anti-mouse IgG secondary antibodies (1:5,000 and 1:3,000, respectively). Immunoreactivity was visualized by enhanced chemiluminescence (Pierce, Rockford, IL) on a Kodak Image Station 440CF (Perkin-Elmer, Wellesley, MA) and bands quantified with Kodak 1D Image Analysis Software (Eastman Kodak, Rochester, NY). Basal forebrain protein immunoreactive signals were normalized to β-tubulin signals. Samples were analyzed in three independent experiments, and a single

band was visualized at the appropriate kilodalton (kDa) weight for each antibody. Controls included elimination of primary antibodies, resulting in no observable immunoreactivity.

Samples were stained for total protein detection using the LI-COR REVERT™ Kit according to the manufacturer's instructions. Briefly, serial dilutions (10-150 μg) of pooled basal forebrain samples were loaded and after transfer membranes were incubated in REVERT for 5 minutes, washed 2x for 30 seconds each in the wash solution (6.7% (v/v) glacial acetic acid, 30% (v/v) methanol, in water) and imaged using the 700 nm channel of the Odyssey imaging system (LI-COR). Densitometry of total protein staining was measured in a rectangular area automatically defined by the software. Manual adjustments were made to contain all detectable signal for a lane and background was subtracted from the lane data. All linear ranges of quantification were obtained by graphing intensities of serial dilutions and choosing a range of dilutions with the highest linearity. A protein concentration of 50 μg was chosen as the desired protein load since it exhibited linearity for all of the antibodies examined.

3.3.5 HDAC2 Immunohistochemistry

Free-floating basal forebrain sections containing the cholinergic subfields Ch4 anteromedial, anterolateral, and intermediate were used for immunohistochemical analysis (Mesulam, Mufson et al. 1983). Serial 40-μm thick sections were washed in PBS and TBS, and then incubated in 0.1 mol/L sodium metaperiodate for 20 minutes (Sigma, St. Louis, IL) to inactivate endogenous peroxidase activity. Tissue was washed in a TBS solution with 0.25% Triton X (Thermo Fisher Scientific, Waltham, MA) and placed in

TBST/Triton 3% goat serum for 1 hour. Sections were then incubated with an HDAC2 rabbit polyclonal antibody (1:500 dilution) overnight in a solution of 0.25% Triton X-100 and 1% goat serum. All washes and incubations were performed at room temperature on a shaker table. Sections were then washed in TBS and 1% goat serum before incubation with a biotinylated secondary antibody goat anti-rabbit IgG (1:200, Vector Laboratories, Burlingame, CA) for 1 hour. After TBS washes, HDAC2 staining was amplified using the Vectastain ABC kit (Vector Laboratories) for 1 hour, rinsed in a 0.2 mol/L sodium acetate solution, 1.0 mol/L imidazole buffer (pH 7.4) and developed in an acetate-imidazole buffer containing 0.05% DAB (Sigma, St. Louis, IL) and 0.0015% H_2O_2. Cytochemical reaction was terminated in an acetate-imidazole buffer, then tissue was mounted on slides and dehydrated through graded alcohols (70%-95%-100%), cleared in xylene, and cover-slipped using DPX mounting medium (Biochemica Fluka, Buchs, Switzerland). Immunohistochemical controls included deletion of the primary antibody, resulting in no observable immunoreaction. Additional HDAC2-immunoreactive (HDAC2-ir) sections were counterstained with cresyl violet to aid cytoarchitectural analysis. For each antibody, staining of all sections was performed at the same time to reduce reagent batch-to-batch variability.

3.3.6 Quantitation of HDAC2 Immunoreactivity

Quantitative HDAC2-ir was performed in 11 NCI, 11 MCI, 10 mAD, and nine sAD cases, with an average of six slides per case and 50 cells per slide. More than 50% of these cases overlapped with the cohort used for western blotting. Measurements were performed blinded to clinical and pathological diagnosis. Cholinergic neurons containing

nuclei positive for HDAC2-ir were identified by location and morphology using parallel sections counterstained with cresyl violet. HDAC2-ir nuclear area and intensity measurements were obtained using a Nikon Microphot-FXA microscope (Nikon Instruments, Melville, NY) at 40 × magnification. An average background value was obtained from 5 microscopic fields lacking HDAC2-ir profiles to yield an average background value, which was subtracted from HDAC2-ir measurements.

3.3.7 Dual $p75^{NTR}$ and AT8 Immunohistochemistry

Adjacent sections were dual immunostained for the pan neurotrophin receptor, $p75^{NTR}$, an excellent marker for human nbM neurons (Mufson, Bothwell et al. 1989), and with the tau pretangle marker AT8 (phosphorylated at Ser202 and Thr205). After development of the first antigen ($p75^{NTR}$, 1:500), tissue was soaked in an avidin/biotin blocking kit (Vector Laboratories). Prior to co-staining, any remaining peroxidase activity was further quenched with 3% H_2O_2 for 30 minutes at room temperature. Blocking buffer was reapplied for 1 hour at room temperature, and tissue was then incubated with the AT8 antibody (1:800) overnight at room temperature. Tissue was then incubated with the appropriate biotinylated secondary antibody (1:200) for 1 hour and placed in an ABC solution as described above. All tissue was developed with the Vector SG Substrate Kit (blue-gray reaction product, Vector Laboratories). Tissue was mounted on slides, dehydrated through a graded series of alcohols, and coverslipped. Immunohistochemical controls were performed to rule out any cross-reactivity or non-specific staining, including omission of the primary and secondary antibodies. Controls

were negative for immunoreactivity (data not shown). The tissue was not prepared for unbiased stereological counting.

3.3.8 Quantitation of nbM NFT Profiles

Counts of single $p75^{NTR}$, AT8, and double AT8/$p75^{NTR}$ neurons within the nbM were performed in the same cases used for single HDAC2 immunostaining. An average of 5 sections per case was analyzed using the Nikon Microphot-FXA microscope at 20× magnification. For each antibody, counts of all AT8- and AT8/$p75^{NTR}$-labeled neurons were averaged per case, as described previously (Perez, Getova et al. 2012), and normalized to the total number of $p75^{NTR}$-positive neurons. Fiduciary landmarks were used to prevent repetitive counting of labeled profiles.

3.3.9 Triple Immunofluorescence and Thioflavin-S Histochemistry

Immunofluorescence was conducted using additional free-floating nbM sections from the same cases used for single HDAC2 and dual $p75^{NTR}$/AT8 immunohistochemistry. Sections were washed 3× for 10 minutes each in PBS, TBS, and TBS/Triton (0.25%), blocked in TBS/Triton/3% donkey serum for 1 hour at room temperature, and incubated overnight in TBS/Triton/1% donkey serum and the primary antibodies ($p75^{NTR}$, HDAC2, AT8, or TauC3), washed in TBS/1% donkey serum, and incubated in TBS/1% donkey serum containing the appropriate secondary antibody for 3 hours at room temperature. Sections were then washed, mounted on glass slides, and dried overnight in the dark. The following day, the sections were defatted in equal parts chloroform and 100% ethanol for 1 hour, rehydrated through graded alcohols (10 seconds), and then placed in dH_2O for 5 minutes. Slides were then incubated in 0.02%

Thioflavin-S for 20 minutes in the dark, differentiated in 80% ethanol for 30 minutes, incubated with an autofluorescence eliminator reagent to eliminate lipofuscin autofluorescence (Millipore, Temecula, CA), and coverslipped with Aqua-Mount (Lerner Laboratories, Cheshire, WA).

HDAC2 immunofluorescent nuclear intensity was measured in nbM neurons positive for $p75^{NTR}$, $p75^{NTR}$/AT8, $p75^{NTR}$/TauC3, $p75^{NTR}$/AT8/Thioflavin-S, and $p75^{NTR}$/TauC3/Thioflavin-S. Immunofluorescence images were acquired using an Echo Revolve R4 microscope (San Diego, CA) at 40× magnification and HDAC2 intensity was analyzed with ImageJ 1.47v. Background measurements were taken and subtracted from all nuclear measurements as described above. Photomicrographs were acquired using a Zeiss LSM 710 confocal microscope (Carl Zeiss Meditec, Oberkochen, Germany) at 40× and 63× magnifications.

3.3.10 Statistical Analysis

The Kruskal-Wallis test was used to compare differences between clinical groups, age at death, education, postmortem interval, brain weight at autopsy, and time between last clinical assessment and autopsy, as well as immunoblotting data, neuronal counts, immunoreactive intensity, and nuclear area. Chi-squared analysis was used to determine whether frequency differences for sex, apolipoprotein E (APOE) ε4 carrier status, Braak stage, CERAD diagnosis, and NIA-Reagan diagnosis were present across clinical groups. The Conover-Iman test was used to discern statistically significant groupwise comparisons. Associations between nuclear area and immunoreactive intensity with demographic, cognitive, and neuropathological variables were assessed using Spearman

correlations. The false discovery rate (FDR) was used to correct for multiple comparisons in the correlation analyses to maintain a significance level of $p < 0.05$ (Glickman, Rao et al. 2014). FDR adjustments were applied to all comparisons to avoid type I error.

3.4 RESULTS

3.4.1 Demographic, Clinical, and Neuropathological Characteristics

Demographic, cognitive, and postmortem characteristics of each clinical group are presented in Table 3.2. The sAD group had a significantly younger age at death (78.75±9.10 years) compared with the MCI group (89.97±4.71 years, $p = 0.01$) and the mAD group (89.90±5.18 years, $p = 0.01$). Since the sAD group had a significantly younger age of death compared to the MCI and mAD groups, it is important to note that the current study was not just comparing different stages in disease progression, but also different disease trajectories/ages of onset. For example, a 78-year-old sAD represented the most aggressive trajectory and the 89-year-old MCI the least aggressive. No statistically significant differences in groups were found for frequency of sex ($p = 0.10$), APOE ε4 carrier status ($p = 0.28$), years of education ($p = 0.87$), postmortem interval ($p = 0.54$), and brain weight at autopsy ($p = 0.26$). Limited demographic information was available for the RADC sAD cases. The mean postmortem interval for the sAD group was 6.78±4.24 (range 2-17.3) hours, 50% were female, and the mean brain weight was 1,077.30±134.71 (range 925-1325) grams.

Although the mAD group displayed significantly lower MMSE and GCS test scores than the NCI and MCI groups ($p < 0.001$, Table 3.2), the latter 2 groups were not

significantly different ($p = 0.07$). A similar relationship was noted for episodic memory, with the mAD group scores significantly lower than those of the NCI and MCI groups ($p < 0.001$), whereas the MCI scores were significantly lower than those of the NCI group ($p = 0.01$). For semantic memory and visuospatial ability, the NCI group had significantly higher scores than both the MCI and mAD cases ($p < 0.001$). For working memory, the NCI group had significantly higher scores than both the MCI ($p = 0.04$) and mAD individuals ($p < 0.001$), whereas the MCI scores were not significantly different from those in the mAD group ($p = 0.06$). No significant differences were noted for perceptual speed between the NCI and MCI groups ($p = 0.87$), whereas mAD had significantly lower scores than both the MCI and NCI groups (both $p < 0.001$). Limited cognitive data were available for the RADC sAD group. The mean MMSE score for this group was 2.50 ± 3.57 (range 0-9).

Neuropathological data for the NCI, MCI, and mAD groups are shown in Table 3.3. No significant differences were found for total neuritic ($p = 0.18$) or diffuse ($p = 0.23$) plaque counts, total NFT counts ($p = 0.28$), CERAD ($p = 0.31$), Braak Stage ($p = 0.17$), or NIA Reagan ($p = 0.37$) among groups. Limited neuropathological data were available for the sAD group. More than 70% of sAD cases were determined to be Braak IV, the rest were Braak stage V.

	NCI	MCI	mAD	p-value	Groupwise Comparisons
N	20	13	12	-	-
Age at Death (years)	86.02±6.18	89.97±4.71	89.90±5.18	0.01	MCI>NCI
Sex (Male/Female)	12/8	3/10	3/9	0.10	-
ApoE ε4 (Carrier/Non-Carrier)	4/15*	1/12	4/8	0.28	-
Education (years)	17.60±4.39	17.38±2.47	17.67±3.34	0.87	-
MMSE	28.15±1.49	25.76±2.84	18.67±5.37	<0.001	NCI, MCI>mAD
Global Cognitive Score (z-score)	0.25±0.43	-0.56±0.35	-1.49±0.56	<0.001	NCI, MCI>mAD
Episodic Memory (z-score)	0.58±0.52	-0.46±0.62	-1.51±0.99	<0.001	NCI, MCI>mAD
Semantic Memory (z-score)	0.22±0.58	-0.46±0.63	-1.06±0.92	<0.001	NCI>MCI, NCI>mAD
Working Memory (z-score)	0.00±0.54	-0.49±0.65	-1.24±0.93	<0.001	NCI>MCI, NCI>mAD
Perceptual Speed (z-score)	-0.35±0.84	-0.77±0.75	-1.96±0.92	<0.001	NCI>mAD, MCI>mAD
Visuospatial (z-score)	0.23±0.62	-0.97±0.73	-0.79±0.70	<0.001	NCI>MCI, NCI>mAD
Post-Mortem Interval (hours)	5.98±1.58	5.61±2.23	5.45±2.33	0.54	-
Brain Weight at Autopsy (grams)	1,225.05±175.00	1,156.77±96.46	1,117.09±102.32	0.26	-

Table 3.2 Demographic and Cognitive Variables

AD, Alzheimer's disease; ApoE, apolipoprotein E; PMI, Postmortem Interval; MCI, mild cognitive impairment; MMSE, Mini-Mental State Examination; NCI, no cognitive impairment.*One individual did not APOE genotype data.

	NCI	MCI	mAD	p-value
Total Neuritic Plaque Count	17.50 [0, 43]	33 [0, 90.25]	55.50 [3, 132.50]	0.18
Total Diffuse Plaque Count	18 [0, 65]	25 [0.75, 52.50]	66 [11.50, 91]	0.23
Total Neurofibrillary Tangle Count	17.50 [7.50, 44]	28 [20.75, 66.50]	44.50 [5.50, 106]	0.28
CERAD Neuropathological Diagnosis				
No AD	9	4	3	
Possible AD	7	5	2	0.31
Probable AD	2	1	1	
Definite AD	2	3	6	
Braak Stage				
0	1	0	0	
I	2	1	2	
II	4	0	2	0.17
III	4	5	1	
IV	9	5	3	
V	0	2	4	
NIA Reagan Diagnosis				
Not AD	1	0	0	
Low Likelihood	11	6	4	0.37
Intermediate Likelihood	8	5	5	
High Likelihood	0	2	3	

Table 3.3 Neuropathological Characteristics

Median [25th %ile, 75th %ile]; AD, Alzheimer's disease; CERAD, Consortium to Establish a Registry for Alzheimer's Disease; MCI, mild cognitive impairment; NCI, no cognitive impairment; NIA, National Institute on Aging.

3.4.2 Reduction in Basal Forebrain HDAC2 and ChAT Protein Levels During AD Progression

Semi-quantitative western blotting was used to identify alterations in HDAC and SIRT protein levels in the basal forebrain region containing the nbM (Figure 3.1). HDAC1, HDAC3 ($p = 0.29$; $p = 0.92$, respectively, Figure 3.1A, C), HDAC4 ($p = 0.18$, Figure 3.1D), HDAC6 ($p = 0.46$, Figure 3.2A), and SIRT1 ($p = 0.20$, Figure 3.2B) levels were stable, whereas HDAC2 levels were significantly decreased in the sAD group compared with the NCI, MCI, and mAD groups ($p = 0.03$, Figure 3.1B). HDAC2 levels in mAD did not reach significance, however, there was a trend for an increase compared to NCI and MCI ($p = 0.12$, Figure 3.1B). ChAT levels (Figure 3.2C) were significantly decreased in the sAD group compared with the NCI ($p < 0.001$) and MCI ($p = 0.04$) groups. ChAT levels were not significantly different between the mAD and sAD groups ($p = 0.07$).

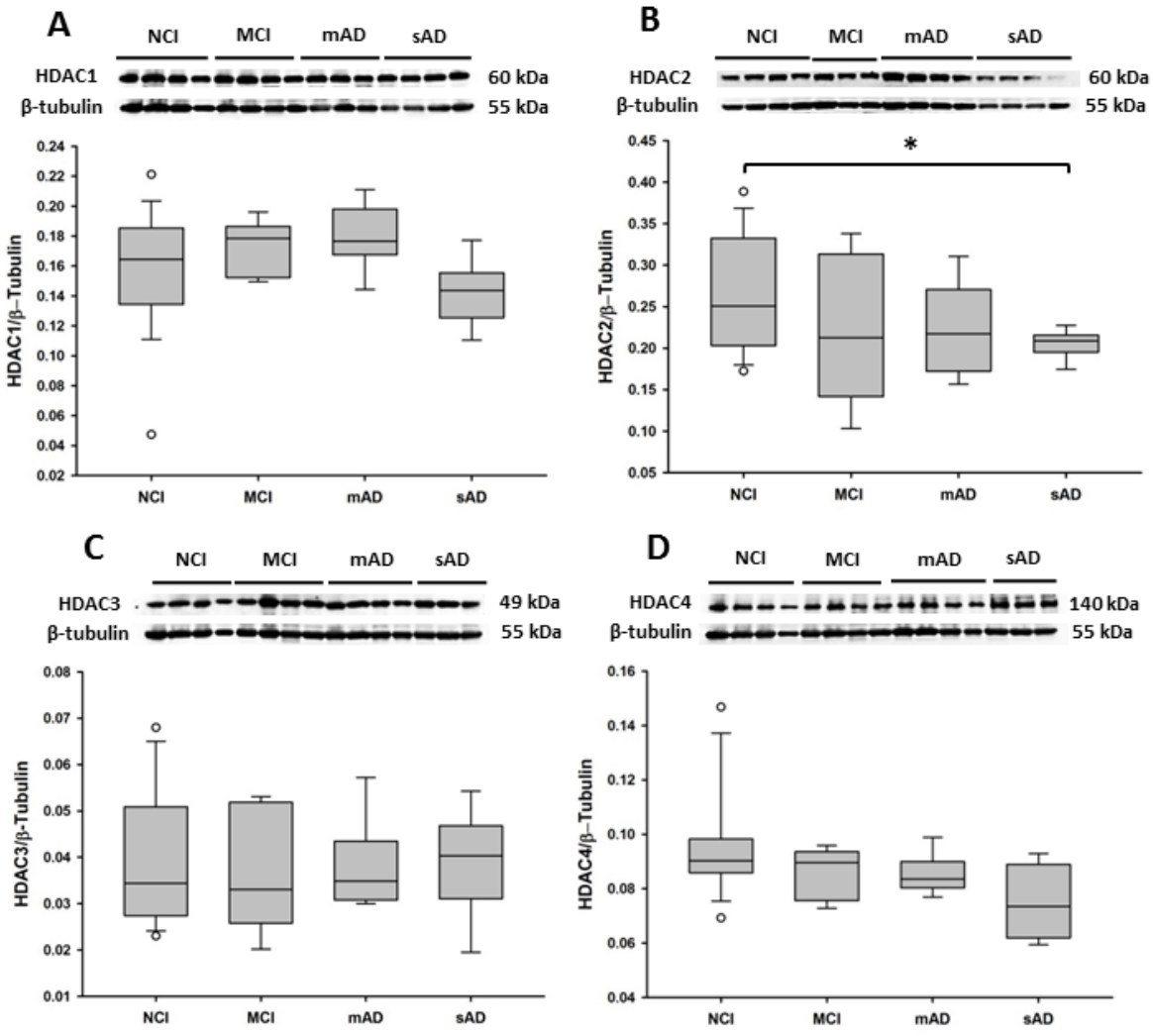

Figure 3.1 HDACs 1-4 Immunoblots and Boxplots

Representative immunoblots and box plots of levels of (A) HDAC1, (B) HDAC2, (C) HDAC3, and (D) HDAC4 in the basal forebrains of non-cognitively impaired (NCI), mild cognitively impaired (MCI), mild/moderate AD (mAD), and severe AD (sAD). Immunoreactive signals obtained by densitometry were normalized to levels of β-tubulin. (A) HDAC1 levels were stable across clinical groups. (B) HDAC2 levels were significantly decreased in the sAD group compared with those in the NCI group ($p = 0.03$). (C) HDAC3 and (D) HDAC4 levels did not change significantly across groups. Circles in box plots indicate outliers. Asterisk indicates $p < 0.05$.

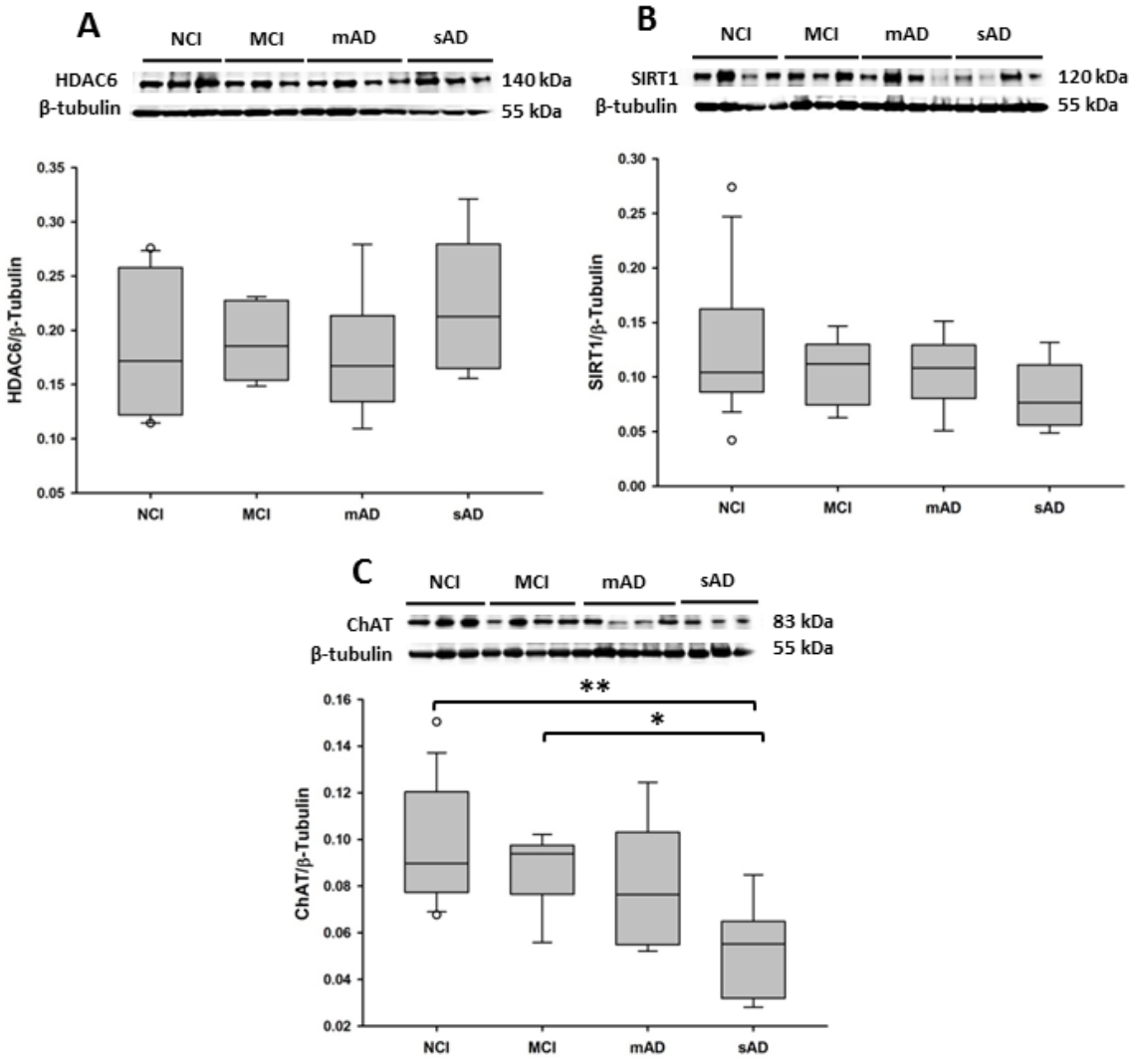

Figure 3.2 HDAC6, SIRT1 and ChAT Immunoblots and Boxplots

Representative immunoblots and box plots of (A) HDAC6, (B) SIRT1, and (C) ChAT basal forebrain levels in the non-cognitively impaired (NCI), mild cognitive impairment (MCI), mild/moderate AD (mAD), and severe AD (sAD) groups. Immunoreactive signals obtained by densitometry were normalized to levels of β-tubulin. HDAC6 (A, $p = 0.46$) and SIRT1 (B, $p = 0.20$) levels were stable across clinical groups. (C) ChAT levels were significantly decreased in the sAD group compared with those in the NCI ($p < 0.001$) and MCI ($p = 0.04$) groups. Circles in box plots indicate outliers. One asterisk indicates $p < 0.05$. Two asterisks indicate $p < 0.001$.

3.4.3 HDAC2 Immunoreactivity Decreases in the nbM in Mild and Severe AD

Since HDAC2 nuclear levels are reduced in entorhinal and hippocampal neurons in persons with AD (Mastroeni, Grover et al. 2010), we evaluated alterations in this protein in the nuclei of individual nbM neurons during AD progression (Figure 3.3). HDAC2-ir nuclei lost their rounded shape, becoming ovoid, flattened, and displaced to the periphery of the soma in the MCI, mAD, and sAD groups (Figure 3.3B-D). HDAC2-ir nuclear intensity was significantly lower in sAD than in the other clinical groups ($p < 0.001$, Figure 3.3E), whereas HDAC2-ir intensity was significantly lower in mAD than in the NCI and MCI groups (both $p < 0.001$, Figure 3.3E). HDAC2-ir intensity in the NCI and MCI groups was not significantly different ($p = 0.54$, Figure 3.3E). Significant group differences were noted for nuclear area: those in the sAD group were significantly smaller (153.32±13.95 μm^2) than NCI (184.93±17.55 μm^2, $p < 0.001$), MCI (175.91±13.07 μm^2, $p < 0.001$), and mAD (166.13±22.66 μm^2, $p = 0.04$, Figure 3.3F). The mAD group also had significantly smaller HDAC2-ir nuclear area than the NCI cases ($p = 0.03$, Figure 3.3F). HDAC2-ir glial profiles were observed surrounding cholinergic neurons in MCI, mAD, and sAD cases, which was confirmed by their smaller HDAC2 nuclear area compared to nbM nuclei positive for HDAC2 (10.71±2.08 μm^2).

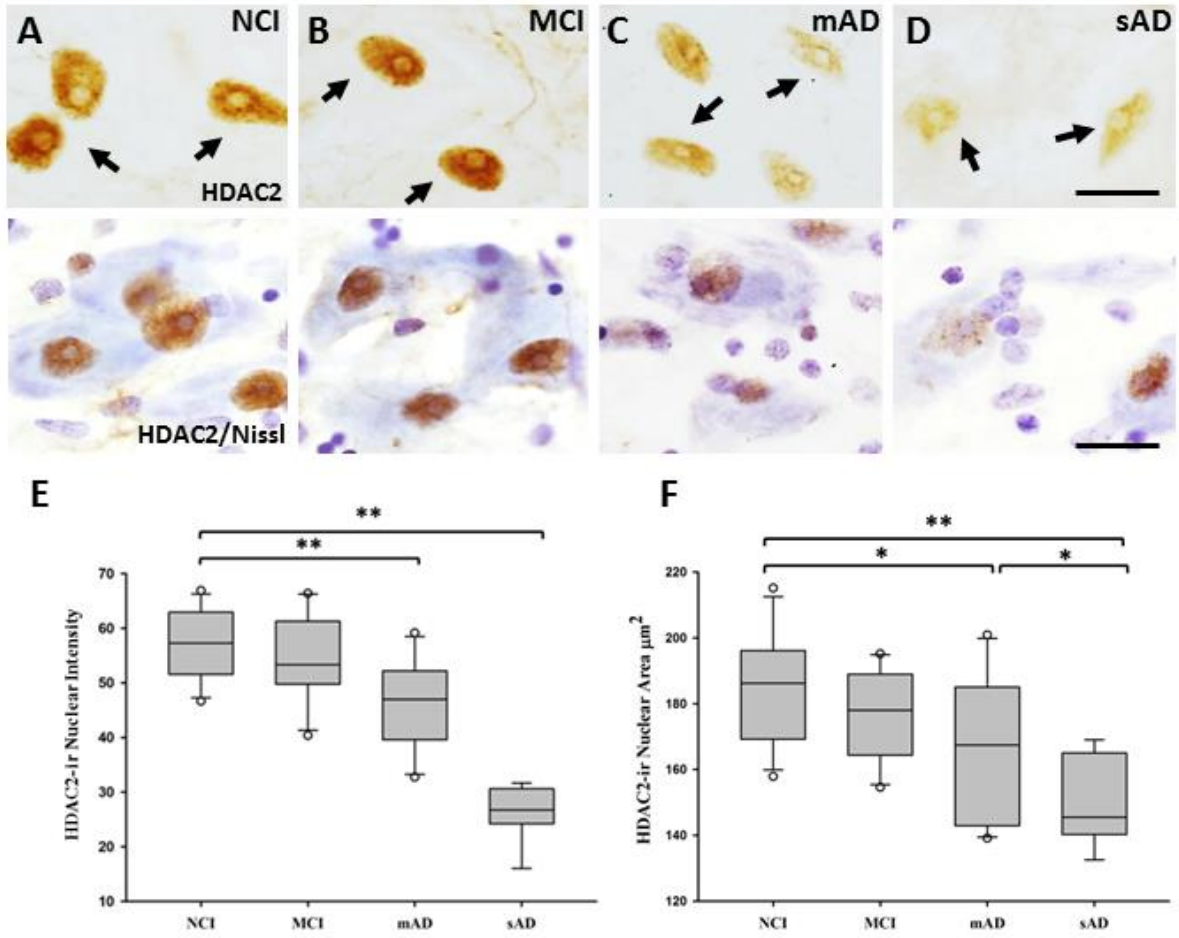

Figure 3.3 HDAC2 Nuclear Immunoreactivity and Area During AD Progression

(A-D) Photomicrographs of sections stained for HDAC2 and cresyl violet, and (E and F) box plots of HDAC2 nuclear intensity and area in non-cognitively impaired (NCI), mild cognitive impairment (MCI), mild/moderate AD (mAD), and severe AD (sAD) groups. Nuclei positive for HDAC2 (black arrows) lost their rounded shape (A) and were displaced to the periphery of the soma in the MCI, mAD, and sAD groups (B, C, and D). (E) HDAC2-ir was significantly decreased in mAD compared to NCI and MCI ($p < 0.001$), and sAD compared to NCI, MCI, and mAD ($p < 0.001$). (F) The area of the nuclei positive for HDAC2-ir was significantly decreased in mAD compared to NCI ($p = 0.03$) and in sAD compared to NCI ($p < 0.001$), MCI ($p < 0.001$), and mAD ($p = 0.04$) groups. Circles in box plots indicate outliers. One asterisk indicates $p < 0.05$; two asterisks indicate a $p < 0.001$. Scale bars: 10µm.

Since HDAC2 is involved in the aberrant expression of genes involved in learning and memory, we examined the association between nbM HDAC2 intensity and area with cognitive test performance (Table 3.4). After correcting for multiple comparisons, we found significant correlations between HDAC2-ir intensity and working memory ($r = 0.56$, $p = 0.003$, Figure 3.4A) and GCS ($r = 0.54$, $p = 0.004$, Figure 3.4B).

3.4.4 Quantitation of AT8 and p75^{NTR} nbM Neuron Numbers Across Clinical Groups

Neuronal counts were performed to determine the number of single p75^{NTR} versus AT8-positive and p75^{NTR}/AT8-positive nbM neurons within the NCI, MCI, mAD, and sAD groups (Figure 3.5). Analysis of variance revealed that the percentage of p75^{NTR}-positive neurons was significantly greater in NCI and MCI compared with mAD and sAD groups ($p < 0.001$, Figure 3.5E), whereas the percentage of AT8-positive nbM neurons increased significantly in mAD and sAD ($p < 0.01$, Figure 3.5E) compared to NCI and MCI. However, no significant differences in the percentage of p75^{NTR}/AT8-positive neurons were detected across the groups ($p = 0.05$, Figure 3.5E). AT8-positive neuropil threads were also scattered within the basal forebrain. Increased HDAC2 nuclear staining strongly correlated with p75^{NTR}-ir neuronal counts across clinical groups ($r = 0.65$, $p < 0.001$, Figure 3.6A). Counts of AT8-positive perikarya were negatively correlated with HDAC2-ir ($r = -0.60$, $p < 0.001$, Figure 3.6B). AT8/p75^{NTR}-positive neuronal counts were negatively correlated with HDAC2-ir in the nbM ($r = -0.59$, $p < 0.001$, Figure 3.6C). HDAC2-ir nuclear area was not correlated with AT8 ($r = -0.33$, $p = 0.06$) or AT8/p75^{NTR} ($r = -0.17$, $p = 0.32$) neuronal counts. The percentage of AT8-positive cells in the nbM was negatively correlated with semantic memory z-scores ($r = -0.50$, $p = 0.008$, Table

	MMSE	GCS	Episodic Memory	Semantic Memory	Working Memory	Perceptual Speed	Visuospatial Ability
HDAC2 immunoreactivity	0.45 p = 0.02	**0.54** **p = 0.004**	0.40 p = 0.04	0.35 p = 0.07	**0.56** **p = 0.003**	0.37 p = 0.06	0.18 p = 0.38
HDAC2 nuclear area	0.23 p = 0.25	0.36 p = 0.07	0.19 p = 0.33	0.33 p = 0.09	0.19 p = 0.34	0.13 p = 0.52	0.29 p = 0.14
% $p75^{NTR}$	0.28 p = 0.16	0.40 p = 0.04	0.32 p = 0.10	0.37 p = 0.06	0.23 p = 0.25	0.15 p = 0.46	0.18 p = 0.38
% AT8	-0.36 p = 0.07	-0.44 p = 0.02	-0.39 p = 0.05	**-0.50** **p = 0.008**	-0.17 p = 0.39	-0.36 p = 0.06	-0.04 p = 0.85
% $p75^{NTR}$/AT8	-0.08 p = 0.69	-0.23 p = 0.26	-0.08 p = 0.67	-0.16 p = 0.43	-0.14 p = 0.49	0.06 p = 0.77	-0.06 p = 0.77

Table 3.4 Correlations Between HDAC2 Immunoreactivity, Percentages of $p75^{NTR}$ and AT8-ir Neurons and Cognitive Domains

False Discovery Rate significance level = 0.01. Bolded r and p values denote statistical significance after correcting for multiple comparisons. MMSE, Mini-Mental state examination; GCS, Global Cognitive score.

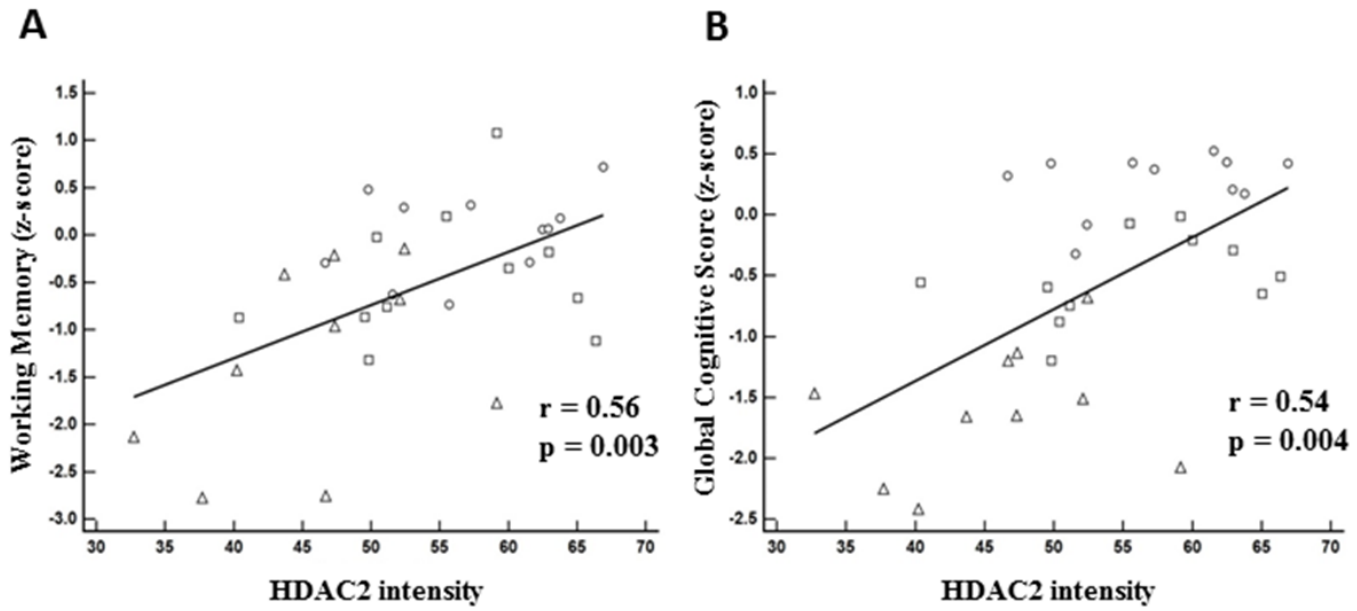

Figure 3.4 Scatter Plots Depicting Correlations Between HDAC2 and Cognitive Tests

(A, B) Scatter plots depicting correlations between HDAC2-ir intensity and cognitive test scores. (A) HDAC2 nuclear intensity correlated positively with working memory z-scores (r=0.56, p = 0.003) and (B) Global cognitive scores (r=0.54, p = 0.004) across disease progression. Cognitive data were not available for sAD cases. NCI, circles; MCI, squares; mAD, triangles.

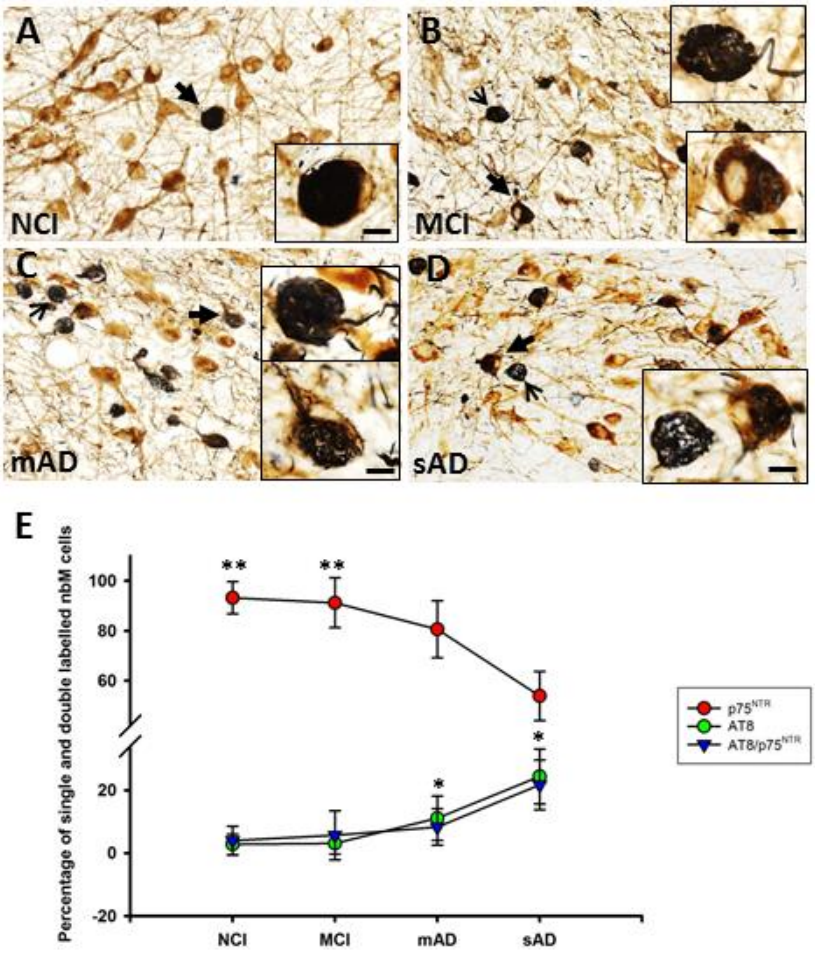

Figure 3.5 Quantitation of AT8 and p75^{NTR} Positive nbM Neurons Across AD Progression

Photomicrographs of nbM tissue dual immunostained for p75^{NTR} (brown) and AT8 (dark blue/black) in (A) NCI, (B) MCI, (C) mAD, and (D) sAD groups. Note the presence of more p75^{NTR}/AT8-positive (closed arrow) and AT8-positive perikarya (open arrow) in (B) MCI, (C) mAD, and (D) sAD. The percentage of p75^{NTR}-positive neurons (red circles, E) was significantly greater in the NCI and MCI groups than in the mAD and sAD groups ($p < 0.001$). The percentage of AT8-positive perikarya (green circles, E) increased significantly in the mAD and sAD groups ($p < 0.01$) compared to the NCI and MCI groups. No significant differences in the percentage of p75^{NTR}/AT8-positive neurons (blue triangle, E) were detected across the groups ($p = 0.05$). One asterisk indicates $p < 0.05$; two asterisks indicate a $p < 0.001$. Scale bars: 50 µm, 10 µm for inset.

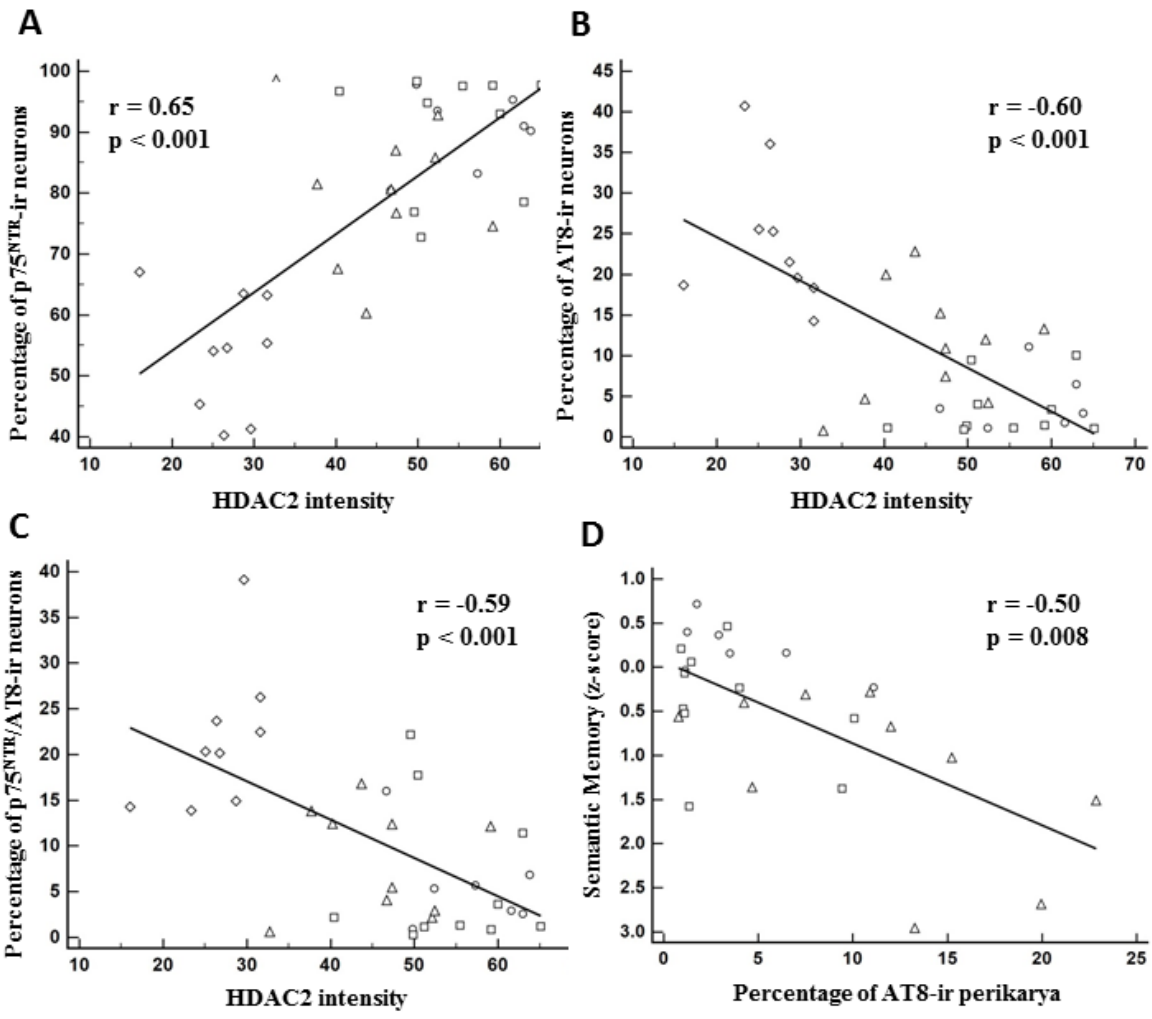

Figure 3.6 Nuclear HDAC2-ir Correlates with the Loss of p75^{NTR} and Gain of AT8 Phenotype in AD

Scatterplots depicting correlations between HDAC2 nuclear intensity and percentages of single-labeled and dual-labeled p75^{NTR}/AT8 perikarya and cognitive measures.HDAC2-ir was positively correlated with the percentage of single-labeled p75^{NTR}-ir neurons (r=0.65, $p < 0.001$, A) and was negatively correlated with the percentage of single-labeled AT8-ir ($r= -0.60$, $p < 0.001$, B) and double-labeled p75^{NTR}/AT8-ir perikarya ($r= -0.59$, $p < 0.001$, C). The percentage of AT8-ir perikarya was negatively correlated with semantic memory z-score ($r= -0.50$, $p = 0.008$, D). NCI, circles; MCI squares; mAD, triangles; sAD, diamonds.

3.4, Figure 3.6D). In addition, the percentage of $p75^{NTR}$ positive nbM neurons was negatively correlated with neuritic plaques (NPs, r= -0.68, p <0.001), diffuse plaques (DPs, r= -0.64, p <0.001), and NFT load (r= -0.51, p = 0.006) in the midfrontal cortex in the same cases (Table 3.5). Counts of single AT8 positive neurons in the nbM were positively correlated with NPs (r=0.68, p<0.001), DPs (r=0.61, p = 0.001), and NFT counts (r=0.56, p = 0.002). Double $p75^{NTR}$/AT8 positive neurons were positively correlated with NPs (r=0.52, p = 0.005) and DPs (r= 0.56, p = 0.002).

	NP Load	DP Load	NFT Load
HDAC2 –ir intensity	-0.13 p = 0.51	-0.24 p = 0.22	0.25 p = 0.22
HDAC2-ir nuclear area	-0.08 p = 0.68	-0.04 p = 0.83	-0.17 p = 0.40
% $p75^{NTR}$-ir neurons	**-0.68** **p<0.001**	**-0.64** **p<0.001**	**-0.51** **p = 0.006**
% AT8-ir neurons	**0.68** **p<0.001**	**0.61** **p = 0.001**	**0.56** **p = 0.002**
% $p75^{NTR}$/AT8-ir neurons	**0.52** **p = 0.005**	**0.56** **p = 0.002**	0.44 p = 0.02

Table 3.5 Protein Correlations with Plaque and Tangle Load

False Discovery Rate significance level = 0.01. Bolded r and p values denote statistical significance after correcting for multiple comparisons. NP, neuritic plaque; DP, diffuse plaque; NFT, neurofibrillary tangle.

3.4.5 HDAC2 Levels Decline in AT8- and TauC3-Positive nbM Neurons

We examined whether HDAC2 nuclear levels were related to the development of NFTs within nbM neurons during disease onset. We identified whether changes in HDAC2-ir nuclei were associated with the early phosphorylation-dependent (AT8) or the later stage caspase cleavage-dependent (TauC3) tau isoform. In addition, we also used Thioflavin-S histochemistry to reveal the presence of β-pleated sheet structures in NFT-bearing cholinergic neurons. Data related to HDAC2 nuclear immunoreactivity in tangle and non-tangle bearing cholinergic neurons is summarized in Table 3.6 and Figure 3.7. HDAC2-ir was significantly decreased in non-NFT–bearing $p75^{NTR}$-positive neurons across disease progression ($p < 0.001$, NCI>mAD and sAD; MCI>mAD and sAD; mAD>sAD, Figure 3.7A, F, K, P, respectively). Moreover, cholinergic neurons, which were AT8-positive (Figure 3.7B, G, L, Q) or TauC3-positive (Figure 3.7D, I, N, S), displayed even less HDAC2 nuclear immunoreactivity across clinical groups ($p < 0.001$, NCI, MCI, and mAD>sAD, Figure 3.7B-E, G-J, L-O, Q-T, respectively). Similarly AT8/Thioflavin-S–positive and TauC3/Thioflavin-S–positive cholinergic nbM neurons showed a greater decrease in HDAC2-ir during disease progression ($p < 0.001$, NCI>sAD, MCI>mAD>sAD; NCI, MCI, and mAD>sAD, respectively, Table 3.6). A within-group analysis across all clinical groups revealed that HDAC2 nuclear immunoreactive levels were highest in single $p75^{NTR}$ neurons negative for AT8, TauC3, AT8/Thioflavin-S, or TauC3/Thioflavin-S ($p < 0.05$, Table 3.6). In the MCI group, HDAC2-ir was greater in cholinergic neurons bearing AT8, TauC3, or AT8/Thioflavin-S than in those bearing TauC3/Thioflavin-S ($p < 0.05$, Table 3.6). In the mAD group,

HDAC2-ir was greater in AT8-positive orTauC3-positive neurons than in AT8/Thioflavin-S–positive or TauC3/Thioflavin-S–positive neurons ($p < 0.05$, Table 3.6). Cholinergic neurons, which were AT8 positive, had greater HDAC2-ir than neurons bearing AT8/Thioflavin-S or TauC3/Thioflavin-S in the sAD group ($p < 0.05$, Table 3.6). Interestingly, nuclear HDAC2-ir in cholinergic nbM neurons labeled for AT8 ($p = 0.03$) or TauC3/Thioflavin-S ($p < 0.05$) was significantly lower in females than males across clinical groups. We previously reported sex differences in trkA mRNA in cholinergic nbM neurons during AD onset (Counts, Che et al. 2011). After correcting for multiple comparisons, within-group correlations revealed a significant correlation between HDAC2-ir intensity in AT8 positive neurons with working memory scores in MCI ($r = -1.0$, $p < 0.0001$), and a significant correlation between HDAC2 nuclear intensity in TauC3 positive cholinergic neurons with visuospatial scores in NCI ($r = -1.0$, $p< 0.0001$).

HDAC2-ir	NCI	MCI	mAD	sAD	p-value	Groupwise Comparisons
$p75^{NTR}$	139.03±19.97	139.46±5.98	116.34±7.97	89.84±8.92	<0.001	NCI>mAD, sAD MCI>mAD, sAD mAD>sAD
$p75^{NTR}$/AT8	81.90±13.91	85.93±12.05	74.64±11.40	41.58±10.13	<0.001	NCI, MCI, mAD>sAD
$p75^{NTR}$/TauC3	93.80±19.14	95.02±6.26	78.13±14.68	36.52±22.26	<0.001	NCI, MCI, mAD>sAD
$p75^{NTR}$/AT8/T	72.15±26.85	84.24±12.16	52.50±7.59	18.91±6.97	<0.001	NCI>sAD MCI>mAD, sAD mAD>sAD
$p75^{NTR}$/TauC3/T	69.90±20.25	64.24±13.15	46.90±15.70	18.20±6.74	<0.001	NCI, MCI, mAD>sAD
Within-Group Comparisons	$p75^{NTR}$ > other groups	$p75^{NTR}$ > other groups; $p75^{NTR}$ /AT8, $p75^{NTR}$ /TauC3, $p75^{NTR}$/AT8/T > $p75^{NTR}$ /TauC3/T	$p75^{NTR}$ > other groups; $p75^{NTR}$ /AT8, $p75^{NTR}$ /TauC3 > $p75^{NTR}$/AT8/T, $p75^{NTR}$/TauC3/T	$p75^{NTR}$ > other groups $p75^{NTR}$ /AT8 > $p75^{NTR}$/AT8/T, $p75^{NTR}$/TauC3/T	$p < 0.05$	N/A

Table 3.6 HDAC2 Nuclear Immunoreactivity in Tangle and Non-tangle Bearing nbM Neurons

Mean ± standard deviation; mAD, mild/moderate Alzheimer's disease; MCI, mild cognitive impairment; NCI, no cognitive impairment, sAD, severe Alzheimer's disease; HDAC2, histone deacetylase 2; $p75^{NTR}$, pan neurotrophin receptor; T, Thioflavin-S.

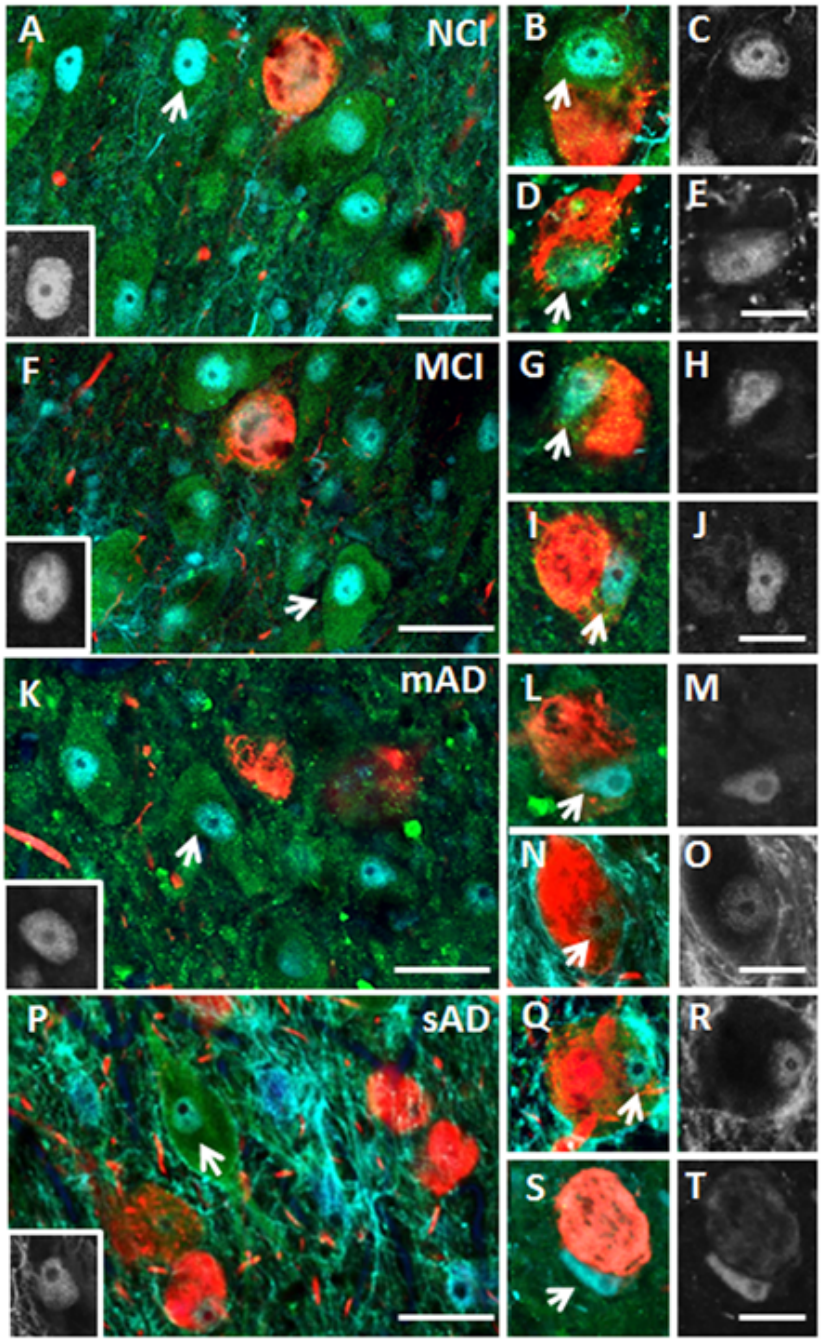

Figure 3.7 HDAC2 Levels Decline in AT8- and TauC3-Positive nbM Neurons

(A-T) Fluorescent photomicrographs of $p75^{NTR}$-ir nbM tissue stained for HDAC2 (cyan), $p75^{NTR}$ (green), AT8 (red), TauC3 (red), and Thioflavin-S (blue). HDAC2-ir decreases in nbM neurons labeled for $p75^{NTR}$ and AT8 from (A) NCI, (F) MCI, to (K) mAD, and (P)

sAD (arrow identifies HDAC2-ir nucleus shown in greyscale inset). Nuclear HDAC2-ir declines in $p75^{NTR}$-positive neurons labeled for AT8/HDAC2 and HDAC2 alone (arrow identifies same nucleus in black and white images) in NCI (B, C), MCI (G, H), mAD (L, M), and sAD (Q, R) and in nbM neurons triple-labeled for $p75^{NTR}$/HDAC2/TauC3, and HDAC2 alone in NCI (D, E), MCI (I, J), mAD (N, O), and sAD (S, T). Note displacement and shrinkage of nuclei positive for HDAC2-ir in tangle-bearing cholinergic nbM neurons. Scale bars: 50 µm (A, F, K, P); 10 µm (B-E, G-J, L-O, Q-T).

3.5 DISCUSSION

HDACs are dynamic enzymes capable of altering chromatin structure and shifting the epigenetic landscape of the brain. These proteins have multiple cellular functions, including gene transcription important for learning, memory, and neuroinflammation (Guan, Haggarty et al. 2009; Graff, Rei et al. 2012; Hsing, Hung et al. 2015; Peng, Zhao et al. 2015), regulation of genome stability (Pan, Penney et al. 2014), and cellular toxicity (Coppede 2014). Increasing evidence from animal studies suggests not only that HDAC2 plays a negative role in hippocampus-dependent cognition in aging but also that protein alterations are present in multiple regions in the AD brain (Julien, Tremblay et al. 2009; Mastroeni, Grover et al. 2010; Graff and Tsai 2013; Mahady, Nadeem et al. 2018). Our data demonstrate that cholinergic nbM HDAC2 levels are selectively altered in AD, correlating with impaired cognitive performance, and are concomitant with NFT formation during disease progression.

Semi-quantitative western blotting revealed that basal forebrain HDAC1, HDAC3, HDAC4, HDAC6, and SIRT1 levels were stable, whereas HDAC2 levels were significantly decreased in the sAD group compared with those in the NCI, MCI and mAD groups. Recent investigations suggest that changes in epigenetic markers are not similar across brain regions in AD. A clinical pathological investigation identified significant increases in protein levels of HDAC1 and HDAC3 in MCI and mAD and a decrease in sAD compared with NCI individuals in the frontal cortex (Mahady, Nadeem et al. 2018). However, HDAC2 levels in the frontal cortex remained stable across clinical groups. HDAC4 was significantly increased in MCI and mAD, but not in sAD compared with

NCI cases. HDAC6 increased significantly during disease onset, whereas SIRT1 decreased in the MCI, mAD, and sAD groups compared with the NCI group (Mahady, Nadeem et al. 2018). These latter results suggest that epigenetic changes differ across brain regions during the progression of AD. This regional specificity of HDAC alterations could differentially affect the suggested epigenetic blockade of neuroplasticity-related gene expression by which memory may become permanently impaired in AD. Functionally, HDAC2 is a modulator of chromatin plasticity that forms co-repressor complexes with HDAC1 to alter gene expression. HDAC2 negatively regulates structural and functional synaptic plasticity (Akhtar, Raingo et al. 2009), altering synaptic transcript levels, immediate early gene expression, and the neuronal survival protein brain-derived neurotrophic factor (Guan, Haggarty et al. 2009; Graff, Rei et al. 2012). In addition, HDAC2 regulates the expression of neuroinflammatory genes, and in combination with other transcription factors mediates the cellular response to oxidative stress and neuronal apoptosis (Hsing, Hung et al. 2015; Peng, Zhao et al. 2015). Thus, HDAC2 is situated in an important position to control expression of multiple proteins important for neuronal survival and programmed cell death in AD.

ChAT mRNA and protein levels are epigenetically regulated via hyperacetylation of the core promoter region of the *ChAT* gene in NG108-15 neuronal cultures (Aizawa, Teramoto et al. 2012). Despite a reduction in HDAC2 nuclear levels in cholinergic nbM neurons in MCI, ChAT protein levels were significantly decreased only in AD compared with NCI and MCI levels; suggesting that the downregulation of HDAC2 does not affect ChAT activity in nbM neurons early in the disease process. The maintenance of basal

forebrain ChAT levels until sAD supports our previous findings showing a reduction in cortical ChAT activity in sAD compared to that in NCI and MCI subjects (DeKosky, Ikonomovic et al. 2002). The stability of ChAT activity in both the basal forebrain and frontal cortex lends support to the suggestion that the cholinergic system displays a neuroplasticity response during the early stages of the disease (DeKosky, Ikonomovic et al. 2002; Mufson, Malek-Ahmadi et al. 2016), which is not affected by changes in HDAC2 levels.

This reduction in HDAC2 within cholinergic nbM neurons is similar to the reduction seen in entorhinal cortex layer II neurons and other methylation factors in AD (Mastroeni, Grover et al. 2010). HDAC2 but not HDAC1 or HDAC3 has been found to be increased in CA1 hippocampal and entorhinal cortex nuclei in AD compared with non-cognitively impaired aged controls (Graff, Rei et al. 2012). The discrepancy between these findings may be related to the case selection criteria used in each study. Graff et al. indicated that their cases were chosen based upon a Braak tangle score (Graff, Rei et al. 2012), whereas the method of selection was not clearly stated by Mastroeni et al (Mastroeni, Grover et al. 2010). Moreover, there is limited clinical information about the control and AD cases in each study. In addition, in MCI we observed a 95% reduction of HDAC2-ir nuclear diameter compared with that in NCI cases. In mAD and sAD, HDAC2-ir nuclear diameter was reduced to 89% and 81%, respectively. Our findings are similar to a reported 79% reduction in the nbM nuclear area of AD patients compared with that of controls (Rinne, Paljarvi et al. 1987). With regard to cognition, impaired spatial and associative memory in murine models of neurodegeneration is rescued by

short-hairpin knockdown of neuronal HDAC2, which has been suggested to accumulate and block transcription of memory-related genes in the rodent hippocampus (Guan, Haggarty et al. 2009; Graff, Rei et al. 2012). We found that nbM HDAC2 levels were correlated positively with working memory and global cognitive z-scores, which indicate that preserved HDAC2 levels in the basal forebrain may be indicative of better cognitive function, thereby supporting the use of HDAC drugs for the treatment of AD.

The decline in nbM nuclear HDAC2 levels is exacerbated by the presence of NFT pathology. The current findings agree with previous reports of a reduction in HDAC2 nuclear reactivity in the entorhinal cortex in AD (Mastroeni, Grover et al. 2010) and its association with early NFT formation (Graff, Rei et al. 2012). We also found that as the number of $p75^{NTR}$ neurons decreased across disease stages, there was a concomitant decrease in HDAC2 nuclear immunoreactivity. Furthermore the reduction in HDAC2 nuclear immunoreactivity inversely correlated with an increase in the number of AT8-positive nbM neurons. Quantitative analysis of the intensity of HDAC2 nuclear immunoreactivity revealed a significant reduction in non-tangle bearing $p75^{NTR}$-positive neurons in the mAD and sAD groups compared with those in the NCI and MCI groups. Cholinergic nbM neurons triple-labeled for $p75^{NTR}$, AT8, or TauC3 displayed an even greater reduction in HDAC2 immunoreactivity in the mAD and sAD groups compared with the non-tangle bearing $p75^{NTR}$ neurons at each disease stage. Within-group analyses indicated that HDAC2 immunoreactivity was highest in non-tangle bearing cholinergic neurons in each clinical group. Interestingly, HDAC2 nuclear immunoreactivity was further reduced in cholinergic nbM neurons co-labeled for either

HDAC2/AT8/Thioflavin-S or HDAC2/TauC3/Thioflavin-S in the MCI and mAD groups. These findings suggest that although a reduction in HDAC2 occurs before the onset of fibrillar tau pathology; this reduction is exacerbated by the presence of phosphorylated and conformational tau epitopes during the progression of AD. Since cholinergic nbM neurons contain oligomeric tau early in the disease process (Tiernan, Mufson et al. 2018), the role that oligomeric tau plays in the reduction of HDAC2 before the development of NFTs remains to be determined.

Abnormal phosphorylation and truncation of tau has not been directly linked to HDAC2 dysregulation in AD; however, aberrant kinase and caspase activation has been associated with alterations in HDAC2 expression (Graff, Rei et al. 2012). In this regard, proline-directed serine/threonine tau kinases, which include cyclin-dependent kinase 5 (Cdk5) (Johnson and Stoothoff 2004) affect tau phosphorylation at Ser202/Thr205 (AT8) and Ser396/Ser404 (PHF-1) sites (Plattner, Angelo et al. 2006). Cdk5 also functions as a glucocorticoid receptor kinase, and when bound to the glucocorticoid responsive element within the proximal HDAC2 promoter region, stimulates HDAC2 expression (Graff, Rei et al. 2012; Graff and Tsai 2013). Thus Cdk5 may be involved in both tau hyperphosphorylation and HDAC2 transcript regulation via glucocorticoid receptor kinase activity in AD. This interaction may underlie the reduction in HDAC2 reactivity observed in AT8-bearing neurons. However, further examination of the relationship among Cdk5, AT8, and HDAC2 in AD is required.

In each clinical group, HDAC2 nuclear immunoreactivity was the lowest in cholinergic TauC3/Thioflavin-S–positive neurons. TauC3 is a caspase-dependent

cleavage epitope associated with apoptotic events and the phenotypic loss of $p75^{NTR}$ in nbM neurons (Vana, Kanaan et al. 2011). Epigenetic shifts are thought to orchestrate entry or reentry into the cell cycle, which would lead to apoptosis in postmitotic neurons, including those in AD (Golubnitschaja 2007). The role of HDAC2 in apoptotic signaling in cancer is well established. Downregulation of HDAC2 expression inhibits cell proliferation, arrests the cell cycle at the G0/G1 phase, and induces cell apoptosis in cell culture models of cancer (Li, Wang et al. 2017). Activation of caspase 3 and caspase 7 is significantly increased *in vivo* upon depletion of HDAC2 (Schuler, Fritsche et al. 2010); silencing HDAC2 is sufficient to decrease NF-κB activity induced by tumor necrosis factor-α (TNFα) and to sensitize cells to TNFα-induced apoptosis (Kaler, Sasazuki et al. 2008). Thus, either HDAC2 changes in combination with the loss of DNA methylation or other factors may explain the reported neuronal cell cycle reentry, apoptosis, or caspase activation in AD (Yang, Mufson et al. 2003).

The current findings indicate that nuclear HDAC2 levels are initially altered in cholinergic nbM neurons in MCI, which suggest that HDAC2 may be a potential preclinical AD biomarker. Neuroepigenetic imaging has recently become available with the advent of HDAC positron emission tomography tracers such as [11C] Martinostat, which detects class I and II HDACs (Wang, Yu et al. 2013; Schroeder, Wang et al. 2014; Wang, Schroeder et al. 2014; Wey, Gilbert et al. 2016). These imaging tools may be used to identify regional HDAC changes in the human brain in light of the apparent complex multiregional response of epigenetic dysregulation observed in the entorhinal cortex (Mastroeni, Grover et al. 2010; Graff, Rei et al. 2012), hippocampus (Graff, Rei et al.

2012), frontal cortex (Mahady, Nadeem et al. 2018), and basal forebrain (current study). Mapping epigenetic alterations in different brain regions and uncovering the molecular and cellular mechanisms related to disease pathogenesis may provide the basis for novel therapeutic platforms for the treatment of dementia.

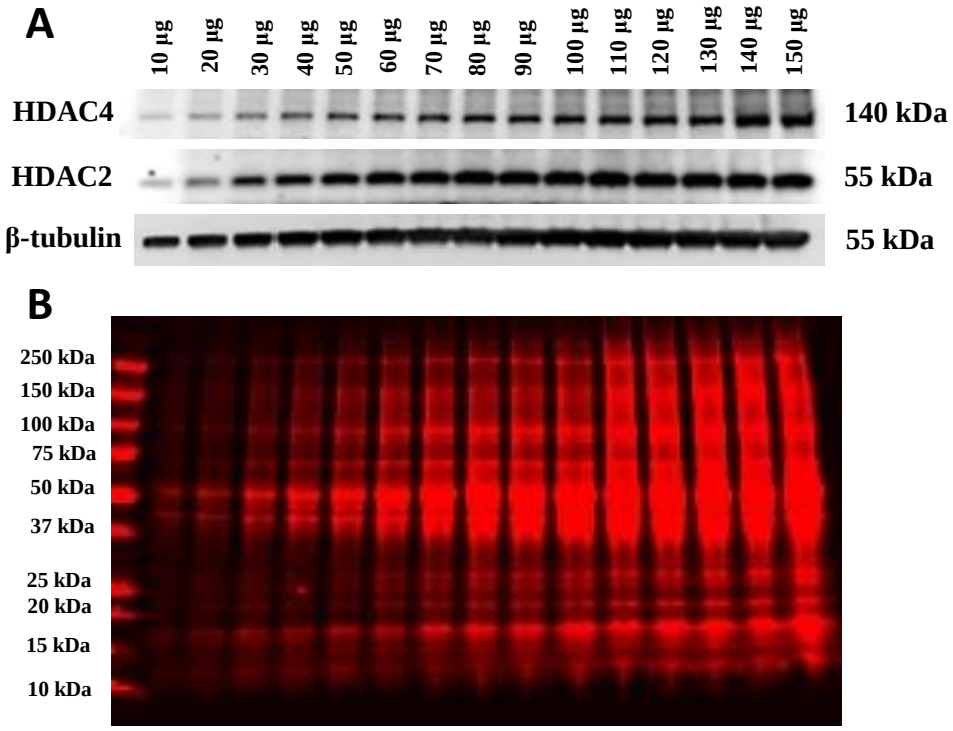

Figure 3.8 Serial Basal Forebrain Protein Dilutions for Linear Dynamic Range

Representative immunoblots (A) of basal forebrain homogenate serial dilutions (10-150 µg) probed for HDAC4, HDAC2, and β-tubulin. (B) Immunoblot stained for total basal forebrain protein.

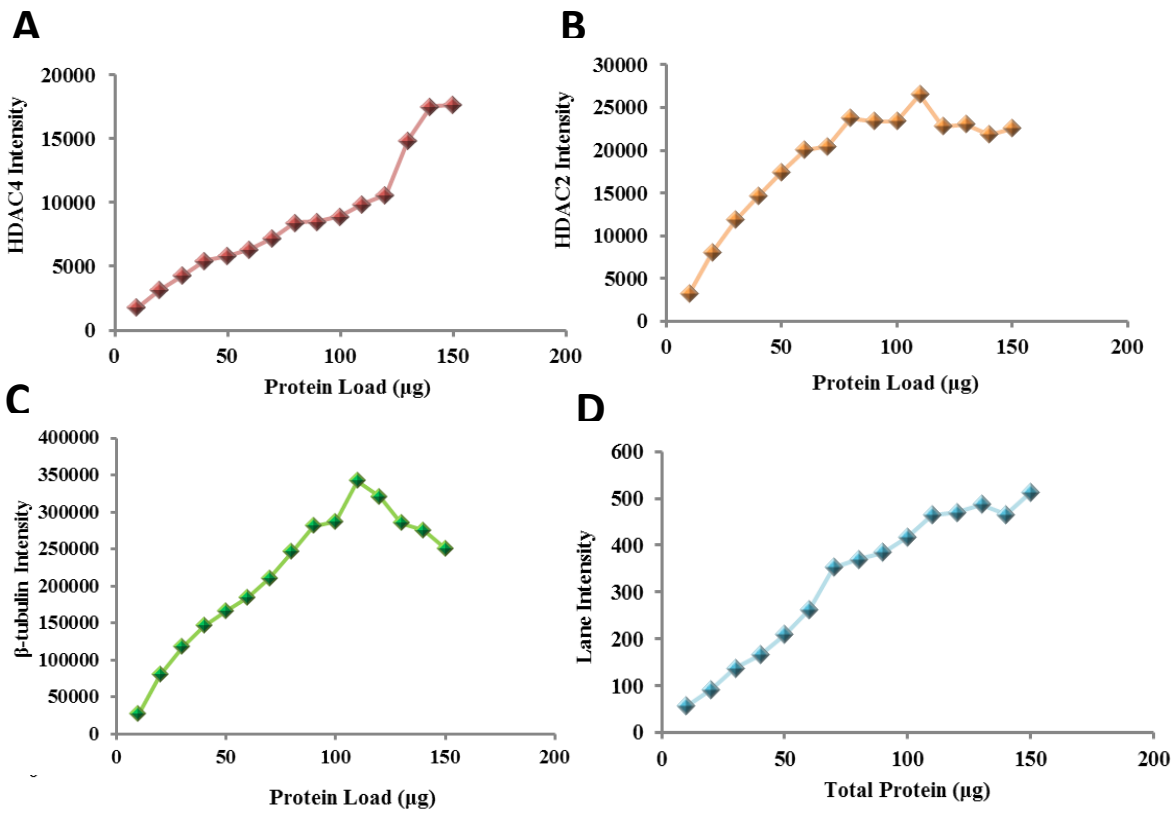

Figure 3.9 Linear Dynamic Ranges for HDAC4, HDAC2, β-tubulin, and Total Protein

(A-D) Basal forebrain homogenates were pooled and dilutions of 10-150 µg total protein were used to determine the linear dynamic range of HDAC4, HDAC2, and β-tubulin. The linear dynamic range for HDAC4 (A) is 10-120 µg, for HDAC2 (B) the range is 10-60 µg, and for β-tubulin (C) the range is 10-70 µg. The linear dynamic range for total protein was wider than β-tubulin (D) with linearity from 10-100 µg.

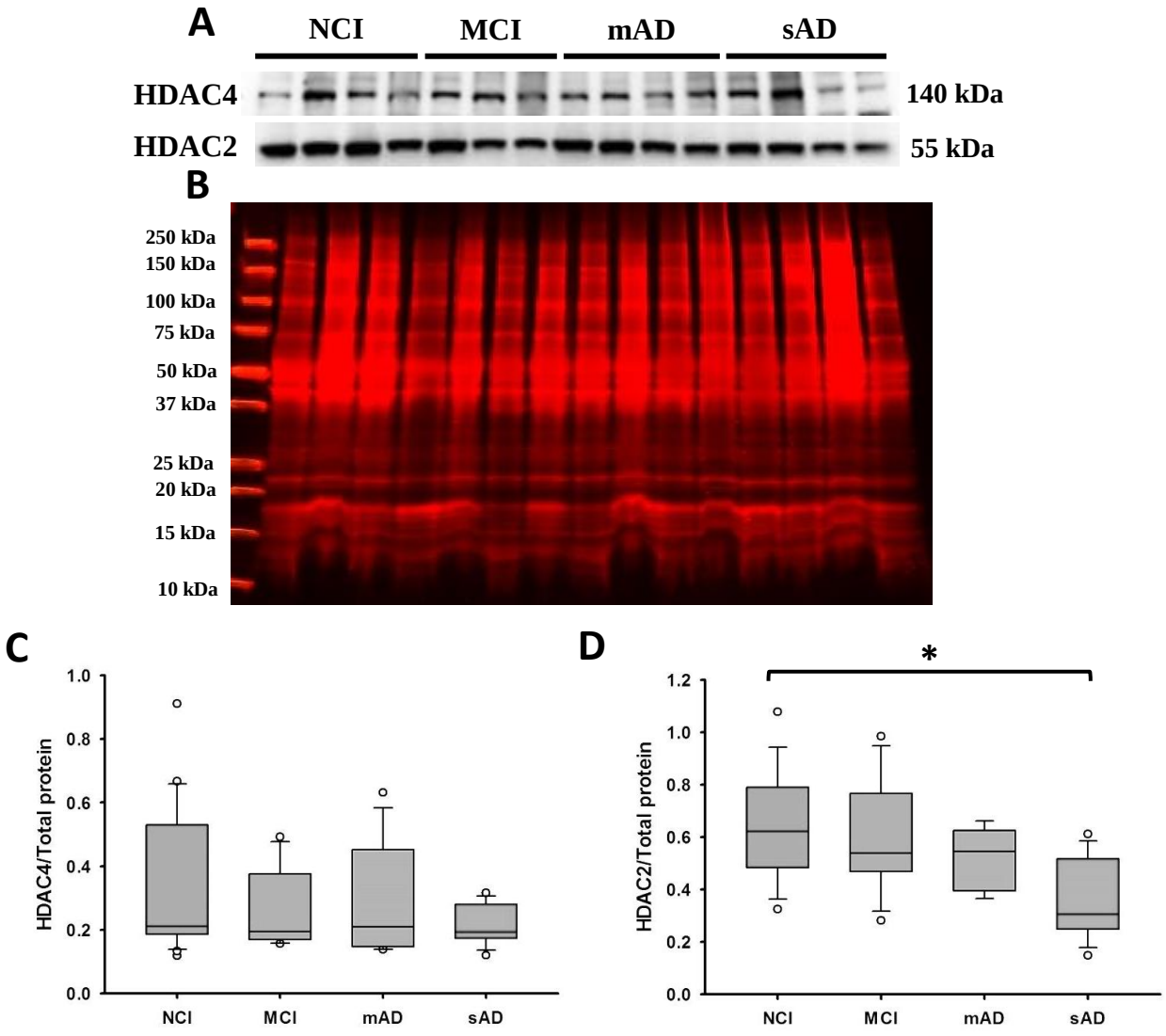

Figure 3.10 HDAC2 and HDAC4 Total Protein Normalization and Quantification

(A) Representative immunoblots probed for HDAC4 and HDAC2 normalized to total basal forebrain protein (B), and quantification across clinical groups HDAC4 (C), and HDAC2 (D). There was no significant change in HDAC4 levels across disease progression ($p = 0.84$; A, C), while HDAC2 levels decreased in the basal forebrain in sAD compared to NCI ($p = 0.02$; A, D).

CHAPTER 4

DISCUSSION

The etiology and molecular pathogenesis of AD is complex, including remarkable heterogeneity of genetic and environmental risk factors, alterations in gene expression, neuropathologic processes, and perhaps most telling, none of these risk factors have complete penetrance in AD (Mastroeni, Grover et al. 2011). Epigenetic modifications can orchestrate gene transcription in numerous cell types and thus may be at the heart of multifactorial diseases such as AD. The studies presented here are the first to investigate epigenetic alterations in the basocortical cholinergic system in AD and provide a foundation for investigating pharmacological treatments targeting chromatin modifiers that alter the cellular pathogenesis underlying the progression of AD. The demonstration of early HDAC dysregulation in the frontal cortex and nuclei of cholinergic nbM neurons suggests that these proteins may be therapeutic targets for AD; perhaps in combination with cholinomimetics and anti-tau and amyloid therapies. Moreover, the present investigations emphasize the importance of applying a "systems biology" approach to tissue obtained from cases that receive extensive premortem clinical and postmortem neuropathological evaluation. These studies recognize the multifactorial, dynamic, and connectivity-based nature of AD and provide novel information about the complex cellular dysfunction that occurs during the course of AD.

4.1 DEACETYLASE LEVELS IN THE BASOCORTICAL CHOLINERGIC SYSTEM DURING THE ONSET OF AD

Although numerous RNA-related and DNA methylation changes are reported in AD, alterations to HDAC proteins are perhaps the best characterized and are highly interactive with other epigenetic mechanisms (Mastroeni, Grover et al. 2011). In the frontal cortex (FC), a diverse number of HDAC classes were altered across disease progression. Cortical HDAC1 and HDAC3 levels were significantly increased in MCI and mAD, while basal forebrain levels of both proteins were unchanged. This may suggest regional differences in these proteins in the AD brain. The upregulation of HDAC1 and HDAC3 in the frontal cortex may be indicative of a neuroplastic response to prodromal/mild AD or the activation of cellular death pathways (Bardai, Price et al. 2012). *In vivo* and *in vitro* studies indicate that an increased interaction between HDAC1 and HDAC3 in neurons is neurotoxic (Bardai, Price et al. 2012). Our data revealed a strong positive correlation between cortical levels of HDAC1 and HDAC3 suggesting that this parallel upregulation reflects an increased interaction between these proteins in MCI and AD. In addition, we observed a downregulation of FC SIRT1 levels in prodromal and mAD. This reduction of SIRT1 may prevent HDAC1 deacetylation and contribute to genomic instability in combination with the neurotoxic effect of an increased HDAC1-HDAC3 interaction (Dobbin, Madabhushi et al. 2013). It will be important to determine in the future which cortical cell types contribute to the global increase in HDAC1 and HDAC3.

HDAC1 and HDAC3 have been shown to deacetylate non-histone proteins, notably transcription factors, indicating an additional layer of gene regulation. HDAC1 binds and deacetylates p53 (Juan, Shia et al. 2000; Luo, Su et al. 2000), YY1, Signal transducer and activator of transcription 3, androgen receptor, Myogenic differentiation 1, E2F transcription factor 1, and Smad family member 7 (Peart, Smyth et al. 2005). Non-histone transcription factor targets for HDAC3 include Smad7, Myocyte enhancer factor 2 (MEF2), Mitogen-activated protein kinase phosphatase-1 (MKP-1), nuclear factor-kappaB (NFkB) (Chen, Fischle et al. 2001; Peart, Smyth et al. 2005; Jeong, Du et al. 2014), with MKP-1 and NFkB being associated with inflammatory processes. A recent report identified that deacetylation by axonal HDAC1 of the dynactin subunit $p150^{Glued}$ mediates retrograde degenerative signaling by $p75^{NTR}$ (Pathak, Stanley et al. 2018). Although HDAC1 is considered a nuclear protein, this deacetylase has been shown to translocate out of the nucleus into axons of hippocampal and cortical neurons when exposed to TNF and glutamate toxicity (Kim, Shen et al. 2010). In addition, axonal HDAC1 disrupts mitochondrial transport through binding to kinesins KIF2a and KIF5 (Kim, Shen et al. 2010). Cholinergic basocortical neurons rely on mitochondrial function and retrograde neurotrophic signaling for survival, and thus would be selectively vulnerable to HDAC1-mediated degenerative cellular mechanisms. However, further studies are necessary to establish if HDAC1 contributes to alterations in $p75^{NTR}$ signaling pathways and mitochondrial dysfunction in the AD brain.

HDAC4 is found in the cytoplasm under normal conditions, and changes in subcellular localization of this protein may contribute to dysregulation of various

signaling pathways. In the frontal cortex, HDAC4 levels were significantly increased in MCI compared to controls and mAD, whereas levels in the basal forebrain were unchanged. HDAC4 is dephosphorylated and translocated to the nucleus in AD, and accumulates in cortical layer III nuclei (Shen, Chen et al. 2016). In addition, treatment with the neuronal survival factor BDNF suppresses HDAC4 nuclear translocation in cerebellar granule neurons, whereas a pro-apoptotic CaMK inhibitor stimulates HDAC4 nuclear accumulation (Bolger and Yao 2005). Although basal forebrain HDAC4 levels were stable, it is possible that HDAC4 is dephosphorylated in cholinergic neurons and the subcellular location is altered in AD. Moreover, ectopic expression of HDAC4 led to neuronal apoptosis and repressed the transcriptional activities of the neuronal survival factors MEF2 and CREB (Bolger and Yao 2005). In contrast, inactivation of HDAC4 by small interfering RNA or HDAC inhibitors suppresses neuronal cell death (Bolger and Yao 2005). Together these data suggest that HDAC4 dysregulation may also contribute to neuronal apoptosis in the AD cortex.

HDAC4 interacts with miR-29b and miR-125 in cellular models of cancer and these miRNAs are dysregulated in AD (Sala Frigerio, Lau et al. 2013; Kiko, Nakagawa et al. 2014; Müller, Jäkel et al. 2016). Whether HDAC4 interacts with miR-29b and miR-125 in AD remains to be determined, but may have importance since these miRNAs are suggested to be CSF biomarkers of AD (Müller, Jäkel et al. 2016). Interestingly, levels of HDAC4 and the cytoplasmic deacetylase HDAC6 were strongly correlated in the cortex, whether these two proteins interact in AD or are linked by their membership to Class II deacetylases is unknown.

HDAC6 is a cytoplasmic deacetylase that interacts with numerous non-histone targets. HDAC6 deacetylates tubulin and the microtubule network *in vivo* (Hubbert, Guardiola et al. 2002; Matsuyama, Shimazu et al. 2002; Zhang, Li et al. 2003). In addition, HDAC6 facilitates the clearance of misfolded ubiquitinated proteins, promoting their accumulation in aggresomes, and protects cells from stress induced by misfolded proteins (Kawaguchi, Kovacs et al. 2003). At the same time, HDAC6 controls induction of heat-shock proteins in response to accumulation of ubiquitinated protein aggregates (Boyault, Sadoul et al. 2007). In the frontal cortex, HDAC6 levels increase in MCI and sAD, while basal forebrain levels remain stable across clinical groups. HDAC6 levels have been shown to increase in the hippocampus in AD (Ding, Dolan et al. 2008). In addition, evidence suggests that increased levels of HDAC6 indicate an initial response to disease onset, which may be indicative of cellular stress. HDAC6 has been linked to suppression of mRNA translation and relocalization of mRNPs into cytoplasmic stress granules, where they are remodeled and protected from degradation (Anderson and Kedersha 2006; Kwon, Zhang et al. 2007). HDAC6 is a critical factor for stress granule assembly, where it binds ubiquitin and dynein motor proteins and acts as an adaptor in both stress granules and the recruitment of misfolded proteins to the aggresome. Perhaps the increase in cortical HDAC6 levels in MCI and AD is an effort by the cell to increase protein clearance and degrade or recycle mRNAs (Kwon, Zhang et al. 2007). This hypothesis would support previous work demonstrating lysosomal/endosomal and autophagic upregulation in the cortex, hippocampus, and basal forebrain in MCI and AD

(Ginsberg, Mufson et al. 2010; Nixon and Yang 2011; Orr and Oddo 2013; Perez, He et al. 2015).

Both HDAC6 and SIRT1 are implicated in tau processing (Cook, Gendron et al. 2012; Tseng, Xie et al. 2017). HDAC6 binds tau directly via its microtubule-binding (MTBR) domain, and HDAC6 levels positively correlate with tau burden, while overexpression of HDAC6 promotes accumulation of PHF1-tau (pS396/S404) (Cook, Gendron et al. 2012). Conversely, loss of SIRT1 has been linked to tau accumulation in AD (Julien, Tremblay et al. 2009). In the frontal cortex, SIRT1 levels steadily decreased from MCI to mAD and sAD. Others have demonstrated decreased SIRT1 expression in early Braak stages in the prefrontal cortex (Bossers, Wirz et al. 2010), and SIRT1 mRNA and protein are decreased in the parietal cortex in AD and parallel NFT accumulation (Julien, Tremblay et al. 2009). SIRT1 deacetylates tau in transgenic tauopathy mouse models and in the human brain (Min, Chen et al. 2015; Min, Sohn et al. 2018). A recent study demonstrated that SIRT1 brain-specific deletion in transgenic tauP301S mice resulted in a significant loss of synaptophysin in the FC and hippocampus, while SIRT1 overexpression significantly reduced spread of MC1-positive tau pathology to the contralateral hippocampus compared with control animals (Min, Sohn et al. 2018). Here we found that SIRT1 levels in the FC were negatively correlated with cortical NFT counts, thus SIRT1 loss in the cortex may be linked to NFT proliferation and may contribute to synaptic loss during AD progression. SIRT1's role in synaptic loss and pathogenic tau during the early stages of AD remain undetermined. Although SIRT1

levels in the basal forebrain were not significantly altered, there was a trend for decreased SIRT1 levels across the clinical groups.

Numerous studies implicate a reduction in SIRT1 with impaired cognitive abilities, including immediate memory, classical conditioning and spatial learning (Gao, Wang et al. 2010; Michan, Li et al. 2010; Ng, Wijaya et al. 2015; Cao, Yan et al. 2017; Min, Sohn et al. 2018). In the current studies, we found significant positive correlations between FC SIRT1 levels and cognitive measures including perceptual speed, GCS, episodic memory, and MMSE. Interestingly, SIRT1 loss in the parietal cortex was correlated with GCS (Julien, Tremblay et al. 2009), indicating that loss of SIRT1 protein in cortical regions may affect cognitive functions during disease progression.

4.2 HDAC2 NUCLEAR LOSS IN CHOLINERGIC NBM NEURONS

A significant decline in HDAC2 basal forebrain protein and cholinergic nbM nuclear levels were observed across the clinical groups. In basal forebrain homogenates, HDAC2 levels did not decline until sAD, while cholinergic nbM nuclear HDAC2 levels were significantly decreased in mAD and sAD. The discrepancy between the western blot and immunocytochemical cellular data may be due to an upregulation in HDAC2 in other cells types included in basal forebrain homogenates. For example, we found HDAC2 positive glial staining surrounding nbM neurons and these cells were not included in the immunocytochemical cellular analysis. In contrast, cortical HDAC2 levels were stable across clinical groups suggesting that this region is not susceptible to HDAC2 dysregulation. Alternatively, it is possible that HDAC2 levels are altered in discrete cortical layers or cell types which are not detectable by analyzing whole FC

homogenates. Future studies of cortical neuronal and glial HDAC2 levels are needed to pin point which cell types within specific cortical layers demonstrate HDAC2 dysregulation, and highlight the importance of studying these complex changes in multiple regions and cellular classes.

Nuclear HDAC2 loss was first described in entorhinal cortex layer II neurons in AD patients (Mastroeni, Grover et al. 2010). In the nbM, both the intensity and area of HDAC2 nuclear immunoreactivity was reduced in mAD and sAD. However, further analysis identified that HDAC2 nuclear levels are highest in neurons that maintain their cholinergic phenotype and did not display NFT pathology across all clinical groups. A recent study demonstrated a significant increase in tau oligomeric complex 1 (TOC1) immunoreactivity in parallel with a decrease in the number of $p75^{NTR}$ positive nbM neurons during the transition from MCI to AD (Tiernan, Mufson et al. 2018). Although HDAC2 levels were not significantly altered in pretangle-bearing nbM neurons in MCI, the effect that TOC1 or other tau oligomeric isoforms have upon HDAC2 or other epigenetic markers remain unknown. Future studies will examine the relationship between TOC1 in cholinergic nbM neurons and HDAC2 nuclear levels to examine if nuclear HDAC2 loss is present earlier during tangle formation.

In cholinergic neurons degeneration and cell loss follows a rostrocaudal topographic progression within the subfields of the nbM, with the posterior Ch4 subfield being the earliest and most severely affected (Arendt, Bigl et al. 1983; Wilcock, Esiri et al. 1983; Mufson, Bothwell et al. 1989; Iraizoz, Guijarro et al. 1999; Liu, Chang et al. 2015; Tiernan, Mufson et al. 2018). Since the current study analyzed HDAC2 nuclear

levels in the anterior and intermediate cholinergic subfields of the nbM, it would be interesting to examine the posterior subfields. Unfortunately, tissue from this region was not consistently available.

Analysis of cholinergic HDAC2 immunoreactive nuclei within the nbM revealed a decrease in size, eccentric location with the soma, and often a flattened appearance in the AD brain in contrast to their large and rounded shape in age-matched cognitively normal individuals. These alterations were first observed in pretangle-bearing neurons, and were exacerbated in nbM neurons containing more mature NFTs that displayed β-pleated sheet structures across disease progression. Displacement of nuclei to the periphery of the soma in cholinergic nbM neurons has been reported before in AT8 positive perikarya (Sassin, Schultz et al. 2000), as has shrinkage of nuclear diameter (Rinne, Paljarvi et al. 1987). The consequences of these cellular alterations on the structural and functional integrity of the nucleus remain unknown. In relation to these findings, a recent report demonstrated that full-length tau interacts with nuclear pore protein Nup98 and to a lesser extent with Nup62 in postmortem AD tissue, transgenic mouse models, and *in vitro* (Eftekharzadeh, Daigle et al. 2018). Evidence of nuclear pore complex (NPC) structural and functional impairments, including Ran mislocalization, alterations in fluorescent protein trafficking, and defects in dextran exclusion was observed in phospho-tau-positive cells obtained from AD patients and rTg4510 transgenic mice (Eftekharzadeh, Daigle et al. 2018). Thus, neurons exposed to exogenous AD brain-derived tau show altered nuclear cytoplasmic Ran distribution and disturbed NPC function and integrity, consequently altering both nuclear protein export and import

(Eftekharzadeh, Daigle et al. 2018). Proteomic analysis of the mammalian NPC identified HDAC2 as a non-NPC core protein that can be considered a nuclear matrix- or chromatin associated protein and therefore may be directly or indirectly associated with NPC function (Cronshaw, Krutchinsky et al. 2002; Pyrzynska, Pilecka et al. 2009). Whether nbM neuronal HDAC2 dysregulation is involved with loss of NPC function or impaired nucleocytoplasmic transport and pathogenic tau is a timely and important area of investigation. Future studies will examine the relationship of nuclear pore structural alterations and HDAC2 nuclear changes in cholinergic nbM neurons during NFT formation.

Cholinergic nbM neurons triple-labeled for $p75^{NTR}$, AT8, or TauC3 displayed a greater reduction in HDAC2 immunoreactivity in mAD and sAD compared with non-tangle bearing $p75^{NTR}$ immunoreactive neurons. HDAC2 nuclear immunoreactivity was further reduced in cholinergic nbM neurons labeled for either HDAC2/AT8/Thioflavin-S or HDAC2/TauC3/Thioflavin-S in MCI and mAD. Thus, although a reduction in HDAC2 occurs before the onset of fibrillar tau pathology, this reduction is exacerbated by the presence of phosphorylated and conformational tau epitopes during the progression of AD. Recent evidence suggests that alterations to HDAC2 induce hyperphosphorylation of tau in AD animal models (Liu, Tang et al. 2017). HDAC2 overexpression mediates hyperphosphorylation of tau indirectly through deacetylation of a transcription factor HNF-4, which suppresses miR-101b expression (Liu, Tang et al. 2017). The loss of miR-101b prevents binding to its target, AMP-activated protein kinase (AMPK), and results in increased AMPK expression, activity, and abnormal hyperphosphorylation and

aggregation of tau (Vingtdeux, Chandakkar et al. 2011). MiR-101 is downregulated in temporal and parietal cortices in AD (Hebert, Horre et al. 2008), however, whether this miRNA is dysregulated and contributes to tau hyperphosphorylation in the cholinergic nbM is unknown.

Another tau kinase, casein kinase 2 (CK2) not only phosphorylates HDAC2, altering its enzymatic activity and complex formation (Tsai and Seto 2002), but is significantly increased in NFTs in hippocampal neurons in AD (Rosenberger, Hilhorst et al. 2016), and at the ultrastructural level CK2 is immunolocalized to paired helical filaments within NFTs and neuropil threads (Masliah, Iimoto et al. 1992). Proline-directed serine/threonine tau kinases including cyclin-dependent kinase 5 (Cdk5) affects tau phosphorylation at Ser202/Thr205 (AT8) and Ser396/Ser404 (PHF-1) sites. Cdk5 functions as a glucocorticoid receptor kinase, and when bound to the glucocorticoid responsive element within the proximal HDAC2 promoter region, stimulates HDAC2 expression. It is possible that aberrant kinase activation is a link between changes in HDAC2 and NFT pathology in the cholinergic nbM and may explain why HDAC2 and the pretangle marker AT8 are inversely related in these neurons. However, further examination of the relationship among HDAC2, hyperphosphorylated tau isoforms, and kinase activity is required to establish this association.

HDAC2 nuclear immunoreactivity was the lowest in cholinergic TauC3/Thioflavin-S–positive neurons across all four clinical groups. TauC3 is a caspase-dependent cleavage epitope associated with apoptotic events and the phenotypic loss of $p75^{NTR}$ in nbM neurons (Vana, Kanaan et al. 2011). While HDAC2 has not been

associated in AD with apoptotic signaling or caspase activation, its role in oxidative stress and neuronal death in cancer has been elucidated. Downregulation of HDAC2 inhibits cell proliferation, arrests cell cycle at G0/G1 phase, and induces apoptosis in cancer cells (Li, Wang et al. 2017). In neurons, HDAC2 forms a complex with the transcription factor FOXO3a which is involved in neuronal apoptosis (Peng, Zhao et al. 2015). Activation of caspase 3 and caspase 7 is significantly increased *in vivo* upon depletion of HDAC2; silencing HDAC2 is sufficient to decrease NF-κB activity induced by TNFα and to sensitize cells to TNFα-induced apoptosis (Kaler, Sasazuki et al. 2008). Thus, HDAC2 has multiple levels of interaction with apoptotic proteins and effectors, and loss of this deacetylase during AD affects neuronal cell cycle reentry, apoptosis, and caspase activation in AD. HDAC2 nuclear levels were significantly correlated with higher z-scores for working memory and global cognitive score, indicating like experimental animal models of HDAC2 knockdown have shown, HDAC2's role in downstream expression of genes important for learning and memory (Guan, Haggarty et al. 2009; Graff, Rei et al. 2012). Future studies will examine single nbM transcript levels of HDAC2 and levels of synaptic and neuroplasticity-related gene transcripts to identify if these targets are downregulated in cholinergic nbM neurons during AD progression.

Overall my thesis spanned from the identification of global basocortical deacetylase dysregulation to the discovery that HDAC2 is selectively dysregulated in cholinergic nbM neurons in AD. The importance of these findings are directly related to recent studies indicating that volumetric reduction of the forebrain region containing the nbM predicts and precedes cortical pathology and memory impairment in prodromal AD

and that changes in nbM grey matter volume are apparent even in clinically silent stages of probable AD (Schmitz and Spreng 2016). These data support the need to develop therapeutic strategies that target epigenetic changes in the basocortical cholinergic system as way of preventing or slowing basal forebrain degeneration. A number of studies have identified HDAC inhibitors as treatments for AD (Tariot, Schneider et al. 2011; Xu, Dai et al. 2011; Cacabelos and Torrellas 2015), specifically in the context of improving learning and memory function (Guan, Haggarty et al. 2009). The data presented in this thesis outlines the importance of studying HDAC levels in multiple regions in prodromal, mild, and severe AD. Inhibition of HDAC2 may be detrimental to cholinergic nbM neuronal function, but may be necessary for cortical or hippocampal function in AD. It is also possible that the upregulation of certain HDACs is neuroprotective and may be a novel biomarker for AD susceptibility. Until specific regional/cell based epigenetic therapies are available, pan-HDAC inhibitors should be used with caution in AD. However, the availability of epigenetic imaging in the brain with the selective class I/IIb HDAC PET tracer [^{11}C]Martinostat (Schroeder, Wang et al. 2014; Wang, Schroeder et al. 2014), may allow for early detection and management of epigenetic dysregulation in the MCI and AD brain.

REFERENCES

(2015). "2015 Alzheimer's disease facts and figures." Alzheimers Dement **11**(3): 332-384.

(2018). "2018 Alzheimer's disease facts and figures." Alzheimers Dement **14**: 367-429.

Adamec, E., J. P. Vonsattel, et al. (1999). "DNA strand breaks in Alzheimer's disease." Brain Res **849**(1-2): 67-77.

Adler, B. L., M. Yarchoan, et al. (2014). "Neuroprotective effects of the amylin analogue pramlintide on Alzheimer's disease pathogenesis and cognition." Neurobiol Aging **35**(4): 793-801.

Aizawa, S., K. Teramoto, et al. (2012). "Histone deacetylase 9 as a negative regulator for choline acetyltransferase gene in NG108-15 neuronal cells." Neuroscience **205**: 63-72.

Aizawa, S. and Y. Yamamuro (2010). "Involvement of histone acetylation in the regulation of choline acetyltransferase gene in NG108-15 neuronal cells." Neurochem Int **56**(4): 627-633.

Akhtar, M., J. Raingo, et al. (2009). "Histone deacetylases 1 and 2 form a developmental switch that controls excitatory synapse maturation and function." J Neurosci **29**: 8288-8297.

Allard, S., W. C. Leon, et al. (2012). "Impact of the NGF maturation and degradation pathway on the cortical cholinergic system phenotype." J Neurosci **32**(6): 2002-2012.

Allen, S. J., D. Dawbarn, et al. (1988). "Morphometric immunochemical analysis of neurons in the nucleus basalis of Meynert in Alzheimer's disease." Brain Res **454**(1-2): 275-281.

Allfrey, V. (1966). "Structural modifications of histones and their possible role in the regulation of ribonucleic acid synthesis." Proc Can Cancer Conf **6**: 313-335.

Alzheimer, A. (1906). "U¨ ber einen eigenartigen schweren Erkrankungsprozeß der Hirnrinde." Neurologisches Centralblatt **23**: 1129-1136.

Anderson, K. W., J. Chen, et al. (2015). "Quantification of histone deacetylase isoforms in human frontal cortex, human retina, and mouse brain." PLoS One **10**(5): e0126592.

Anderson, P. and N. Kedersha (2006). "RNA granules." J Cell Biol **172**(6): 803-808.

Araki, T., Y. Sasaki, et al. (2004). "Increased nuclear NAD biosynthesis and SIRT1 activation prevent axonal degeneration." Science **305**(5686): 1010-1013.

Arendt, T., V. Bigl, et al. (1983). "Loss of neurons in the nucleus basalis of Meynert in Alzheimer's disease, paralysis agitans and Korsakoff's Disease." Acta Neuropathol **61**(2): 101-108.

Arnold, S. E., N. Louneva, et al. (2013). "Cellular, synaptic, and biochemical features of resilient cognition in Alzheimer's disease." Neurobiol Aging **34**(1): 157-168.

Arrighetti, N., C. Corno, et al. (2015). "Drug Combinations with HDAC Inhibitors in Antitumor Therapy." Crit Rev Oncog **20**(1-2): 83-117.

Bahari-Javan, S., A. Maddalena, et al. (2012). "HDAC1 regulates fear extinction in mice." J Neurosci **32**(15): 5062-5073.

Ballinger, E. C., M. Ananth, et al. (2016). "Basal Forebrain Cholinergic Circuits and Signaling in Cognition and Cognitive Decline." Neuron **91**(6): 1199-1218.

Bandyopadhyay, D. and E. E. Medrano (2003). "The emerging role of epigenetics in cellular and organismal aging." Exp Gerontol **38**(11-12): 1299-1307.

Bao, J., L. Zheng, et al. (2016). "Deacetylation of TFEB promotes fibrillar Abeta degradation by upregulating lysosomal biogenesis in microglia." Protein Cell **7**(6): 417-433.

Bardai, F., V. Price, et al. (2012). "Histone Deacetylase-1 (HDAC1) Is a Molecular Switch between Neuronal Survival and Death." Journal of Biological Chemistry **287**: 35444-35453.

Barker, P. (2004). "p75NTR Is Positively Promiscuous: Novel Partners and New Insights." Neuron **42**: 529-533.

Barrachina, M. and I. Ferrer (2009). "DNA methylation of Alzheimer disease and tauopathy-related genes in postmortem brain." J Neuropathol Exp Neurol **68**(8): 880-891.

Bartus, R. T., R. L. Dean, 3rd, et al. (1982). "The cholinergic hypothesis of geriatric memory dysfunction." Science **217**(4558): 408-414.

Baudic, S., G. Barba, et al. (2006). "Executive function deficits in early Alzheimer's disease and their relations with episodic memory." Arch Clin Neuropsychol **21**: 15-21.

Baxter, M. G. and A. A. Chiba (1999). "Cognitive functions of the basal forebrain." Curr Opin Neurobiol **9**(2): 178-183.

Behera, J., V. Jayprakash, et al. (2015). "Histone deacetylase inhibitors: a review on class-I specific inhibition." Mini Rev Med Chem **15**(9): 731-750.

Bekdash, R. (2016). Choline and the Brain: An Epigenetic Perspective. The Benefits of Natural Products for Neurodegenerative Diseases. A. M. Essa M, Guillemin G, Springer, Cham. **12:** 381-399.

Benjamini, Y. and Y. Hochberg (1995). "Controlling the False Discovery Rate: A Practical and Powerful Approach to Multiple Testing." J Royal Stat Soc **57**: 289-300.

Bennett, D., A. Buchman, et al. (2018). "Religious Orders Study and Rush Memory and Aging Project." J Alzheimers Dis **64**: 161-189.

Bennett, D., J. Schneider, et al. (2006). "Neuropathology of older persons without cognitive impairment from two community-based studies." Neurology **66**: 1837-1844.

Bennett, D., J. Schneider, et al. (2005). "Mild cognitive impairment is related to Alzheimer disease pathology and cerebral infarctions." Neurology **64**: 834-841.

Bennett, D. A., J. A. Schneider, et al. (2012). "Overview and findings from the religious orders study." Curr Alzheimer Res **9**(6): 628-645.

Bennett, D. A., J. A. Schneider, et al. (2004). "Neurofibrillary tangles mediate the association of amyloid load with clinical Alzheimer disease and level of cognitive function." Arch Neurol **61**(3): 378-384.

Bennett, D. A., R. S. Wilson, et al. (2002). "Natural history of mild cognitive impairment in older persons." Neurology **59**(2): 198-205.

Bicknell, L. S., S. Walker, et al. (2011). "Mutations in ORC1, encoding the largest subunit of the origin recognition complex, cause microcephalic primordial dwarfism resembling Meier-Gorlin syndrome." Nat Genet **43**(4): 350-355.

Bierer, L. M., V. Haroutunian, et al. (1995). "Neurochemical correlates of dementia severity in Alzheimer's disease: relative importance of the cholinergic deficits." J Neurochem **64**(2): 749-760.

Binder, L., A. Guillozet-Bongaarts, et al. (2005). "Tau, tangles, and Alzheimer's disease." Biochem Biophys Acta **1739**: 216-223.

Binder, L. I., A. L. Guillozet-Bongaarts, et al. (2005). "Tau, tangles, and Alzheimer's disease." Biochim Biophys Acta **1739**(2-3): 216-223.

Bird, A. and A. Wolffe (1999). " Methylation-induced repression--belts, braces, and chromatin." Cell **99**: 451-454.

Bird, A. P. (1978). "The occurrence and transmission of a pattern of DNA methylation in Xenopus laevis ribosomal DNA." Philos Trans R Soc Lond B Biol Sci **283**(997): 325-327.

Bird, T. D., S. Stranahan, et al. (1983). "Alzheimer's disease: choline acetyltransferase activity in brain tissue from clinical and pathological subgroups." Ann Neurol **14**(3): 284-293.

Blair, J. A., C. Wang, et al. (2016). "Individual Case Analysis of Postmortem Interval Time on Brain Tissue Preservation." PLoS One **11**(3): e0151615.

Blake, M. G. and M. M. Boccia (2018). "Basal Forebrain Cholinergic System and Memory." Curr Top Behav Neurosci **37**: 253-273.

Bolger, T. A. and T. P. Yao (2005). "Intracellular trafficking of histone deacetylase 4 regulates neuronal cell death." J Neurosci **25**(41): 9544-9553.

Bonner, M. and A. Price (2013). "Where is the anterior temporal lobe and what does it do?" J Neurosci **33**: 4213-4215.

Bordone, L., D. Cohen, et al. (2007). "SIRT1 transgenic mice show phenotypes resembling calorie restriction." Aging Cell **6**: 759-767.

Bossers, K., K. T. Wirz, et al. (2010). "Concerted changes in transcripts in the prefrontal cortex precede neuropathology in Alzheimer's disease." Brain **133**(Pt 12): 3699-3723.

Bowen, D. M., C. B. Smith, et al. (1976). "Neurotransmitter-related enzymes and indices of hypoxia in senile dementia and other abiotrophies." Brain **99**(3): 459-496.

Boyault, C., B. Gilquin, et al. (2006). "HDAC6-p97/VCP controlled polyubiquitin chain turnover." EMBO J **25**(14): 3357-3366.

Boyault, C., K. Sadoul, et al. (2007). "HDAC6, at the crossroads between cytoskeleton and cell signaling by acetylation and ubiquitination." Oncogene **26**: 5468-5476.

Braak, H. and E. Braak (1991). "Neuropathological stageing of Alzheimer-related changes." Acta Neuropathol **82**(4): 239-259.

Bradley-Whitman, M. A. and M. A. Lovell (2013). "Epigenetic changes in the progression of Alzheimer's disease." Mech Ageing Dev **134**(10): 486-495.

Bredy, T. W., H. Wu, et al. (2007). "Histone modifications around individual BDNF gene promoters in prefrontal cortex are associated with extinction of conditioned fear." Learn Mem **14**(4): 268-276.

Bruijn, R. d. and M. Ikram (2014). "Cardiovascular risk factors and future risk of Alzheimer's disease." BMC Med **12**: 1-9.

Brunet, A., L. B. Sweeney, et al. (2004). "Stress-dependent regulation of FOXO transcription factors by the SIRT1 deacetylase." Science **303**(5666): 2011-2015.

Buckner, R., A. Snyder, et al. (2005). "Molecular, Structural, and Functional Characterization of Alzheimer's Disease: Evidence for a Relationship Between Default Activity, Amyloid, and Memory." J Neurosci **25**: 7709-7717.

Buckner, R. L., J. Sepulcre, et al. (2009). "Cortical hubs revealed by intrinsic functional connectivity: mapping, assessment of stability, and relation to Alzheimer's disease." J Neurosci **29**(6): 1860-1873.

Burd, C., H. Kinyamu, et al. (2008). "UV radiation regulates Mi-2 through protein translation and stability." J Biol Chem **283**: 34976-34982.

Cacabelos, R. and C. Torrellas (2015). "Epigenetics of Aging and Alzheimer's Disease: Implications for Pharmacogenomics and Drug Response." Int J Mol Sci **16**(12): 30483-30543.

Cao, Y., Z. Yan, et al. (2017). "SIRT1 Regulates Cognitive Performance and Ability of Learning and Memory in Diabetic and Nondiabetic Models." J Diabetes Res **2017**: 7121827.

Carlesimo, G. A. and M. Oscar-Berman (1992). "Memory deficits in Alzheimer's patients: a comprehensive review." Neuropsychol Rev **3**(2): 119-169.

Cavedo, E., B. Dubois, et al. (2016). "Reduced regional cortical thickness rate of change in donepe- zil-treated subjects with suspected prodromal Alzheimer's disease." **77**: 1631-1638.

Cavedo, E., M. J. Grothe, et al. (2017). "Reduced basal forebrain atrophy progression in a randomized Donepezil trial in prodromal Alzheimer's disease." Sci Rep **7**(1): 11706.

Ceccacci, E. and S. Minucci (2016). "Inhibition of histone deacetylases in cancer therapy: lessons from leukaemia." Br J Cancer **114**(6): 605-611.

Chao, M. V., M. A. Bothwell, et al. (1986). "Gene transfer and molecular cloning of the human NGF receptor." Science **232**(4749): 518-521.

Chen, J., Y. Zhou, et al. (2005). "SIRT1 protects against microglia-dependent amyloid-beta toxicity through inhibiting NF-kappaB signaling." J Biol Chem **280**: 40364-40374.

Chen, K. S. and F. H. Gage (1995). "Somatic gene transfer of NGF to the aged brain: behavioral and morphological amelioration." J Neurosci **15**(4): 2819-2825.

Chen, L., W. Fischle, et al. (2001). "Duration of nuclear NF-kappaB action regulated by reversible acetylation." Science **293**(5535): 1653-1657.

Chen, S., G. C. Owens, et al. (2010). "HDAC6 regulates mitochondrial transport in hippocampal neurons." PLoS One **5**(5): e10848.

Chouliaras, L., D. v. d. Hove, et al. (2012). "Age-related increase in levels of 5-hydroxymethylcytosine in mouse hippocampus is prevented by caloric restriction." Curr Alzheimer Res **9**: 536-544.

Chouliaras, L., D. Mastroeni, et al. (2013). "Consistent decrease in global DNA methylation and hydroxymethylation in the hippocampus of Alzheimer's disease patients." Neurobiol Aging **34**(9): 2091-2099.

Chuang, M. J., S. T. Wu, et al. (2013). "The HDAC inhibitor LBH589 induces ERK-dependent prometaphase arrest in prostate cancer via HDAC6 inactivation and down-regulation." PLoS One **8**(9): e73401.

Clewes, O., M. Fahey, et al. (2008). "Human ProNGF: biological effects and binding profiles at TrkA, P75NTR and sortilin." J Neurochem **107**: 1124-1135.

Cogswell, J., J. Ward, et al. (2008). "Identification of miRNA Changes in Alzheimer's Disease Brain and CSF Yields Putative Biomarkers and Insights into Disease Pathways." Journal of Alzheimer's Disease **14**: 1-11.

Combs, B., C. Hamel, et al. (2016). "Pathological conformations involving the amino terminus of tau occur early in Alzheimer's disease and are differentially detected by monoclonal antibodies." Neurobiol Dis **94**: 18-31.

Condliffe, D., A. Wong, et al. (2014). "Cross-region reduction in 5-hydroxymethylcytosine in Alzheimer's disease brain." Neurobiol Aging **35**(8): 1850-1854.

Conner, J., K. Franks, et al. (2009). "NGF Is Essential for Hippocampal Plasticity and Learning." **29**: 10883-10889.

Cook, C., T. F. Gendron, et al. (2012). "Loss of HDAC6, a novel CHIP substrate, alleviates abnormal tau accumulation." Hum Mol Genet **21**(13): 2936-2945.

Coppede, F. (2014). "The potential of epigenetic therapies in neurodegenerative diseases." Front Genet **5**: 220.

Coppieters, N., B. V. Dieriks, et al. (2014). "Global changes in DNA methylation and hydroxymethylation in Alzheimer's disease human brain." Neurobiol Aging **35**(6): 1334-1344.

Coppieters, N. and M. Dragunow (2011). "Epigenetics in Alzheimer's disease: a focus on DNA modifications." Curr Pharm Des **17**(31): 3398-3412.

Corder, E. H., A. M. Saunders, et al. (1993). "Gene dose of apolipoprotein E type 4 allele and the risk of Alzheimer's disease in late onset families." Science **261**(5123): 921-923.

Counts, S., M. Nadeem, et al. (2004). "Reduction of cortical TrkA but not p75(NTR) protein in early-stage Alzheimer's disease." Ann Neurol **56**: 520-531.

Counts, S. E., S. Che, et al. (2011). "Gender differences in neurotrophin and glutamate receptor expression in cholinergic nucleus basalis neurons during the progression of Alzheimer's disease." J Chem Neuroanat **42**(2): 111-117.

Counts, S. E., B. He, et al. (2012). "Hippocampal drebrin loss in mild cognitive impairment." Neurodegener Dis **10**(1-4): 216-219.

Cronshaw, J. M., A. N. Krutchinsky, et al. (2002). "Proteomic analysis of the mammalian nuclear pore complex." J Cell Biol **158**(5): 915-927.

Cruz, J., D. Kim, et al. (2006). "p25/Cyclin-Dependent Kinase 5 Induces Production and Intraneuronal Accumulation of Amyloid β In Vivo." J Neurosci **26**: 10536-10541.

Cruz, J. C., H. C. Tseng, et al. (2003). "Aberrant Cdk5 activation by p25 triggers pathological events leading to neurodegeneration and neurofibrillary tangles." Neuron **40**(3): 471-483.

Cuello, A. C., M. A. Bruno, et al. (2007). "NGF-cholinergic dependency in brain aging, MCI and Alzheimer's disease." Curr Alzheimer Res **4**(4): 351-358.

D'Addario, C., S. B. Candia, et al. (2017). "Transcriptional and epigenetic phenomena in peripheral blood cells of monozygotic twins discordant for alzheimer's disease, a case report." J Neurol Sci **372**: 211-216.

Davies, P. and A. J. Maloney (1976). "Selective loss of central cholinergic neurons in Alzheimer's disease." Lancet **2**(8000): 1403.

Dawbarn, D., S. J. Allen, et al. (1988). "Coexistence of choline acetyltransferase and nerve growth factor receptors in the rat basal forebrain." Neurosci Lett **94**(1-2): 138-144.

Dawson, M. A. and T. Kouzarides (2012). "Cancer epigenetics: from mechanism to therapy." Cell **150**(1): 12-27.

de Calignon, A., M. Polydoro, et al. (2012). "Propagation of tau pathology in a model of early Alzheimer's disease." Neuron **73**(4): 685-697.

Dekker, A. J., J. Winkler, et al. (1994). "Grafting of nerve growth factor-producing fibroblasts reduces behavioral deficits in rats with lesions of the nucleus basalis magnocellularis." Neuroscience **60**(2): 299-309.

DeKosky, S., R. Harbaugh, et al. (1992). "Cortical biopsy in Alzheimer's disease: diagnostic accuracy and neurochemical, neuropathological, and cognitive correlations." Ann Neurol **32**: 625-632.

DeKosky, S. T., M. D. Ikonomovic, et al. (2002). "Upregulation of choline acetyltransferase activity in hippocampus and frontal cortex of elderly subjects with mild cognitive impairment." Ann Neurol **51**(2): 145-155.

Delcuve, G. P., D. H. Khan, et al. (2012). "Roles of histone deacetylases in epigenetic regulation: emerging paradigms from studies with inhibitors." Clin Epigenetics **4**(1): 5.

Ding, H., P. J. Dolan, et al. (2008). "Histone deacetylase 6 interacts with the microtubule-associated protein tau." J Neurochem **106**(5): 2119-2130.

Divac, I. (1975). "Magnocellular nuclei of the basal forebrain project to neocortex, brain stem, and olfactory bulb. Review of some functional correlates." Brain Res **93**: 385-398.

Dobbin, M. M., R. Madabhushi, et al. (2013). "SIRT1 collaborates with ATM and HDAC1 to maintain genomic stability in neurons." Nat Neurosci **16**(8): 1008-1015.

Dompierre, J. P., J. D. Godin, et al. (2007). "Histone deacetylase 6 inhibition compensates for the transport deficit in Huntington's disease by increasing tubulin acetylation." J Neurosci **27**(13): 3571-3583.

Doucette, R., Fisman M, Hachinski VC, Mersky H (1986). "Cell loss from the nucleus basalis of Meynert in Alzheimer's disease." The Canadian journal of neurological sciences **13**: 435-440.

Drachman, D. A. and J. Leavitt (1974). "Human memory and the cholinergic system. A relationship to aging?" Arch Neurol **30**(2): 113-121.

Dressel, U., P. J. Bailey, et al. (2001). "A dynamic role for HDAC7 in MEF2-mediated muscle differentiation." J Biol Chem **276**(20): 17007-17013.

Dubois, B., H. H. Feldman, et al. (2007). "Research criteria for the diagnosis of Alzheimer's disease: revising the NINCDS-ADRDA criteria." Lancet Neurol **6**(8): 734-746.

Dunnett, S. B. (1990). "Neural Transplantation in Animal Models of Dementia." Eur J Neurosci **2**(7): 567-587.

Eftekharzadeh, B., J. G. Daigle, et al. (2018). "Tau Protein Disrupts Nucleocytoplasmic Transport in Alzheimer's Disease." Neuron **99**(5): 925-940 e927.

Erten-Lyons, D., R. L. Woltjer, et al. (2009). "Factors associated with resistance to dementia despite high Alzheimer disease pathology." Neurology **72**(4): 354-360.

Etienne, P., Y. Robitaille, et al. (1986). "Nucleus basalis neuronal loss, neuritic plaques and choline acetyltransferase activity in advanced Alzheimer's disease." Neuroscience **19**(4): 1279-1291.

Fahnestock, M., B. Michalski, et al. (2001). "The precursor pro-nerve growth factor is the predominant form of nerve growth factor in brain and is increased in Alzheimer's disease." Mol Cell Neurosci **18**: 210-220.

Fahnestock, M., G. Yu, et al. (2004). "The nerve growth factor precursor proNGF exhibits neurotrophic activity but is less active than mature nerve growth factor." J Neurochem **89**: 581-592.

Feldman, H., S. Gauthier, et al. (2003). "Efficacy of donepezil on maintenance of activities of daily living in patients with moderate to severe Alzheimer’s disease and the effect on caregiver burden." J Am Geriatr Soc **51**: 737-744.

Feldman, H., T. Pirttila, et al. (2009). "Treatment with galantamine and time to nursing home placement in Alzheimer’s disease patients with and without cerebrovascular disease." Int J Geriatr Psychiatry **32**: 479-488.

Feng, Q. and Y. Zhang (2001). "The MeCP1 complex represses transcription through preferential binding, remodeling, and deacetylating methylated nucleosomes." Genes Dev **15**: 827-832.

Ferris, S. and M. Farlow (2013). "Language impairment in Alzheimer's disease and benefits of acetylcholinesterase inhibitors." Clin Interv Aging **8**: 1007-1014.

Fiorino, E., M. Giudici, et al. (2014). "The sirtuin class of histone deacetylases: regulation and roles in lipid metabolism." IUBMB Life **66**(2): 89-99.

Fischer, A., F. Sananbenesi, et al. (2005). "Opposing roles of transient and prolonged expression of p25 in synaptic plasticity and hippocampus-dependent memory." Neuron **48**(5): 825-838.

Fischer, A., F. Sananbenesi, et al. (2007). "Recovery of learning and memory is associated with chromatin remodelling." Nature **447**: 178-182.

Fischer, D. D., R. Cai, et al. (2002). "Isolation and characterization of a novel class II histone deacetylase, HDAC10." J Biol Chem **277**(8): 6656-6666.

Fischle, W., F. Dequiedt, et al. (2002). "Enzymatic activity associated with class II HDACs is dependent on a multiprotein complex containing HDAC3 and SMRT/N-CoR." Mol Cell **9**: 45-57.

Fleming, S. M., J. Huijgen, et al. (2012). "Prefrontal contributions to metacognition in perceptual decision making." J Neurosci **32**(18): 6117-6125.

Forman, J., A. Legesse-Miller, et al. (2008). "A search for conserved sequences in coding regions reveals that the let-7 microRNA targets Dicer within its coding sequence." Proc Natl Acad Sci U S A **105**: 14879-14884.

Fraga, M. F. and M. Esteller (2007). "Epigenetics and aging: the targets and the marks." Trends Genet **23**(8): 413-418.

Francis, Y. I., M. Fa, et al. (2009). "Dysregulation of histone acetylation in the APP/PS1 mouse model of Alzheimer's disease." J Alzheimers Dis **18**(1): 131-139.

French, P. J., V. O'Connor, et al. (2001). "Subfield-specific immediate early gene expression associated with hippocampal long-term potentiation in vivo." Eur J Neurosci **13**(5): 968-976.

Fritah, S., E. Col, et al. (2009). "Heat-shock factor 1 controls genome-wide acetylation in heat-shocked cells." Mol Biol Cell **20**(23): 4976-4984.

Gallinari, P., S. Di Marco, et al. (2007). "HDACs, histone deacetylation and gene transcription: from molecular biology to cancer therapeutics." Cell Res **17**(3): 195-211.

Gao, J., W. Y. Wang, et al. (2010). "A novel pathway regulates memory and plasticity via SIRT1 and miR-134." Nature **466**(7310): 1105-1109.

Gao, L., M. A. Cueto, et al. (2002). "Cloning and functional characterization of HDAC11, a novel member of the human histone deacetylase family." J Biol Chem **277**(28): 25748-25755.

Gao, Y. S., C. C. Hubbert, et al. (2010). "The microtubule-associated histone deacetylase 6 (HDAC6) regulates epidermal growth factor receptor (EGFR) endocytic trafficking and degradation." J Biol Chem **285**(15): 11219-11226.

Garcia-Sierra, F., N. Ghoshal, et al. (2003). "Conformational changes and truncation of tau protein during tangle evolution in Alzheimer's disease." J Alzheimers Dis **5**(2): 65-77.

Geula, C., C. Schatz, et al. (1993). "Differential localization of NADPH-diaphorase and calbindin-D within the cholinergic neurons of the basal forebrain, striatum and brainstem in the rat, monkey, baboon and human." Neuroscience **54**: 461-476.

Ghoshal, N., F. Garcia-Sierra, et al. (2001). "Tau-66: evidence for a novel tau conformation in Alzheimer's disease." J Neurochem **77**(5): 1372-1385.

Ghoshal, N., F. Garcia-Sierra, et al. (2002). "Tau conformational changes correspond to impairments of episodic memory in mild cognitive impairment and Alzheimer's disease." Exp Neurol **177**(2): 475-493.

Gilmor, M. L., J. D. Erickson, et al. (1999). "Preservation of nucleus basalis neurons containing choline acetyltransferase and the vesicular acetylcholine transporter in the elderly with mild cognitive impairment and early Alzheimer's disease." J Comp Neurol **411**(4): 693-704.

Ginsberg, S., S. Che, et al. (2006). "Down regulation of trk but not p75NTR gene expression in single cholinergic basal forebrain neurons mark the progression of Alzheimer's disease." J Neurochem **97**: 475-487.

Ginsberg, S., E. Mufson, et al. (2010). "Regional selectivity of rab5 and rab7 protein upregulation in mild cognitive impairment and Alzheimer's disease." J Alzheimers Dis **5**: 631-639.

Glickman, M., S. Rao, et al. (2014). "False discovery rate control is a recommended alternative to Bonferroni-type adjustments in health studies." J Clin Epidemiol **67**: 850-857.

Gold, C. A. and A. E. Budson (2008). "Memory loss in Alzheimer's disease: implications for development of therapeutics." Expert Rev Neurother **8**(12): 1879-1891.

Golomb, J., M. J. de Leon, et al. (1993). "Hippocampal atrophy in normal aging. An association with recent memory impairment." Arch Neurol **50**(9): 967-973.

Golubnitschaja, O. (2007). "Cell cycle checkpoints: the role and evaluation for early diagnosis of senescence, cardiovascular, cancer, and neurodegenerative diseases." Amino Acids **32**(3): 359-371.

Grady, C. L., M. L. Furey, et al. (2001). "Altered brain functional connectivity and impaired short-term memory in Alzheimer's disease." Brain **124**(Pt 4): 739-756.

Graff, J., D. Rei, et al. (2012). "An epigenetic blockade of cognitive functions in the neurodegenerating brain." Nature **483**(7388): 222-226.

Graff, J. and L. H. Tsai (2013). "Histone acetylation: molecular mnemonics on the chromatin." Nat Rev Neurosci **14**(2): 97-111.

Guan, J. S., S. J. Haggarty, et al. (2009). "HDAC2 negatively regulates memory formation and synaptic plasticity." Nature **459**(7243): 55-60.

Guardiola, A. R. and T. P. Yao (2002). "Molecular cloning and characterization of a novel histone deacetylase HDAC10." J Biol Chem **277**(5): 3350-3356.

Guillozet-Bongaarts, A., M. Cahill, et al. (2006). "Pseudophosphorylation of tau at serine 422 inhibits caspase cleavage: in vitro evidence and implications for tangle formation in vivo." J Neurochem **97**: 1005-1014.

Guillozet-Bongaarts, A. L., F. Garcia-Sierra, et al. (2005). "Tau truncation during neurofibrillary tangle evolution in Alzheimer's disease." Neurobiol Aging **26**(7): 1015-1022.

Guillozet, A. L., S. Weintraub, et al. (2003). "Neurofibrillary tangles, amyloid, and memory in aging and mild cognitive impairment." Arch Neurol **60**(5): 729-736.

Gupta-Agarwal, S., A. Franklin, et al. (2012). "G9a/GLP histone lysine dimethyltransferase complex activity in the hippocampus and the entorhinal cortex is required for gene activation and silencing during memory consolidation." J Neurosci **32**: 5440-5453.

Gupta, M. P., S. A. Samant, et al. (2008). "HDAC4 and PCAF bind to cardiac sarcomeres and play a role in regulating myofilament contractile activity." J Biol Chem **283**(15): 10135-10146.

Guzowski, J. F., G. L. Lyford, et al. (2000). "Inhibition of activity-dependent arc protein expression in the rat hippocampus impairs the maintenance of long-term potentiation and the consolidation of long-term memory." J Neurosci **20**(11): 3993-4001.

Haass, C. and D. J. Selkoe (1993). "Cellular processing of beta-amyloid precursor protein and the genesis of amyloid beta-peptide." Cell **75**(6): 1039-1042.

Haberland, M., R. L. Montgomery, et al. (2009). "The many roles of histone deacetylases in development and physiology: implications for disease and therapy." Nat Rev Genet **10**(1): 32-42.

Hall, J., K. L. Thomas, et al. (2000). "Rapid and selective induction of BDNF expression in the hippocampus during contextual learning." Nat Neurosci **3**(6): 533-535.

Hallows, W. C., S. Lee, et al. (2006). "Sirtuins deacetylate and activate mammalian acetyl-CoA synthetases." Proc Natl Acad Sci U S A **103**(27): 10230-10235.

Hampel, H., M. M. Mesulam, et al. (2018). "The cholinergic system in the pathophysiology and treatment of Alzheimer's disease." Brain.

Hansen, R., G. Gartlehner, et al. (2008). "Efficacy and safety of donepezil, galantamine, and rivastigmine for the treatment of Alzheimer's disease: a systematic review and meta-analysis." Clin Interv Aging **3**: 211-225.

Hashimoto, M., Y. Yatabe, et al. (2009). "Impact of donepezil hydrochloride on the care burden of family caregivers of patients with Alzheimer's disease." Psychogeriatrics **9**: 196-203.

Hebert, L., P. Scherr, et al. (1995). "Age-Specific Incidence of Alzheimer's Disease in a Community Population." JAMA **273**: 1354-1359.

Hebert, S. S., K. Horre, et al. (2009). "MicroRNA regulation of Alzheimer's Amyloid precursor protein expression." Neurobiol Dis **33**(3): 422-428.

Hebert, S. S., K. Horre, et al. (2008). "Loss of microRNA cluster miR-29a/b-1 in sporadic Alzheimer's disease correlates with increased BACE1/beta-secretase expression." Proc Natl Acad Sci U S A **105**(17): 6415-6420.

Hempen, B. and J. P. Brion (1996). "Reduction of acetylated alpha-tubulin immunoreactivity in neurofibrillary tangle-bearing neurons in Alzheimer's disease." J Neuropathol Exp Neurol **55**(9): 964-972.

Herrup, K., J. Li, et al. (2013). "The role of ATM and DNA damage in neurons: upstream and downstream connections." DNA Repair (Amst) **12**(8): 600-604.

Heyn, H., N. Li, et al. (2012). "Distinct DNA methylomes of newborns and centenarians." Proc Natl Acad Sci U S A **109**(26): 10522-10527.

Hildmann, C., D. Riester, et al. (2007). "Histone deacetylases--an important class of cellular regulators with a variety of functions." Appl Microbiol Biotechnol **75**: 487-497.

Hirono, N., E. Mori, et al. (1997). "Procedural memory in patients with mild Alzheimer's disease." Dement Geriatr Cogn Disord **8**(4): 210-216.

Hof, P. R. and J. H. Morrison (1990). "Quantitative analysis of a vulnerable subset of pyramidal neurons in Alzheimer's disease: II. Primary and secondary visual cortex." J Comp Neurol **301**(1): 55-64.

Hsing, C. H., S. K. Hung, et al. (2015). "Histone Deacetylase Inhibitor Trichostatin A Ameliorated Endotoxin-Induced Neuroinflammation and Cognitive Dysfunction." Mediators Inflamm **2015**: 163140.

Huang, E. J. and L. F. Reichardt (2001). "Neurotrophins: roles in neuronal development and function." Annu Rev Neurosci **24**: 677-736.

Huang, R., S. P. Langdon, et al. (2016). "The role of HDAC2 in chromatin remodelling and response to chemotherapy in ovarian cancer." Oncotarget **7**(4): 4695-4711.

Hubbert, C., A. Guardiola, et al. (2002). "HDAC6 is a microtubule-associated deacetylase." Nature **417**: 455-458.

Humphries, C., M. A. Kohli, et al. (2015). "Alzheimer disease (AD) specific transcription, DNA methylation and splicing in twenty AD associated loci." Mol Cell Neurosci **67**: 37-45.

Huynh, J. L. and P. Casaccia (2013). "Epigenetic mechanisms in multiple sclerosis: implications for pathogenesis and treatment." Lancet Neurol **12**(2): 195-206.

Imai, S., C. Armstrong, et al. (2000). "Transcriptional silencing and longevity protein Sir2 is an NAD-dependent histone deacetylase." Nature **403**: 795-800.

Imamura, T., Y. Takatsuki, et al. (1998). "Age at onset and language disturbances in Alzheimer's disease." Neuropsychologia **36**: 945-949.

Iraizoz, I., J. L. Guijarro, et al. (1999). "Neuropathological changes in the nucleus basalis correlate with clinical measures of dementia." Acta Neuropathol **98**(2): 186-196.

Iraizoz, I., S. d. Lacalle, et al. (1991). "Cell loss and nuclear hypertrophy in topographical subdivisions of the nucleus basalis of Meynert in Alzheimer's disease." Neuroscience **41**: 33-40.

Iulita, M. F. and A. C. Cuello (2016). "The NGF Metabolic Pathway in the CNS and its Dysregulation in Down Syndrome and Alzheimer's Disease." Curr Alzheimer Res **13**(1): 53-67.

Iwata, A., K. Nagata, et al. (2014). "Altered CpG methylation in sporadic Alzheimer's disease is associated with APP and MAPT dysregulation " Human Mol Gen **23**: 648-656.

Jager, P. D., G. Srivastava, et al. (2014). "Alzheimer's disease: early alterations in brain DNA methylation at ANK1, BIN1, RHBDF2 and other loci." Nat Neurosci **17**: 1156-1163.

Jahn, H. (2013). "Memory loss in Alzheimer's disease." Dialogues Clin Neurosci **15**(4): 445-454.

Jakovcevski, M. and S. Akbarian (2012). "Epigenetic mechanisms in neurological disease." Nat Med **18**(8): 1194-1204.

Jeong, H., F. Then, et al. (2009). "Acetylation targets mutant huntingtin to autophagosomes for degradation." Cell **137**(1): 60-72.

Jeong, Y., R. Du, et al. (2014). "Histone deacetylase isoforms regulate innate immune responses by deacetylating mitogen-activated protein kinase phosphatase-1." J Leukoc Biol **95**(4): 651-659.

Jiao, Y., Z. Zheng, et al. (2014). "Identification and Characterization of Micro-RNAs in Pearl Oyster Pinctada martensii by Solexa Deep Sequencing." Marine Biotechnology **16**: 54-62.

Johnson, G. V. and W. H. Stoothoff (2004). "Tau phosphorylation in neuronal cell function and dysfunction." J Cell Sci **117**(Pt 24): 5721-5729.

Johnson, J., N. Phillips, et al. (2010). "Baseline predictors of clinical progression among patients with dysexecutive mild cognitive impairment." Dement Geriatr Cogn Disord **30**: 344-351.

Jones, P. L., G. J. Veenstra, et al. (1998). "Methylated DNA and MeCP2 recruit histone deacetylase to repress transcription." Nat Genet **19**(2): 187-191.

Jonhagen, M., A. Nordberg, et al. (1998). " Intra-cerebroventricular infusion of nerve growth factor in three patients with Alzheimer's disease." Dement Geriatr Cogn Disord **9**: 246-257.

Juan, L. J., W. J. Shia, et al. (2000). "Histone deacetylases specifically down-regulate p53-dependent gene activation." J Biol Chem **275**(27): 20436-20443.

Julien, C., C. Tremblay, et al. (2009). "SIRT1 decrease parallels the accumulation of tau in Alzheimer disease." J Neuropathol Exp Neurol **68**(1): 48-58.

Kaler, P., T. Sasazuki, et al. (2008). "HDAC2 deficiency sensitizes colon cancer cells to TNFalpha-induced apoptosis through inhibition of NF-kappaB activity." Experimental Cell Research **314**: 1507-1518.

Kaplan, D. R. and F. D. Miller (2000). "Neurotrophin signal transduction in the nervous system." Curr Opin Neurobiol **10**(3): 381-391.

Karres, J. S., V. Hilgers, et al. (2007). "The conserved microRNA miR-8 tunes atrophin levels to prevent neurodegeneration in Drosophila." Cell **131**(1): 136-145.

Kawaguchi, Y., J. J. Kovacs, et al. (2003). "The deacetylase HDAC6 regulates aggresome formation and cell viability in response to misfolded protein stress." Cell **115**(6): 727-738.

Kievit, J. and H. Kuypers (1975). "Basal forebrain and hypothalamic connections to frontal and parietal cortex in the rhesus monkey." Science **187**: 660-662.

Kiko, T., K. Nakagawa, et al. (2014). "MicroRNAs in plasma and cerebrospinal fluid as potential markers for Alzheimer's disease." J Alzheimers Dis **39**: 253-259.

Kim, D., C. L. Frank, et al. (2008). "Deregulation of HDAC1 by p25/Cdk5 in neurotoxicity." Neuron **60**(5): 803-817.

Kim, D., M. Nguyen, et al. (2007). "SIRT1 deacetylase protects against neurodegeneration in models for Alzheimer's disease and amyotrophic lateral sclerosis." EMBO J **26**: 3169-3179.

Kim, J., S. Shen, et al. (2010). "HDAC1 nuclear export induced by pathological conditions is essential for the onset of axonal damage." Nat Neurosci **13**: 180-189.

Kim, M. S., M. W. Akhtar, et al. (2012). "An essential role for histone deacetylase 4 in synaptic plasticity and memory formation." J Neurosci **32**(32): 10879-10886.

Kong, X., G. Li, et al. (2012). "MicroRNA-7 inhibits epithelial-to-mesenchymal transition and metastasis of breast cancer cells via targeting FAK expression." PLoS One **7**(8): e41523.

Konsoula, Z. and F. A. Barile (2012). "Epigenetic histone acetylation and deacetylation mechanisms in experimental models of neurodegenerative disorders." J Pharmacol Toxicol Methods **66**(3): 215-220.

Kopito, R. R. (2000). "Aggresomes, inclusion bodies and protein aggregation." Trends Cell Biol **10**(12): 524-530.

Kordower, J. H., E. Y. Chen, et al. (1994). "trk-immunoreactivity in the monkey central nervous system: forebrain." J Comp Neurol **349**(1): 20-35.

Korsching, S., G. Auburger, et al. (1985). "Levels of nerve growth factor and its mRNA in the central nervous system of the rat correlate with cholinergic innervation." EMBO J **4**(6): 1389-1393.

Kosik, K. S., P. R. Rapp, et al. (2012). "Mechanisms of age-related cognitive change and targets for intervention: epigenetics." J Gerontol A Biol Sci Med Sci **67**(7): 741-746.

Kouzarides, T. (2007). "Chromatin Modifications and Their Function." Cell **128**: 693-705.

Kovacs, J. J., P. J. Murphy, et al. (2005). "HDAC6 regulates Hsp90 acetylation and chaperone-dependent activation of glucocorticoid receptor." Mol Cell **18**(5): 601-607.

Kriaucionis, S. and N. Heintz (2009). "The nuclear DNA base 5-hydroxymethylcytosine is present in Purkinje neurons and the brain." Science **324**: 929-930.

Krichevsky, A. M., K. S. King, et al. (2003). "A microRNA array reveals extensive regulation of microRNAs during brain development." RNA **9**(10): 1274-1281.

Kumar, R., P. Chaterjee, et al. (2013). "Sirtuin1: a promising serum protein marker for early detection of Alzheimer's disease." PLoS One **8**(4): e61560.

Kwon, S., S. Seok, et al. (2017). "Obesity and aging diminish sirtuin 1 (SIRT1)-mediated deacetylation of SIRT3, leading to hyperacetylation and decreased activity and stability of SIRT3." J Biol Chem **292**(42): 17312-17323.

Kwon, S., Y. Zhang, et al. (2007). "The deacetylase HDAC6 is a novel critical component of stress granules involved in the stress response." Genes Dev **21**: 3381-3394.

Lalla, R. and G. Donmez (2013). "The role of sirtuins in Alzheimer's disease." Front Aging Neurosci **5**: 16.

Lambert, J. C., C. A. Ibrahim-Verbaas, et al. (2013). "Meta-analysis of 74,046 individuals identifies 11 new susceptibility loci for Alzheimer's disease." Nat Genet **45**(12): 1452-1458.

Lashley, T., P. Gami, et al. (2015). "Alterations in global DNA methylation and hydroxymethylation are not detected in Alzheimer's disease." Neuropathol Appl Neurobiol **41**: 497-506.

Lee, J., Y. Kim, et al. (2018). "SIRT3 deregulation is linked to mitochondrial dysfunction in Alzheimer's disease." Aging Cell **17**: 1-12.

Lee, R., P. Kermani, et al. (2001). "Regulation of cell survival by secreted proneurotrophins." Science **294**(5548): 1945-1948.

Lee, T., S. Murthy, et al. (2011). "An N-terminal truncated carboxypeptidase E splice isoform induces tumor growth and is a biomarker for predicting future metastasis in human cancers." J Clin Invest **121**.

Lehmann, S. M., C. Kruger, et al. (2012). "An unconventional role for miRNA: let-7 activates Toll-like receptor 7 and causes neurodegeneration." Nat Neurosci **15**(6): 827-835.

Levenson, J. M., K. J. O'Riordan, et al. (2004). "Regulation of histone acetylation during memory formation in the hippocampus." J Biol Chem **279**(39): 40545-40559.

Levine, M., A. Lu, et al. (2015). "Epigenetic age of the pre-frontal cortex is associated with neuritic plaques, amyloid load, and Alzheimer's disease related cognitive functioning." AGING-US **7**: 1198-1211.

Levine, M. E., A. T. Lu, et al. (2018). "An epigenetic biomarker of aging for lifespan and healthspan." Aging (Albany NY) **10**(4): 573-591.

Lewis, J., R. Meehan, et al. (1992). "Purification, sequence, and cellular localization of a novel chromosomal protein that binds to methylated DNA." Cell **69**: 905-914.

Li, S., F. Wang, et al. (2017). "HDAC2 regulates cell proliferation, cell cycle progression and cell apoptosis in esophageal squamous cell carcinoma EC9706 cells." Oncol Lett **13**(1): 403-409.

Lindsay, M. A. (2008). "microRNAs and the immune response." Trends Immunol **29**(7): 343-351.

Linnarsson, S., A. Bjorklund, et al. (1997). "Learning deficit in BDNF mutant mice." Eur J Neurosci **9**(12): 2581-2587.

Liu, A. K., R. C. Chang, et al. (2015). "Nucleus basalis of Meynert revisited: anatomy, history and differential involvement in Alzheimer's and Parkinson's disease." Acta Neuropathol **129**(4): 527-540.

Liu, C., T. Kanekiyo, et al. (2013). "Apolipoprotein E and Alzheimer disease: risk, mechanisms and therapy." Nat Rev Neurol **9**: 106-118.

Liu, D., H. Tang, et al. (2017). "Targeting the HDAC2/HNF-4A/miR-101b/AMPK Pathway Rescues Tauopathy and Dendritic Abnormalities in Alzheimer's Disease." Mol Ther **25**(3): 752-764.

Liu, H., Q. Hu, et al. (2008). "Developmental expression of histone deacetylase 11 in the murine brain." J Neurosci Res **86**(3): 537-543.

Liu, L., V. Drouet, et al. (2012). "Trans-synaptic spread of tau pathology in vivo." PLoS One **7**(2): e31302.

Liu, L., R. C. Wylie, et al. (2003). "Aging, cancer and nutrition: the DNA methylation connection." Mech Ageing Dev **124**(10-12): 989-998.

Liu, X., X. Chen, et al. (2013). "Regulation of microRNAs by epigenetics and their interplay involved in cancer." Journal of Experimental & Clinical Cancer Research **32**: 1-8.

Loewi, O. (1921). "Über humorale Übertragbarkeit der Herznervenwirkung." Pflügers Arch Ges Physiol **189**: 239-242.

Lonze, B. E. and D. D. Ginty (2002). "Function and regulation of CREB family transcription factors in the nervous system." Neuron **35**(4): 605-623.

Lukiw, W. J. (2007). "Micro-RNA speciation in fetal, adult and Alzheimer's disease hippocampus." Neuroreport **18**(3): 297-300.

Luo, J., F. Su, et al. (2000). "Deacetylation of p53 modulates its effect on cell growth and apoptosis." Nature **408**(6810): 377-381.

Lutz, L., I. C. Fitzner, et al. (2016). "Histone modifiers and marks define heterogeneous groups of colorectal carcinomas and affect responses to HDAC inhibitors in vitro." Am J Cancer Res **6**(3): 664-676.

Lyketsos, C. G., M. C. Carrillo, et al. (2011). "Neuropsychiatric symptoms in Alzheimer's disease." Alzheimers Dement **7**(5): 532-539.

Mahady, L., M. Nadeem, et al. (2018). "Frontal Cortex Epigenetic Dysregulation During the Progression of Alzheimer's Disease." Journal of Alzheimer's Disease **62**: 115-131.

Markesbery, W. R. (2010). "Neuropathologic alterations in mild cognitive impairment: a review." J Alzheimers Dis **19**(1): 221-228.

Markesbery, W. R., F. A. Schmitt, et al. (2006). "Neuropathologic substrate of mild cognitive impairment." Arch Neurol **63**(1): 38-46.

Marks, P. A. and W. S. Xu (2009). "Histone deacetylase inhibitors: Potential in cancer therapy." J Cell Biochem **107**(4): 600-608.

Masliah, E., D. S. Iimoto, et al. (1992). "Casein kinase II alteration precedes tau accumulation in tangle formation." Am J Pathol **140**(2): 263-268.

Masoudi, R., M. Ioannou, et al. (2009). "Biological activity of nerve growth factor precursor is dependent upon relative levels of its receptors." J Biol Chem **284**: 18424-18433.

Massoud, F. and S. Gauthier (2010). "Update on the pharmacological treatment of Alzheimer's disease." Curr Neuropharmacol **8**: 69-80.

Mastroeni, D., E. Delvaux, et al. (2015). "Aberrant intracellular localization of H3k4me3 demonstrates an early epigenetic phenomenon in Alzheimer's disease." Neurobiol Aging **36**: 3121-3129.

Mastroeni, D., A. Grover, et al. (2010). "Epigenetic changes in Alzheimer's disease: decrements in DNA methylation." Neurobiol Aging **31**(12): 2025-2037.

Mastroeni, D., A. Grover, et al. (2011). "Epigenetic mechanisms in Alzheimer's disease." Neurobiol Aging **32**(7): 1161-1180.

Mastroeni, D., A. McKee, et al. (2009). "Epigenetic differences in cortical neurons from a pair of monozygotic twins discordant for Alzheimer's disease." PLoS One **4**(8): e6617.

Matsuyama, A., T. Shimazu, et al. (2002). "In vivo destabilization of dynamic microtubules by HDAC6-mediated deacetylation." EMBO J **21**(24): 6820-6831.

Maurer, S. V. and C. L. Williams (2017). "The Cholinergic System Modulates Memory and Hippocampal Plasticity via Its Interactions with Non-Neuronal Cells." Front Immunol **8**: 1489.

McKhann, G., D. Drachman, et al. (1984). "Clinical diagnosis of Alzheimer's disease: report of the NINCDS-ADRDA Work Group under the auspices of Department of Health and Human Services Task Force on Alzheimer's Disease." Neurology **34**(7): 939-944.

McKhann, G., D. Knopman, et al. (2011). "The diagnosis of dementia due to Alzheimer's disease: recommendations from the National Institute on Aging-Alzheimer's Association workgroups on diagnostic guidelines for Alzheimer's disease." Alzheimers Dementia **7**: 263-269.

McQuown, S., R. Barrett, et al. (2011). "HDAC3 is a critical negative regulator of long-term memory formation." J Neurosci **31**: 764-774.

Mesulam, M. (1999). "Neuroplasticity failure in Alzheimer's disease: bridging the gap between plaques and tangles." Neuron **24**: 521-529.

Mesulam, M. (2013). "Cholinergic circuitry of the human nucleus basalis and its fate in Alzheimer's disease." J Comp Neurol **521**: 4124-4144.

Mesulam, M. and G. V. Hoesen (1976). "Acetylcholinesterase-rich projections from the basal forebrain of the rhesus monkey to neocortex." Neurology **109**: 152-157.

Mesulam, M. and E. Mufson (1984). "Neural inputs into the nucleus basalis of the substantia innominata in the rhesus monkey." Brain **107**: 253–274.

Mesulam, M., P. Shaw, et al. (2004). "Cholinergic nucleus basalis tauopathy emerges early in the aging-MCI-AD continuum." Ann Neurol **55**(6): 815-828.

Mesulam, M. M., E. J. Mufson, et al. (1983). "Cholinergic innervation of cortex by the basal forebrain: cytochemistry and cortical connections of the septal area, diagonal band

nuclei, nucleus basalis (substantia innominata), and hypothalamus in the rhesus monkey." J Comp Neurol **214**(2): 170-197.

Mesulam, M. M., E. J. Mufson, et al. (1986). "Three-dimensional representation and cortical projection topography of the nucleus basalis (Ch4) in the macaque: concurrent demonstration of choline acetyltransferase and retrograde transport with a stabilized tetramethylbenzidine method for horseradish peroxidase." Brain Res **367**(1-2): 301-308.

Mesulam, M. M., E. J. Mufson, et al. (1983). "Central cholinergic pathways in the rat: an overview based on an alternative nomenclature (Ch1-Ch6)." Neuroscience **10**(4): 1185-1201.

Michan, S., Y. Li, et al. (2010). "SIRT1 is essential for normal cognitive function and synaptic plasticity." Journal of Neuroscience **30**: 9695-9707.

Mietelska-Porowska, A., U. Wasik, et al. (2014). "Tau Protein Modifications and Interactions: Their Role in Function and Dysfunction." Int J Mol Sci **15**: 4671-4713.

Miller, K. M., J. V. Tjeertes, et al. (2010). "Human HDAC1 and HDAC2 function in the DNA-damage response to promote DNA nonhomologous end-joining." Nat Struct Mol Biol **17**(9): 1144-1151.

Min, S. W., X. Chen, et al. (2015). "Critical role of acetylation in tau-mediated neurodegeneration and cognitive deficits." Nat Med **21**(10): 1154-1162.

Min, S. W., S. H. Cho, et al. (2010). "Acetylation of tau inhibits its degradation and contributes to tauopathy." Neuron **67**(6): 953-966.

Min, S. W., P. D. Sohn, et al. (2018). "SIRT1 Deacetylates Tau and Reduces Pathogenic Tau Spread in a Mouse Model of Tauopathy." J Neurosci **38**(15): 3680-3688.

Mirra, S. S. (1997). "The CERAD neuropathology protocol and consensus recommendations for the postmortem diagnosis of Alzheimer's disease: a commentary." Neurobiol Aging **18**(4 Suppl): S91-94.

Morris, M. J., M. Mahgoub, et al. (2013). "Loss of histone deacetylase 2 improves working memory and accelerates extinction learning." J Neurosci **33**(15): 6401-6411.

Motta, M. C., N. Divecha, et al. (2004). "Mammalian SIRT1 represses forkhead transcription factors." Cell **116**(4): 551-563.

Mucha, L., S. Shaohung, et al. (2008). "Comparison of cholinesterase inhibitor utilization patterns and associated health care costs in Alzheimer’s disease." J Manag Care Pharm **14**: 451-461.

Mufson, E., M. Bothwell, et al. (1989). "Loss of nerve growth factor receptor-containing neurons in Alzheimer's disease: a quantitative analysis across subregions of the basal forebrain." Experimental Neurology **105**: 221-232.

Mufson, E., S. Ma, et al. (2000). "Loss of nucleus basalis neurons containing trkA immunoreactivity in individuals with mild cognitive impairment and early Alzheimer's disease." Journal of Comparative Neurology **427**: 19-30.

Mufson, E., S. Ma, et al. (2002). "Loss of basal forebrain P75(NTR) immunoreactivity in subjects with mild cognitive impairment and Alzheimer's disease." Journal of Comparative Neurology **443**: 136-153.

Mufson, E., L. Mahady, et al. (2015). "Hippocampal plasticity during the progression of Alzheimer's disease." Neuroscience **309**: 51-67.

Mufson, E., M. Malek-Ahmadi, et al. (2016). "Braak staging, plaque pathology, and APOE status in elderly persons without cognitive impairment." Neurobiol Aging **37**: 147-153.

Mufson, E. J., T. Brashers-Krug, et al. (1992). "p75 nerve growth factor receptor immunoreactivity in the human brainstem and spinal cord." Brain Res **589**(1): 115-123.

Mufson, E. J., E. Y. Chen, et al. (1999). "Entorhinal cortex beta-amyloid load in individuals with mild cognitive impairment." Exp Neurol **158**(2): 469-490.

Mufson, E. J., S. D. Ginsberg, et al. (2003). "Human cholinergic basal forebrain: chemoanatomy and neurologic dysfunction." J Chem Neuroanat **26**(4): 233-242.

Mufson, E. J., B. He, et al. (2012). "Hippocampal proNGF signaling pathways and beta-amyloid levels in mild cognitive impairment and Alzheimer disease." J Neuropathol Exp Neurol **71**(11): 1018-1029.

Mufson, E. J., G. A. Higgins, et al. (1991). "Nerve growth factor receptor immunoreactivity in the new world monkey (Cebus apella) and human cerebellum." J Comp Neurol **308**(4): 555-575.

Mufson, E. J., M. Malek-Ahmadi, et al. (2016). "Braak stage and trajectory of cognitive decline in noncognitively impaired elders." Neurobiol Aging **43**: 101-110.

Muller-Spahn, F. (2003). "Behavioral disturbances in dementia." Dialogues Clin Neurosci **5**: 49-59.

Müller, M., L. Jäkel, et al. (2016). "MicroRNA-29a Is a Candidate Biomarker for Alzheimer's Disease in Cell-Free Cerebrospinal Fluid." Molecular Neurobiology **53**: 2894-2899.

Namekawa, Y., H. Baba, et al. (2013). "Heterogeneity of elderly depression: increased risk of Alzheimer's disease and Abeta protein metabolism." Prog Neuropsychopharmacol Biol Psychiatry **43**: 203-208.

Nativio, R., G. Donahue, et al. (2018). "Dysregulation of the epigenetic landscape of normal aging in Alzheimer's disease." Nat Neurosci **21**(4): 497-505.

Nelson, P. and W. Wang (2010). "MiR-107 is reduced in Alzheimer's disease brain neocortex: validation study." J Alzheimers Dis **21**: 75-79.

Newell, K. L., B. T. Hyman, et al. (1999). "Application of the National Institute on Aging (NIA)-Reagan Institute criteria for the neuropathological diagnosis of Alzheimer disease." J Neuropathol Exp Neurol **58**(11): 1147-1155.

Ng, F., L. Wijaya, et al. (2015). "SIRT1 in the brain-connections with aging-associated disorders and lifespan." Front Cell Neurosci **9**: 64.

Nixon, R. and D. Yang (2011). "Autophagy failure in Alzheimer's disease--locating the primary defect." Neurobiol Dis **43**: 38-45.

Nykjaer, A., R. Lee, et al. (2004). "Sortilin is essential for proNGF-induced neuronal cell death.

." Nature **427**: 843-848.

O'Hagan, H., H. Mohammad, et al. (2008). "Double stranded breaks can initiate gene silencing and SIRT-1 dependent onset of DNA methylation in an exogenous promoter CpG island." PLoS Genet **4**: 1-16.

Opris, I., L. Santos, et al. (2013). "Prefrontal cortical microcircuits bind perception to executive control." Sci Rep **3**: 2285.

Orr, M. and S. Oddo (2013). "The role of autophagy in Alzheimer's disease." Alzheimers Dement **9**.

Pan, L., J. Penney, et al. (2014). "Chromatin regulation of DNA damage repair and genome integrity in the central nervous system." J Mol Biol **426**(20): 3376-3388.

Pandey, U., Z. Nie, et al. (2007). "HDAC6 rescues neurodegeneration and provides an essential link between autophagy and the UPS." Nature **447**: 859-863.

Pandey, U., J. Taylor, et al. (2007). "HDAC6 at the Intersection of Autophagy, the Ubiquitin-proteasome System, and Neurodegeneration." Autophagy **3**: 643-645.

Pasinetti, G. and J. Eberstein (2008). "Metabolic syndrome and the role of dietary lifestyles in Alzheimer's disease." J Neurochem **106**: 1502-1514.

Pathak, A., E. M. Stanley, et al. (2018). "Retrograde Degenerative Signaling Mediated by the p75 Neurotrophin Receptor Requires p150(Glued) Deacetylation by Axonal HDAC1." Dev Cell **46**(3): 376-387 e377.

Patrick, G. N., L. Zukerberg, et al. (1999). "Conversion of p35 to p25 deregulates Cdk5 activity and promotes neurodegeneration." Nature **402**(6762): 615-622.

Peart, M. J., G. K. Smyth, et al. (2005). "Identification and functional significance of genes regulated by structurally different histone deacetylase inhibitors." Proc Natl Acad Sci U S A **102**(10): 3697-3702.

Peng, S., J. Wuu, et al. (2004). "Increased proNGF levels in subjects with mild cognitive impairment and mild Alzheimer disease." J Neuropathol Exp Neurol **63**(6): 641-649.

Peng, S., S. Zhao, et al. (2015). "HDAC2 selectively regulates FOXO3a-mediated gene transcription during oxidative stress-induced neuronal cell death." J Neurosci **35**(3): 1250-1259.

Perez, M., I. Santa-Maria, et al. (2009). "Tau – an inhibitor of deacetylase HDAC6 function." J Neurochem **109**: 1756-1766.

Perez, S., D. Getova, et al. (2012). "Rac1b increases with progressive tau pathology within cholinergic nucleus basalis neurons in Alzheimer's disease." Am J Pathol **180**: 526-540.

Perez, S. E., B. He, et al. (2015). "Hippocampal endosomal, lysosomal, and autophagic dysregulation in mild cognitive impairment: correlation with abeta and tau pathology." J Neuropathol Exp Neurol **74**(4): 345-358.

Perez, S. E., M. Nadeem, et al. (2017). "Neocortical and hippocampal TREM2 protein levels during the progression of Alzheimer's disease." Neurobiol Aging **54**: 133-143.

Pernet, L., V. Faure, et al. (2014). "HDAC6-ubiquitin interaction controls the duration of HSF1 activation after heat shock." Mol Biol Cell **25**(25): 4187-4194.

Perry, E. K., M. Johnson, et al. (1992). "Convergent cholinergic activities in aging and Alzheimer's disease." Neurobiol Aging **13**(3): 393-400.

Perry, E. K., B. E. Tomlinson, et al. (1978). "Correlation of cholinergic abnormalities with senile plaques and mental test scores in senile dementia." Br Med J **2**(6150): 1457-1459.

Peters, M., P. Rosenberg, et al. (2013). "Neuropsychiatric symptoms as risk factors for progression from CIND to dementia: the Cache County Study." Am J Geriatr Psychiatry **21**: 1116-1124.

Petersen, R. (2004). "Mild cognitive impairment as a diagnostic entity." J Intern Med **256**(3): 183-194.

Petersen, R. C., G. E. Smith, et al. (1999). "Mild cognitive impairment: clinical characterization and outcome." Arch Neurol **56**(3): 303-308.

Phipps, A. J., J. C. Vickers, et al. (2016). "Neurofilament-labeled pyramidal neurons and astrocytes are deficient in DNA methylation marks in Alzheimer's disease." Neurobiol Aging **45**: 30-42.

Plattner, F., M. Angelo, et al. (2006). "The roles of cyclin-dependent kinase 5 and glycogen synthase kinase 3 in tau hyperphosphorylation." J Biol Chem **281**(35): 25457-25465.

Poleshko, A., I. Palagin, et al. (2008). "Identification of cellular proteins that maintain retroviral epigenetic silencing: Evidence for an antiviral response." J Virol **82**: 2313-2323.

Poulsen, P., M. Esteller, et al. (2007). "The epigenetic basis of twin discordance in age-related diseases." Pediatr Res **61**(5 Pt 2): 38R-42R.

Pratt, A. J. and I. J. MacRae (2009). "The RNA-induced silencing complex: a versatile gene-silencing machine." J Biol Chem **284**(27): 17897-17901.

Price, J. and D. Amaral (1981). "An autoradiographic study of the projections of the central nucleus of the monkey amygdala." J Neurosci **1**: 1242-1259.

Price, J., D. McKeel, et al. (2009). "Neuropathology of Nondemented Aging: Presumptive Evidence for Preclinical Alzheimer Disease." Neurobiol Aging **30**: 1026-1036.

Price, J. L. and J. C. Morris (1999). "Tangles and plaques in nondemented aging and "preclinical" Alzheimer's disease." Ann Neurol **45**(3): 358-368.

Pujol Lopez, Y., G. Kenis, et al. (2016). "Effects of prenatal Poly I:C exposure on global histone deacetylase (HDAC) and DNA methyltransferase (DNMT) activity in the mouse brain." Mol Biol Rep **43**(7): 711-717.

Pyrzynska, B., I. Pilecka, et al. (2009). "Endocytic proteins in the regulation of nuclear signaling, transcription and tumorigenesis." Mol Oncol **3**(4): 321-338.

Quental, N., S. Brucki, et al. (2009). "Visuospatial function in early Alzheimer's disease: Preliminary study." Dement Neuropsychol **3**: 234-240.

Rahnev, D., H. Lau, et al. (2011). "Prior expectation modulates the interaction between sensory and prefrontal regions in the human brain." J Neurosci **31**: 10741-10748.

Rahnev, D., D. E. Nee, et al. (2016). "Causal evidence for frontal cortex organization for perceptual decision making." Proc Natl Acad Sci U S A **113**(21): 6059-6064.

Rao, J. S., V. L. Keleshian, et al. (2012). "Epigenetic modifications in frontal cortex from Alzheimer's disease and bipolar disorder patients." Transl Psychiatry **2**: e132.

Rashid, S., I. Pilecka, et al. (2009). "Endosomal adaptor proteins APPL1 and APPL2 are novel activators of beta-catenin/TCF-mediated transcription." J Biol Chem **284**(27): 18115-18128.

Rasool, C., C. Svendsen, et al. (1986). "Neurofibrillary degeneration of cholinergic and noncholinergic neurons of the basal forebrain in Alzheimer's disease." Annals of Neurology **20**: 482-488.

Ratti, F., F. Ramond, et al. (2015). "Histone deacetylase 6 is a FoxO transcription factor-dependent effector in skeletal muscle atrophy." J Biol Chem **290**: 4215-4224.

Reynolds, R., P. Casaccia, et al. (2010). "HDAC1 nuclear export induced by pathological conditions is essential for the onset of axonal damage." Nat Neurosci **13**: 180-189.

Ringholm, S., R. S. Bienso, et al. (2011). "Bed rest reduces metabolic protein content and abolishes exercise-induced mRNA responses in human skeletal muscle." Am J Physiol Endocrinol Metab **301**(4): E649-658.

Rinne, J., L. Paljarvi, et al. (1987). " Neuronal size and density in the nucleus basalis of Meynert in Alzheimer's disease." The Journal of Neurological Sciences **79**: 67-76.

Riopelle, R. J., V. M. Verge, et al. (1987). "Properties of receptors for nerve growth factor in the mature rat nervous system." Brain Res **427**(1): 45-53.

Roberts, T. C., K. V. Morris, et al. (2014). "Perspectives on the mechanism of transcriptional regulation by long non-coding RNAs." Epigenetics **9**(1): 13-20.

Robertson, J., A. Robertson, et al. (2011). "The presence of 5-hydroxymethylcytosine at the gene promoter and not in the gene body negatively regulates gene expression." Biochem Biophys Res Commun **411**: 40-43.

Rodenhiser, D. and M. Mann (2006). "Epigenetics and human disease: translating basic biology into clinical applications." CMAJ **174**: 341-348.

Rodriguez-Otero, P., J. Roman-Gomez, et al. (2011). "Deregulation of FGFR1 and CDK6 oncogenic pathways in acute lymphoblastic leukaemia harbouring epigenetic modifications of the MIR9 family." Br J Haematol **155**(1): 73-83.

Ronn, T., P. Volkov, et al. (2013). "A six months exercise intervention influences the genome-wide DNA methylation pattern in human adipose tissue." PLoS Genet **9**(6): e1003572.

Rosenberger, A. F., R. Hilhorst, et al. (2016). "Protein Kinase Activity Decreases with Higher Braak Stages of Alzheimer's Disease Pathology." J Alzheimers Dis **49**(4): 927-943.

Rossor, M. and C. Mountjoy (1986). "Postmortem neurochemical changes in Alzheimer's disease compared with normal aging." Can J Neurol Sci **13**: 499-502.

Rotkrua, P., Y. Akiyama, et al. (2011). "MiR-9 downregulates CDX2 expression in gastric cancer cells." Int J Cancer **129**(11): 2611-2620.

Rouaux, C., N. Jokic, et al. (2003). "Critical loss of CBP/p300 histone acetylase activity by caspase-6 during neurodegeneration." EMBO J **22**(24): 6537-6549.

Rye, D. B., B. H. Wainer, et al. (1984). "Cortical projections arising from the basal forebrain: a study of cholinergic and noncholinergic components employing combined retrograde tracing and immunohistochemical localization of choline acetyltransferase." Neuroscience **13**(3): 627-643.

Saito, T., M. Nagai, et al. (2006). "SYT-SSX1 and SYT-SSX2 interfere with repression of E-cadherin by snail and slug: a potential mechanism for aberrant mesenchymal to epithelial transition in human synovial sarcoma." Cancer Res **66**(14): 6919-6927.

Sala Frigerio, C., P. Lau, et al. (2013). "Reduced expression of hsa-miR-27a-3p in CSF of patients with Alzheimer disease." Neurology **81**(24): 2103-2106.

Salat, D., J. Kaye, et al. (2001). "Selective Preservation and Degeneration Within the Prefrontal Cortex in Aging and Alzheimer Disease." Arch of Neurol **58**: 1403-1408.

Sassin, I., C. Schultz, et al. (2000). "Evolution of Alzheimer's disease-related cytoskeletal changes in the basal nucleus of Meynert." Acta Neuropathol **100**: 259-269.

Scheff, S. W. and D. A. Price (1998). "Synaptic density in the inner molecular layer of the hippocampal dentate gyrus in Alzheimer disease." J Neuropathol Exp Neurol **57**(12): 1146-1153.

Scheff, S. W. and D. A. Price (2003). "Synaptic pathology in Alzheimer's disease: a review of ultrastructural studies." Neurobiol Aging **24**(8): 1029-1046.

Scheff, S. W., D. A. Price, et al. (2006). "Hippocampal synaptic loss in early Alzheimer's disease and mild cognitive impairment." Neurobiol Aging **27**(10): 1372-1384.

Schipper, H. M., O. C. Maes, et al. (2007). "MicroRNA expression in Alzheimer blood mononuclear cells." Gene Regul Syst Bio **1**: 263-274.

Schmitt, M. and H. Matthies (1979). "Biochemical studies on histones of the central nervous system. III. Incorporation of [14C]-acetate into the histones of different rat brain regions during a learning experiment." Acta Biol Med Ger **38**: 683-689.

Schmitz, T. and R. N. Spreng (2016). "Basal forebrain degeneration precedes and predicts the cortical spread of Alzheimer's pathology." Nat Commun **7**: 13249.

Schneider, J., N. Aggarwal, et al. (2009). "The neuropathology of older persons with and without dementia from community versus clinic cohorts." J Alzheimers Dis **18**: 691-701.

Schoenmakers, B., F. Buntinx, et al. (2009). "Can pharmacological treatment of behavioural disturbances in elderly patients with dementia lower the burden of their family caregiver?" Fam Pract **26**: 279-286.

Schonrock, N., D. Humphreys, et al. (2012). "Target gene repression mediated by miRNAs miR-181c and miR-9 both of which are down-regulated by amyloid-β." J Mol Neurosci **46**: 324-335.

Schonrock, N., Y. D. Ke, et al. (2010). "Neuronal microRNA deregulation in response to Alzheimer's disease amyloid-beta." PLoS One **5**(6): e11070.

Schroeder, F. A., C. Wang, et al. (2014). "PET imaging demonstrates histone deacetylase target engagement and clarifies brain penetrance of known and novel small molecule inhibitors in rat." ACS Chem Neurosci **5**(10): 1055-1062.

Schuler, S., P. Fritsche, et al. (2010). "HDAC2 attenuates TRAIL-induced apoptosis of pancreatic cancer cells." Mol Cancer **9**: 80.

Seiler, M. and M. E. Schwab (1984). "Specific retrograde transport of nerve growth factor (NGF) from neocortex to nucleus basalis in the rat." Brain Res **300**(1): 33-39.

Shen, X., J. Chen, et al. (2016). "Neurons in Vulnerable Regions of the Alzheimer's Disease Brain Display Reduced ATM Signaling." eNeuro **3**(1).

Shi, Y., K. Yamada, et al. (2017). "ApoE4 markedly exacerbates tau-mediated neurodegeneration in a mouse model of tauopathy." Nature **549**(7673): 523-527.

Shoji, M., T. E. Golde, et al. (1992). "Production of the Alzheimer amyloid beta protein by normal proteolytic processing." Science **258**(5079): 126-129.

Simic, G., M. Babic, et al. (2014). "Early failure of the default-mode network and the pathogenesis of Alzheimer's disease." CNS Neurosci Ther **20**(7): 692-698.

Slack, J., L. J. LE, et al. (2011). "Autodeimination of protein arginine deiminase 4 alters protein-protein interactions but not activity." Biochemistry **50**: 3997-4010.

Sobreviela, T., D. O. Clary, et al. (1994). "TrkA-immunoreactive profiles in the central nervous system: colocalization with neurons containing p75 nerve growth factor receptor, choline acetyltransferase, and serotonin." J Comp Neurol **350**(4): 587-611.

Soreq, H. and Y. Wolf (2011). "NeurimmiRs: microRNAs in the neuroimmune interface." Trends Mol Med **17**(10): 548-555.

Sparks, D. L., J. C. Hunsaker, 3rd, et al. (1992). "Monoaminergic and cholinergic synaptic markers in the nucleus basalis of Meynert (nbM): normal age-related changes and the effect of heart disease and Alzheimer's disease." Ann Neurol **31**(6): 611-620.

Sperling, R., E. Mormino, et al. (2014). "The evolution of preclinical Alzheimer's disease: implications for prevention trials." Neuron **84**(3): 608-622.

Swank, M. and J. Sweatt (2001). "Increased histone acetyltransferase and lysine acetyltransferase activity and biphasic activation of the ERK/RSK cascade in insular cortex during novel taste learning." J Neurosci Res **21**: 3383-3391.

Tagliavini, F. and G. Pilleri (1983). "Neuronal counts in basal nucleus of Meynert in Alzheimer disease and in simple senile dementia." Lancet **1**(8322): 469-470.

Tahiliani, M., K. P. Koh, et al. (2009). "Conversion of 5-methylcytosine to 5-hydroxymethylcytosine in mammalian DNA by MLL partner TET1." Science **324**(5929): 930-935.

Tang, L. Y., M. N. Reddy, et al. (2003). "The eukaryotic DNMT2 genes encode a new class of cytosine-5 DNA methyltransferases." J Biol Chem **278**(36): 33613-33616.

Tang, X., J. S. Gao, et al. (2007). "Acetylation-dependent signal transduction for type I interferon receptor." Cell **131**(1): 93-105.

Tariot, P. N., L. S. Schneider, et al. (2011). "Chronic divalproex sodium to attenuate agitation and clinical progression of Alzheimer disease." Arch Gen Psychiatry **68**(8): 853-861.

Teipel, S., W. Flatz, et al. (2005). "Measurement of basal forebrain atrophy in Alzheimer's disease using MRI." Brain **128**: 2626-2644.

Thangavel, R., S. Sahu, et al. (2009). "Loss of non-phosphorylated neurofilament immunoreactivity in temporal cortical areas in Alzheimer's disease." Neuroscience **160**: 427-433.

Thies, W. and L. Bleiler (2013). "2013 Alzheimer's disease facts and figures." Alzheimers Dement **9**(2): 208-245.

Thinakaran, G. and E. H. Koo (2008). "Amyloid precursor protein trafficking, processing, and function." J Biol Chem **283**(44): 29615-29619.

Tiernan, C. T., E. J. Mufson, et al. (2018). "Tau Oligomer Pathology in Nucleus Basalis Neurons During the Progression of Alzheimer Disease." J Neuropathol Exp Neurol **77**(3): 246-259.

Trojanowski, J. (1993). "The molecular and genetic basis of neurological disease." J Neuropathol Exp Neurol **52**: 550.

Tsai, S. C. and E. Seto (2002). "Regulation of histone deacetylase 2 by protein kinase CK2." J Biol Chem **277**(35): 31826-31833.

Tseng, J. H., L. Xie, et al. (2017). "The Deacetylase HDAC6 Mediates Endogenous Neuritic Tau Pathology." Cell Rep **20**(9): 2169-2183.

Tulving, E. and H. J. Markowitsch (1998). "Episodic and declarative memory: role of the hippocampus." Hippocampus **8**(3): 198-204.

Tuszynski, M. H., J. Roberts, et al. (1996). "Gene therapy in the adult primate brain: intraparenchymal grafts of cells genetically modified to produce nerve growth factor prevent cholinergic neuronal degeneration." Gene Ther **3**(4): 305-314.

Tuszynski, M. H., L. Thal, et al. (2005). "A phase 1 clinical trial of nerve growth factor gene therapy for Alzheimer disease." Nat Med **11**(5): 551-555.

Valinluck, V. and L. C. Sowers (2007). "Endogenous cytosine damage products alter the site selectivity of human DNA maintenance methyltransferase DNMT1." Cancer Res **67**(3): 946-950.

Valinluck, V., H. H. Tsai, et al. (2004). "Oxidative damage to methyl-CpG sequences inhibits the binding of the methyl-CpG binding domain (MBD) of methyl-CpG binding protein 2 (MeCP2)." Nucleic Acids Res **32**(14): 4100-4108.

van Gent, R., C. Di Sanza, et al. (2014). "SIRT1 mediates FOXA2 breakdown by deacetylation in a nutrient-dependent manner." PLoS One **9**(5): e98438.

Vana, L., N. Kanaan, et al. (2011). "Progression of tau pathology in cholinergic basal forebrain neurons in MCI and AD." Am J Pathol **179**: 2533-2550.

Vaquero, A., M. Scher, et al. (2004). "Human SirT1 interacts with histone H1 andpromotes formation of facultative heterochromatin." Mol Cell **16**: 93-105.

Vaziri, H., S. Dessain, et al. (2001). "hSIR2(SIRT1) functions as an NAD-dependent p53 deacetylase." Cell **107**: 149-159.

Vickers, J. C., B. M. Riederer, et al. (1994). "Alterations in neurofilament protein immunoreactivity in human hippocampal neurons related to normal aging and Alzheimer's disease." Neuroscience **62**(1): 1-13.

Vilalta-Franch, J., S. Lopez-Pousa, et al. (2013). "Psychosis of Alzheimer disease: prevalence, incidence, persistence, risk factors, and mortality." Am J Geriatr Psychiatry **21**(11): 1135-1143.

Vingtdeux, V., P. Chandakkar, et al. (2011). "Novel synthetic small-molecule activators of AMPK as enhancers of autophagy and amyloid-β peptide degradation." FASEB **25**: 219-231.

Volmar, C. and C. Wahlestedt (2015). "Histone deacetylases (HDACs) and brain function." Neuroepigenetics **1**: 20-27.

Wade, P. A. (2001). "Methyl CpG-binding proteins and transcriptional repression." Bioessays **23**(12): 1131-1137.

Wade, P. A., P. L. Jones, et al. (1998). "Histone deacetylase directs the dominant silencing of transcription in chromatin: association with MeCP2 and the Mi-2 chromodomain SWI/SNF ATPase." Cold Spring Harb Symp Quant Biol **63**: 435-445.

Wang, C., F. A. Schroeder, et al. (2014). "In vivo imaging of histone deacetylases (HDACs) in the central nervous system and major peripheral organs." J Med Chem **57**(19): 7999-8009.

Wang, J., J. T. Yu, et al. (2013). "Epigenetic mechanisms in Alzheimer's disease: implications for pathogenesis and therapy." Ageing Res Rev **12**(4): 1024-1041.

Wang, S. C., B. Oelze, et al. (2008). "Age-specific epigenetic drift in late-onset Alzheimer's disease." PLoS One **3**(7): e2698.

Wang, W., B. Rajeev, et al. (2008). "The Expression of MicroRNA miR-107 Decreases Early in Alzheimer's Disease and May Accelerate Disease Progression through Regulation of β-Site Amyloid Precursor Protein-Cleaving Enzyme 1." J Neurosci **28**: 1213-1223.

Wang, W. Y., L. Pan, et al. (2013). "Interaction of FUS and HDAC1 regulates DNA damage response and repair in neurons." Nat Neurosci **16**(10): 1383-1391.

Wegiel, J., M. Flory, et al. (2017). "Multiregional Age-Associated Reduction of Brain Neuronal Reserve Without Association With Neurofibrillary Degeneration or β-Amyloidosis." J Neuropathol Exp Neurol **76**: 439-457.

Wey, H., T. Gilbert, et al. (2016). "Insights into neuroepigenetics through human histone deacetylase PET imaging." Sci Transl Med **8**.

Whitehouse, P. J., D. L. Price, et al. (1981). "Alzheimer disease: evidence for selective loss of cholinergic neurons in the nucleus basalis." Ann Neurol **10**(2): 122-126.

Wilcock, G. K., M. M. Esiri, et al. (1982). "Alzheimer's disease. Correlation of cortical choline acetyltransferase activity with the severity of dementia and histological abnormalities." J Neurol Sci **57**(2-3): 407-417.

Wilcock, G. K., M. M. Esiri, et al. (1983). "The nucleus basalis in Alzheimer's disease: cell counts and cortical biochemistry." Neuropathol Appl Neurobiol **9**(3): 175-179.

Wilson, R. S., L. A. Beckett, et al. (2002). "Individual differences in rates of change in cognitive abilities of older persons." Psychol Aging **17**(2): 179-193.

Wilson, V. and P. Jones (1983). "DNA methylation decreases in aging but not in immortal cells." Science **220**: 1055-1057.

Wimo, A., M. Guerchet, et al. (2017). "The worldwide costs of dementia 2015 and comparisons with 2010." Alzheimers Dement **13**(1): 1-7.

Winkler, J., A. E. Power, et al. (1998). "Short-term and complete reversal of NGF effects in rats with lesions of the nucleus basalis magnocellularis." Brain Res **788**(1-2): 1-12.

Xu, K., X. L. Dai, et al. (2011). "Targeting HDACs: a promising therapy for Alzheimer's disease." Oxid Med Cell Longev **2011**: 143269.

Xu, X., J. Vatsyayan, et al. (2010). "HDAC2 promotes eIF4E sumoylation and activates mRNA translation gene specifically." J Biol Chem **285**(24): 18139-18143.

Yang, Y., H. Hou, et al. (2005). "Suppression of FOXO1 activity by FHL2 through SIRT1-mediated deacetylation." EMBO J **24**: 1021-1032.

Yang, Y., E. Mufson, et al. (2003). "Neuronal Cell Death Is Preceded by Cell Cycle Events at All Stages of Alzheimer's Disease." Journal of Neuroscience **23**: 2557-2563.

Yoshiyama, Y., V. M. Lee, et al. (2013). "Therapeutic strategies for tau mediated neurodegeneration." J Neurol Neurosurg Psychiatry **84**(7): 784-795.

Yu, Z., W. Li, et al. (2015). "Relationship between Adiponectin Gene Polymorphisms and Late-Onset Alzheimer's Disease." PLoS One **10**: 1-11.

Zahodne, L. B., J. J. Manly, et al. (2013). "Cognitive declines precede and predict functional declines in aging and Alzheimer's disease." PLoS One **8**(9): e73645.

Zhang, C., T. McKinsey, et al. (2002). "Class II Histone Deacetylases Act as Signal-Responsive Repressors of Cardiac Hypertrophy." Cell **110**: 479-488.

Zhang, K., M. Schrag, et al. (2012). "Targeted proteomics for quantification of histone acetylation in Alzheimer's disease." Proteomics **12**(8): 1261-1268.

Zhang, X., Z. Yuan, et al. (2007). "HDAC6 modulates cell motility by altering the acetylation level of cortactin." Mol Cell **27**(2): 197-213.

Zhang, Y., N. Li, et al. (2003). "HDAC-6 interacts with and deacetylates tubulin and microtubules in vivo." EMBO J **22**(5): 1168-1179.

Zhang, Y. and D. Reinberg (2001). "Transcription regulation by histone methylation: interplay between different covalent modifications of the core histone tails." Genes and Development **15**: 2343-2360.

Zovoilis, A., H. Agbemenyah, et al. (2011). "microRNA-34c is a novel target to treat dementias." EMBO J **30**: 4299-4308.

Zusso, M., M. Barbierato, et al. (2018). "Neuroepigenetics and Alzheimer's Disease: An Update." J Alzheimers Dis **64**(3): 671-688.

APPENDIX A

COPYRIGHT PERMISSION

Laura Mahady has permission from all co-authors to include the following published works in her dissertation:

Chapter 2 of this dissertation is published in: Mahady, L., M. Nadeem, et al. (2018). "Frontal Cortex Epigenetic Dysregulation During the Progression of Alzheimer's Disease." Journal of Alzheimer's Disease **62**: 115-131.

Chapter 3 of this dissertation is published in: Mahady, L., M. Nadeem, et al. (2018). "HDAC2 dysregulation in the nucleus basalis of Meynert during the progression of Alzheimer's disease." Neuropathol Appl Neurobiol.